UNIL | Université de Lausanne

Unicentre
CH-1015 Lausanne
http://serval.unil.ch

Year : 2019

Contracting CAG/CTG repeats using the CRISPR-Cas9 nickase

Cinesi Cinzia

Cinesi Cinzia, 2019, Contracting CAG/CTG repeats using the CRISPR-Cas9 nickase

Originally published at : Thesis, University of Lausanne

Posted at the University of Lausanne Open Archive http://serval.unil.ch
Document URN : urn:nbn:ch:serval-BIB_BDA89CB72B699

Droits d'auteur
L'Université de Lausanne attire expressément l'attention des utilisateurs sur le fait que tous les documents publiés dans l'Archive SERVAL sont protégés par le droit d'auteur, conformément à la loi fédérale sur le droit d'auteur et les droits voisins (LDA). A ce titre, il est indispensable d'obtenir le consentement préalable de l'auteur et/ou de l'éditeur avant toute utilisation d'une oeuvre ou d'une partie d'une oeuvre ne relevant pas d'une utilisation à des fins personnelles au sens de la LDA (art. 19, al. 1 lettre a). A défaut, tout contrevenant s'expose aux sanctions prévues par cette loi. Nous déclinons toute responsabilité en la matière.

Copyright
The University of Lausanne expressly draws the attention of users to the fact that all documents published in the SERVAL Archive are protected by copyright in accordance with federal law on copyright and similar rights (LDA). Accordingly it is indispensable to obtain prior consent from the author and/or publisher before any use of a work or part of a work for purposes other than personal use within the meaning of LDA (art. 19, para. 1 letter a). Failure to do so will expose offenders to the sanctions laid down by this law. We accept no liability in this respect.

UNIL | Université de Lausanne
Faculté de biologie et de médecine

Ecole de Biologie

Contracting CAG/CTG repeats using the CRISPR-Cas9 nickase

Thèse de doctorat ès sciences de la vie (PhD)

présentée à la

Faculté de biologie et de médecine
de l'Université de Lausanne

par

Cinzia CINESI

Master de l'Université de Lausanne

Jury

Prof. Laurent Lehmann, Président
Prof. Alexandre Reymond, Directeur de thèse
Prof. Vincent Dion Co-directeur de thèse
Prof. Nicole Déglon, Experte
Prof. Geneviève Gourdon, Experte

Lausanne
May 2019

UNIL | Université de Lausanne
Faculté de biologie
et de médecine

Ecole Doctorale
Doctorat ès sciences de la vie

Imprimatur

Vu le rapport présenté par le jury d'examen, composé de

Président·e	Monsieur	Prof.	Laurent	**Lehmann**
Directeur·trice de thèse	Monsieur	Prof.	Alexandre	**Reymond**
Co-directeur·trice	Monsieur	Prof.	Vincent	**Dion**
Expert·e·s	Madame	Prof.	Nicole	**Déglon**
	Madame	Prof.	Geneviève	**Gourdon**

le Conseil de Faculté autorise l'impression de la thèse de

Madame Cinzia Cinesi

Master en sciences moléculaires du vivant, Université de Lausanne

intitulée

Contracting CAG/CTG repeats using the CRISPR-Cas9 nickase

Lausanne, le 21 juin 2019

pour le Doyen
de la Faculté de biologie et de médecine

Prof. Laurent Lehmann

Acknowledgments

I would like to thank my thesis professor Vincent Dion for this great opportunity. I have learned so much and improved in many different aspects during these years thanks to your guidance. Support, new ideas, smiles and positive words made my project a beautiful experience. Thank you for everything.

Thank you to Prof. Alexandre Reymond for being my co-Director and especially for allowing me to finish this project in a more relaxed and focused way.
My Committee experts, Prof. Nicole Déglon and Prof. Geneviève Gourdon, offered me the opportunity to have great scientific discussions and feedbacks. I always left our meetings with a big smile, satisfaction and new ideas in mind, thanks for your supportive comments.

I would like to thank all the collaborators that took part to my PhD project.
Prof. Vanessa Wheeler gave me the opportunity to be hosted in her laboratory and work under her supervision. It was a great experience where I enriched my scientific knowledge and techniques.
Prof. Beverly Davidson and Dr. Alejandro Monteys took part in this project and I am really happy I could visit and experience the great team and science they are doing. Particularly I would like to thank Alejandro for the nice conversations we had and the warm welcome I received in Philadelphia from the entire research team.
I had the pleasure to work under the supervision of Prof. Geneviève Gourdon. I had a really enriching experience working with her team, scientifically and personally. I really felt part of a big family fighting for the same goal. I would like to particularly mention Stephanie for being so supportive and a great friend since the first minute I joined the team. Many thanks to Aline, who patiently taught me so many new things, French included! Thank you to Antoine, my exchange-lab buddy, for your smile and our chats.

The Dion's team has been my family for 5 years and I couldn't have asked for more. We have been a great group, and the amazing memories and time spent together is an indelible record in my mind. The coordination and support from every single member brought everyone's project to success. I am glad I could be part of this team during these years, allowing me to grow up in many aspects to a better me.

Thank you to Lorène, without whom our life in the lab would have not been the same. Lorène patiently answered all my doubts, helped me in many experiments and was a supportive voice during dark days when nothing was working.
Bin has been a great colleague and my best friend. I will always be thankful for her presence and support. Thank you for being a great listener and sharing dreams with me.
Thank you to Gustavo and Oscar without whom the lab's vibe wouldn't be so much fun.
Nathalie has been the angel, saving me from many paper work headaches. Thank you for the great time we spent together, in and outside of the lab.

If I am here I mostly owe it to my parents, without whom I couldn't have afford any of this, career and life achievements, surprising myself solving any issue I faced. Thank you for believing in me, following me in my decisions and never discouraging me.

I would never stop thanking my friends, who made my life in Lausanne, Boston and Paris a great experience. I need to thank my three first supporters, Patrick, Andrea and Matteo who have always found a way to put a smile on my face, even during difficult moments. Thank you for the really inspiring conversations and for pushing me to do better.
Alessia has been my conscience and my bravery at the same time. Thank you for being present and for all the sweet and revealing words.
I cannot forget to mention the person who helped me when I was on the other side of the ocean and believed in me without really knowing each other: Maria. Thank you for your help, for our chats and for our great friendship.

Abstract

Expanded trinucleotide repeats (TNRs) are responsible for at least 20 neurological, neuromuscular, and neurodegenerative diseases, 14 of which are caused by CAG/CTG repeats. No effective therapy has been found yet. Since repeat expansions induce the onset and are thought to precipitate pathogenesis, contractions to a normal size may alleviate the symptoms. Unfortunately, there is currently no efficient way to induce specifically contractions. As a therapeutic approach, here I tested whether engineered nucleases, specifically (Zinc Finger Nucleases (ZFNs) and CRISPR-Cas9, can induce contractions in expanded CAG repeats. Using a GFP reporter assay, I found that a ZFN and the Cas9 nuclease activity induced both contractions and expansions. Surprisingly, the nickase version of Cas9 (D10A) selectively induced repeat contractions. Moreover, ATR and ATM, two kinases involved in the DNA damage response, controlled the generation of contractions and expansions induced by the nickase. We proposed a model in which DNA gaps created by the nickase lead to contractions. Therefore, my results show that contraction bias is possible in human cells. Cas9 nickase showed repeat contractions events in patient-derived cells for Myotonic Dystrophy type 1 (DM1) and Huntington's Disease (HD). Since gene therapy holds the promise for curing genetic disorders, a viral vector has been tested as delivery tool for Cas9 nickase. It is also not clear whether delivery of Cas9 nickase with a gene therapy approach can result in contraction events and reversion of pathogenic phenotypes in affected tissues. We injected Adeno-associated Viruses (AAVs) expressing the Cas9 nickase and a gRNA against the repeat tract into DM1 and HD mouse models. I started to assess whether this treatment induces repeat contractions and reversion of pathogenic phenotypes *in vivo*. This Cas9 nickase-based gene therapy approach remains to be optimized to develop an efficient therapeutic tool. Nevertheless, my work has opened the door towards a novel therapeutic avenue for 14 different expanded TNR disorders.

Sommaire

Les répétitions trinucléotides expansé (TNR) sont responsables d'au moins 20 maladies neurologiques, neuromusculaires and neurodégénératives, de les quelles 14 sont causée par répétitions de CAG/CTG. Aucune thérapie efficace n'a été trouvée. De nombreuses études sont en cours mais aucune n'est dirigés directement sur la cause de la maladie: la répétition CTG étendu. Depuis qu'on sait que les expansions de répétition induisent l'apparition de phénotype pathogène, il a été proposé que les contractions de longues répétitions en dessous de la longueur limite pourraient soulager les symptômes. Mais pour le moment il n'existe actuellement pas de moyens efficaces pour induire spécifiquement les contractions de répétitions. Avec le bout de développer un traitement thérapeutique, ici J'ai testé si l'ingénierie nucléases, comme ″Nucléase à doigt de zinc″ (ZFN) et CRISPR-Cas9, peuvent induire des contractions spécifiquement dans répétitions de CAG expansés. Dans un dosage de GFP sur un système cellulaire, les ZFN et Cas9 nucléase introduisent des contractions et expansions de répétitions. Différemment, Cas9 nickase (D10A) qui crée des nick dans l'ADN introduise des contractions dans les répétitions. ATR et ATM, deux kinases qui font part de mécanisme de réponse après dommage dans l'ADN, contrôlent la génération des contractions et expansions. Nous proposons un modèle dans lequel des gaps de ADN crées par l'activité du nickase produite des contractions des répétitions. Donc, mes résultats montrent qu'induire des contractions est possible dans des cellules humaines.

Pour mieux comprendre si Cas9 nickase peut vraiment être un traitement pour des maladies causés par the répétitions expansés, nous avons testé le nickase sous des modèles des maladies. Avec l'utilise des lentiviruses, nous avons exprimés Cas9 nickase dans des cellules de patinent affecté par la Dystrophie Myotonique type 1 (DM1) and la maladie de Huntington (HD). Cas9 nickase a montré sa capacité d'induire contractions des répétitions déjà dans 3 jours d'activité avec une gRNA pour les répétitions de CAG/CTG. Pour tester si l'utilise des virus peut être un

moyen efficace pour la livraison de Cas9, la méthode de thérapie génique a été testé. Nous avons produit des AAV qui expressent Cas9 nickase et log RNA, et des souris modèl pour DM1 et HD ont été injecté. Malheureusement, il n'est pas encore possible d'avoir une conclusion à propos de l'efficacité de Cas9 nickase dans le modèle de souri pour DM1 et HD. Évaluation de capacité Cas9 nickase en reversant les symptômes pathogéniques est une important resultat pour développer un traitement efficace. Les résultats de ce projet vont élever les connaissances sur les désordres du TNR, spécifiquement l'efficacité des Cas9 nickase dirigées vers TNR comme des traitements thérapeutiques.

List of Abbreviations

AAV	Adeno-associated virus
ALS/FTD	Amyotrophic lateral sclerosis/frontotemporal dementia
CANVAS	Cerebellar ataxia neuropathy bilaterlal vestibular areflexia syndrome
CELF1	CUGBP1/Elav-like family protein 1
CRISPR-Cas9	Clustered regularly interspaced short palindromic repeats-associated Cas9
dCas9	Catalytic dead Cas9
DM1	Myotonic Dystrophy type 1
DMPK	Myotonic dystrophy protein kinase
DRPLA	Dentatorubral-pallidoluysian atrophy
DSB	Double strand break
EPM1	Unverricht-Lungborg Disease
FECD	Fuchs endothelial Corneal Dystrophy
FRAXE MR	Fragile XE syndrome
FRDA	Friedreich's ataxia syndrome
FRT	Flippase recognition target
FXPOI	Fragile X associated primary ovarian insufficiency
FXS	Fragile X syndrome
FXTAS	Fragile X-associated tremor/ataxia syndrome
GFP	Green Fluorescent Protein
gRNA	Single Guide RNA
HD	Huntington Disease
HDL2	Huntington disease-like 2 syndrome
HR	Homologous recombination
HSA	Human skeletal actin
iPSCs	Induced Pluripotent Stem Cells
IR	Insulin receptor
LCLs	Lymphoblastoid cell lines
MBNL1	Muscle blind-like 1
NHEJ	Non-homologous end joining
nmCas9	*Neisseria meningitidis* CRISPR-Cas9
PAM	Protospacer adjacent motif
PCR	Polymerase chain reaction
qPCR	Quantitative PCR
RNPs	Ribonucleoproteins
saCas9	*Staphylococcus aureus* CRISPR-Cas9
SBMA	Spinal and bulbar muscular atrophy
SCA	Spinocerebellar ataxia
SNPs	Single nucleotide polymorphisms
SP-PCR	Small-Pool PCR

spCas9	*Streptococcus pyogenens* CRISPR-Cas9
TALEN	Transcription activator-like effector nuclease
TNR	Trinucleotide repeat
UTR	Untranslated region
WB	Western Blot
ZFN	Zinc-finger nuclease

Table of Contents

List of Figures

List of Tables

Chapter I

Introduction

I.I Trinucleotide repeat disorders

Repetitive sequences are commonly present in the human genome at different locations. Expansions of short repeats are responsible and associated with numerous neurological diseases (Gomes-Pereira, Cooper, and Gourdon 2011a; Ami Mankodi et al. 2000; Orr and Zoghbi 2007a; Zhao and Usdin 2015) (Table I.I.1), 14 of them are caused by expanded CAG/CTG trinucleotide repeats (TNRs) (López Castel, Cleary, and Pearson 2010). In different disorders, the expanded repeat tract is located in distinct loci. The nature of the pathogenic symptoms and the affected cellular functions is determined by the expanded repeat locus. Since expanded CAG/CTGs are the most common repeat units causing diseases, in this study I focused on CAG/CTG disorders, such as Myotonic Dystrophy type 1 (DM1) and Huntington's disease (HD).

CAG/CTG TNRs present in unaffected people are short, generally less than 30 units. When TNRs expand over a threshold of 35 repeats – this exact number depends somewhat on the disorder – they become highly unstable leading to the appearance of the pathogenic symptoms. The repeat length in patients is directly correlated with the severity of the symptoms (Holmans, Massey, and Jones 2017; Pešović et al. 2017) and determines much of the variation in the onset age, which can vary from childhood to late onset. Affected families display anticipation, a phenomenon characterized by repeat expansion events and increased disease severity over generations, as evidenced by an earlier age of onset (Cynthia T. McMurray 2010; Mirkin 2007).

Table I.I.1 TNR disorders. Adapted from Zhao and Usdin 2015, Cortese et al. 2019.

Disease	Repeat unit	Gene	Normal repeat	Expanded repeat	Repeat location
DRPLA	CAG	*ATN1*	7-35	49-93	Exon
HD	CAG	*HTT*	9-35	36-121	Exon
SBMA	CAG	*AR*	9-34	38-62	Exon
SCA1	CAG	*ATXN1*	6-42	39-83	Exon
SCA2	CAG	*ATXN2*	14-31	32-200	Exon
SCA3	CAG	*ATXN3*	12-44	52-86	Exon
SCA6	CAG	*CACNAIA*	4-18	21-33	Exon
SCA7	CAG	*ATXN7*	4-35	37-306	Exon
SCA12	CAG	*PPP2R2B*	7-28	55-78	5'UTR
SCA17	CAG	*TBP*	25-42	45-66	Exon
DM1	CTG	*DMPK*	5-38	>50	3'UTR
FECD	CTG	*TCF4*	10-37	>50	Intron
HDL2	CTG	*JPH3*	6-28	40-59	3'UTR
SCA8	CTG	*ATXN8*	16-34	>74	3'UTR
FRA7A	CGG	*ZNF13*	5-22	68, 72, ~450	Intron
FXPOI	CGG	*FMR1*	<55	55-200	5'UTR
FXTAS	CGG	*FMR1*	<55	55-200	5'UTR
FXS	CGG	*FMR1*	<55	>200	5'UTR
FRAXE MR	GCC	*AFF/FMR2*	6-25	>200	5'UTR
FRDA	GAA	*FXN*	8-33	>90	Intron
DM2	CCTG	*ZFN9*	<30	75-11000	Intron
SCA10	ATTCT	*ATXN10*	9-32	800-4500	Intron
CANVAS	AAGGG	*RFC1*	NA	NA	Intron
SCA36	G_2C_2TG	*NOP56*	3-8	1500-2500	Intron
ALS/FTD	G_4CC	C9orf72	2-22	700-1600	Intron
EPM1	C4GC4GCG	CSTB	2-3	30-78	Promoter

Myotonic Dystrophy type 1

DM1 is the most common adult form of muscular dystrophy (Gourdon and Meola 2017). It is an autosomal dominant multisystemic disorder characterized by myotonia, muscle weakness and wasting, cataracts, and by defects in cardiac conduction (Gomes-Pereira, Cooper, and Gourdon 2011b; A Mankodi 2000; Udd and Krahe 2012a). It is categorized as a rare disorder and has a frequency of 1 case in a population of 8000 (Hammans 2002). It exists in 4 different forms which differ in the underlying repeat lengths leading to different ages of onset: congenital, childhood-onset, adult-onset and late onset oligosymptomatic (Udd and Krahe 2012b).

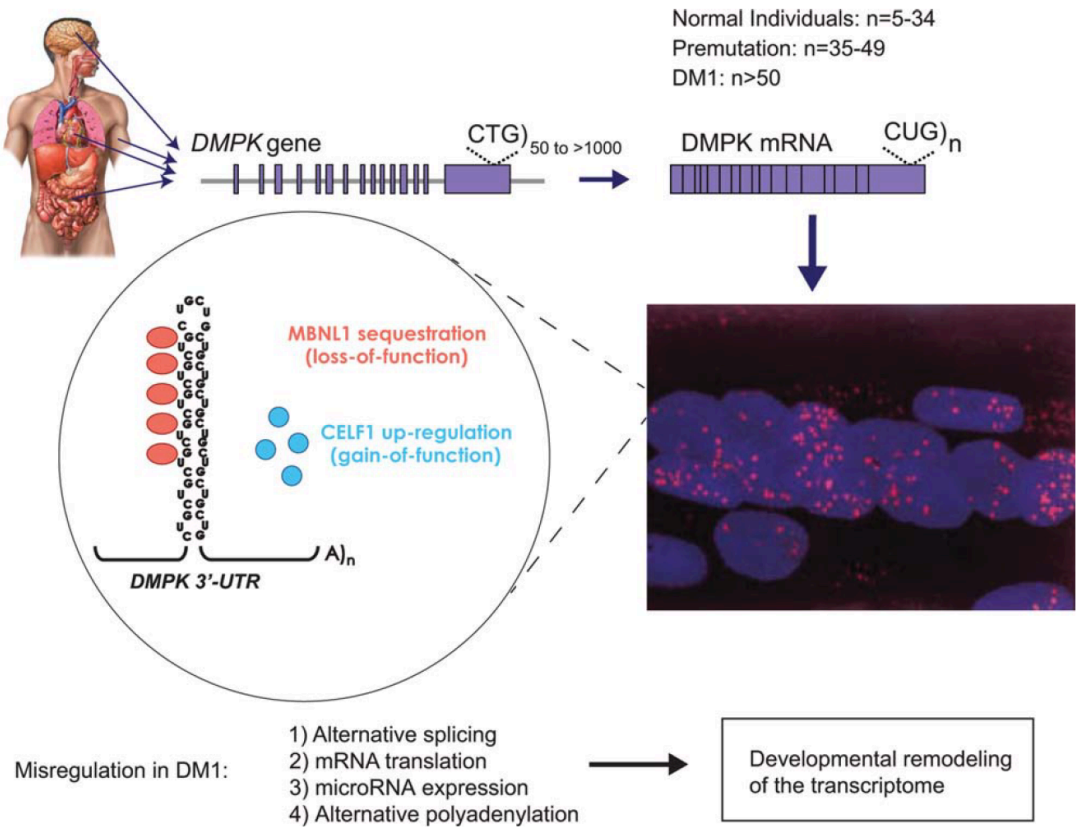

Figure I.I.1 Model of DM1 cellular pathogenesis induced by expanded CTG repeats in *DMPK* gene.
Expanded CTG repeats in DMPK gene affect multiple tissues: brain, heart, skeletal muscles. CUG hairpins in the DMPK mRNA lead to the formation of nuclear foci alterning the right metabolism of the cells. The sequestration of MBNL1 and up-regulation of CELF1 induce affected splicing regulation of targeted genes and developmental remodeling of the transcriptome (Chau and Kalsotra 2015).

DM1 is characterized by a toxic RNA-mediated gain of function mechanism. The presence and expression of an expanded CTG repeat localized in the 3'UTR of the myotonic dystrophy protein kinase (*DMPK*) gene, located on chromosome 19, is sufficient to induce DM1 pathogenesis (Figure I.I.1) (A Mankodi 2000). The expanded CUGs in the *DMPK* mRNA fold into hairpin-like structures and interact with proteins forming aggregates inside the nucleus. This leads to the direct sequestration of muscleblind-like 1 protein (MBNL1) and by consequent stabilization of CUGBP/Elav-like family protein 1 (CELF1). The imbalance of these two antagonistic splicing regulators induces the dysregulation of several muscle-specific genes, such as chloride channel (*CLC1*), bridging integrator 1 (*BIN1*), insulin receptor (*IR*), and others. This in turn produces the DM1 pathogenic phenotype in central nervous system, heart and skeletal muscles (G.-S. Wang et al. 2007; Hernández-Hernández et al. 2013).

Currently there is no cure available for this disorder. Medications helping affected patients are aimed to alleviate the motor impairments: physiotherapy and specific drugs, such as mexiletine, an anti-myotonia treatment (Logigian et al. 2010), and anti-inflammatories to manage muscle pain. Psychiatric support is also needed. The direct action on the ultimate cause of these disorders, the expanded repeats, can be the winning approach to definitely reverse the pathogenic symptoms.

Huntington's Disease

George Huntington described HD for the first time as an inherited neurodegenerative disorder mainly causing symptoms such as chorea, depression, and memory deficits (Huntington 1872; Orr and Zoghbi 2007b). HD is an autosomal dominant disorder and manifests at different ages and with different severity based largely on the size of the repeat tract (Holmans, Massey, and

Jones 2017). The frequency rate is 1 in 7000 individuals in Western countries (Rawlins et al. 2016).

The expanded CAG repeat is located in the first exon of the Huntingtin gene (*Htt*) in chromosome 4. Th repeat size ranges in 36-121 units in the affected patients (Group 1993). As a gain-of-function pathogenic mechanism, the expanded CAG repeats translate into long polyglutamine tract that causes protein misfolding and aggregate formation. These inclusion bodies in neural cells are characteristic of neurodegenerative diseases. Mutated huntingtin proteins accumulate and result in neuronal dysfunction and neurodegeneration (Orr and Zoghbi 2007b; Saudou et al. 1998). Although the *HTT* gene is ubiquitously expressed, HD pathology develops only in distinct brain areas, particularly in the striatum.

Similar to DM1, no drug has been found for patients that definitely cure HD yet. Medical treatments to reduce movement impairment symptoms, such as Tetrabenazine, are the only solutions available at the moment (Yero and Rey 2008). Psychiatric support is also necessary to help patients against psychosis.

Treating expanded CAG/CTG repeat disorders

To date, there is no effective therapy for expanded TNR disorders but some potential strategies of therapeutic interventions have been expressed. The most promising approaches in a clinical point view are aimed in targeting mRNA or DNA of the mutant allele. Targeting of the mRNA can be achieved by antisense oligonucleotides (ASOs), RNA interference (RNAi) or chemical inhibitors. ASOs are synthetic nucleotide molecules that bind pre-mRNA and induce degradation by RNase H in the nucleus. ASO targeted against the CUG repeat in *DMPK* mRNA has been shown to be successful in alleviating DM1 cellular symptoms (Johanna E. Lee, Bennett, and Cooper 2012). Lee et al. were able to induce RNase-H mediated degradation of

CUG-repeat transcript in DM1 cell lines and transgenic mice. They found gapmers able to specifically disrupt the RNA foci formed by the pathological *DMPK* transcripts and MBNL1 (J. E. Lee, Bennett, and Cooper 2012). Similar therapeutic strategy has been found by other teams where silencing of the expanded *DMPK* transcript reduced foci accumulation and DM1 symptoms (Mulders et al. 2009; Furling et al. 2003). Silencing of the mutant allele with ASOs has also been shown to be successful in HD models (J. B. Carroll et al. 2011; Kordasiewicz et al. 2012; Drouet et al. 2009). The reduction of mutant HTT presence by ASOs reversed motor coordination in HD mouse models (Kordasiewicz et al. 2012). Kordasiewicz et al. injected *HTT* targeted ASOs into cerebrospinal fluid of BACHD mice and *HTT* mRNA degradation resulted in delayed disease progression and improvement of motor deficits. Similar improvement of HD pathology has been observed by Drouet et al. Moreover, they showed that silencing of *HTT,* non-allele dependently, did not induce deleterious toxicity in striata cells (Drouet et al. 2009).

Another study approach is to induce the degradation of the expanded repeats mRNA with synthetic RNAi molecules. Differently from ASOs, RNAi works on mature mRNA and triggers its degradation in the cytoplasm. In an *in vivo* study, synthetic siRNA targeting the CUG^{exp} RNA was injected into the muscles of HSA^{LR} mice (Sobczak et al. 2013). Treated mice showed reduced ribonuclear foci and CUG transcript levels. Moreover, they exhibited almost complete reversion of aberrantly spliced transcript as well as of the myotonia. RNAi approach has also been tested in HD mouse model where AAV delivered shRNA targeted to *HTT* mRNA. Reduced *HTT* expression by shRNA activity resulted in improved pathological and behavioral features (Harper et al. 2005).These are promising results that require further insights to exclude possible off target effects, which are common in siRNA approaches.

The steric inhibition of interaction between the mutant mRNA and interacting protein has been the basis of small molecules-based strategies. A methylene linker that prevents the binding

between expanded CUG repeats and MBNL1, has been proposed by Coonrod et al. as therapeutic small molecule against DM1. The administration of heptamidine to mice model for DM1 also reversed splicing defects and reduced significantly myotonia (Coonrod et al. 2013). Other small molecules have shown positive results or are ongoing in ameliorating DM1 and HD symptoms (García-lópez et al. 2011; Warf et al. 2009; E M Doherty 2017).

All these approaches, which would hopefully alleviate the phenotype in patients, need to be administrated for long periods. Unfortunately, prolonged administration could increase toxicity, already generated by low specificity, resulting in a not optimal solution for affected patients.

I.II CAG/CTG instability and pathogenesis

The primary cause of the TNR disorder symptoms is the presence of a long repeat tract, characterized by high instability and frequency of expansion and contraction events. The longer the repeat tract is, the more unstable the repeats are. TNR instability results from multiple mechanisms related to DNA metabolism, concerning processes such as DNA repair, replication and transcription (Pearson, Nichol Edamura, and Cleary 2005; Moss et al. 2017; Bettencourt et al. 2016; J.-M. Lee et al. 2015). TNR expansions vary in different disorders and from tissue to tissue (Dion 2014). Due to their propensity to form non-B DNA structures, long TNRs tend to be highly unstable, leading to expansions and contractions (Kohwi, Wang, and Kohwi-Shigematsu 1993; Marquis Gacy et al. 1995; Axford et al. 2013; Lin et al. 2010; López Castel, Cleary, and Pearson 2010). These unusual structures are recognized as damaged DNA and are processed aberrantly due to their repetitive nature. Moreover, these structures interfere with proper DNA repair in cis. Thus, the longer the repeat tract is, the more unstable it becomes, establishing a positive feedback loop in which expansions induce more expansions (C. T. McMurray 2011).

Somatic instability plays an important role in the disease progression, as shown by studies in HD mouse models where somatic instability correlated with disease progression (Kennedy and Shelbourne 2000; Kumar et al. 2016, 201; Kielar and Morton 2018; Huguet et al. 2012). In fact, Wheeler et al. confirmed this hypothesis by showing the stabilization of CAG repeats in an *in vivo* model for HD induced by the complete lack of Msh2, which is essential for DNA mismatch repair (Wheeler et al. 2003; Kovalenko et al. 2012). Moreover, Msh2 deficiency delayed the accumulation of mutant huntingtin in the nucleus and, thus, the onset of the disease (Wheeler et al. 2003). This was in line with previous studies showing a central role of Msh2 in

promoting repeat expansion (Wheeler et al. 2003; Broek et al. 2002; Tomé et al. 2009; C. Savouret et al. 2004; Â. Savouret et al. 2003; Manley et al. 1999; Kovtun, Thornhill, and McMurray 2004; Kovtun and Mcmurray 2001). This and other subsequent studies suggest that somatic repeat instability greatly influences disease progression.

Since disease onset and progression is affected by repeat size and instability, variations in repeat size could impact and reverse pathogenesis. Reversion of DM1 and HD pathogenic symptoms has already been shown to be possible in different models (Yamamoto, Lucas, and Hen 2000; Díaz-Hernández et al. 2005; Garriga-Canut et al. 2012; Mahadevan et al. 2006a; S. Yang et al. 2017). The induction of repeat contraction by using pharmacological stabilizers of repeats or genetic modifications, such as gene silencing, could lead to the alleviation of pathological symptoms by removing the underlying cause of the disease. Mahadevan et al. developed a mouse wherein the overexpression of a normal *DMPK* 3‘UTR linked to a GFP sequence led to the generation of some of the main DM1 symptoms. Shutting off the expression of this transgene, alleviated the myotonia, cardiac conduction abnormalities, histopathology, RNA splicing defects, and nuclear inclusion disappeared in skeletal and cardiac muscles (Mahadevan et al. 2006b). Similarly, in multiple studies repression of *HTT* expression corrected behavioural symptoms and molecular pathogenesis in HD mouse models (Díaz-Hernández et al. 2005; Yamamoto, Lucas, and Hen 2000; Garriga-Canut et al. 2012). In fact, the silencing of the mutant *HTT* gene reversed the cellular phenotype in HD mouse models (Yamamoto, Lucas, and Hen 2000; Díaz-Hernández et al. 2005). This mouse model carries a tetracycline-inducible promoter that activates/deactivates the expression of a truncated N-terminal *HTT* sequence with 94 CAGs. The expression of this truncated *HTT* led to neuropathology, such as Htt aggregate formation, small brain size, and behavioral deficits. Blocking transgene expression by doxycycline administration reversed aggregate formation and motor dysfunction (Yamamoto, Lucas, and Hen 2000). Even more, the excision of repeats

in a mutant *HTT* allele induced by Clustered regularly interspaced short palindromic repeats Cas9 (CRISPR-Cas9) combined with two gRNAs resulted in gene silencing. Consequently, transcription blockade led to attenuated neuropathology in this HD mouse model (S. Yang et al. 2017). Thus, reversibility of DM1 and HD pathogenic phenotypes is possible and targeting the expanded repeats could be a successful strategy to tackle expanded TNR disorders.

Even if more than 25 years have passed since the discovery of the expanded repeat toxicity in TNR disorders, no cure has been developed yet. Finding a tool able to contract repeats and alleviate pathogenic symptoms is a challenge. Thus, we decided to tackle this question and investigate how to specifically induce contractions using gene editing techniques.

A requirement to recognize which specific players affect TNR instability is a system in which instability can be directly traced. Understanding how repeat contractions, without concomitant expansions, can be produced is important to develop efficient therapeutic approaches to tackle TNR disorders. Since a long time, many research teams are working on better understanding the mechanisms of repeat instability. There have been studies aiming at inducing repeat contractions specifically. Most of these are focused on the induction of DNA damage, specifically double-strand breaks (DSBs) within or near the repeat tract (G. F. Richard, Dujon, and Haber 1999; B. a Santillan et al. 2014; Mittelman et al. 2009a). Different techniques have been used to measure the ability of different tools in inducing repeat instability. Small-Pool PCR (SP-PCR) and sequencing are the most used techniques to determine repeat instability at the moment (Monckton et al. 1995; Dandelot and Gourdon 2018; Mangiarini et al. 1996; Aeschbach and Dion 2017). Specifically, SP-PCR consists in the amplification of only few alleles per reaction through big dilutions of genomic DNA. An electrophoresis run followed by a southern blot, due to the low DNA quantity, are the fundamental steps that allow to

visualize repeat instability in SP-PCR (Monckton et al. 1995; Aeschbach and Dion 2017). However, these available assays hide weak points that slow down the understanding of repeat instability dynamics and the discovery of tools capable of specifically inducing repeat contractions. In fact, these techniques are time consuming and show lack in sensitivity. The development of new reporters able to measure repeat instability efficiently is fundamental for the discover of therapeutic tools for expanded TNR disorders.

In 2003, a new cell line reporter for repeat instability detection was developed. This selectable chromosomal reporter allowed to determine repeat size variations in CHO cells (Gorbunova et al. 2003). The integrated *APRT* mini gene and *HPRT* transgene have been modified to carry an intron containing a CAG repeat tract. In the presence of long repeat tracts, the CAGs enhance the inclusion of the repeat itself into an alternative exon, leading to loss of the APRT function (Gorbunova et al. 2003). By selecting for $APRT^+$ and $HPRT^+$ cells, large contraction events can be measured in the surviving colonies. This system allows test of experimental treatments, such as DNA plasmid transfection and selection of repeat contraction inducers in mammalian cells (Mittelman et al. 2009b; Lin, Dion, and Wilson 2005). Unfortunately, the sensitivity of this reporter is limited to large repeat contraction events and is blind for expansions.

In 2014, a new instability assay was presented by John Wilson's group (B. A. Santillan et al. 2014). They showed the ability of a new reporter in measuring repeat instability by detection of GFP fluorescence intensity expressed in mammalian cells. A single copy of a GFP mini gene carrying a CAG repeat sequence was integrated into the genome of HEK 293 T-Rex Flp-In cells. The GFP sequence is divided in two exons by an intron within which a CAG repeat tract is present. The shortening of the repeat tract results in stronger GFP expression in these cells. Similar to the *APRT* and *HPRT* systems, expanded CAG repeats affect the correct splicing of GFP mRNA, resulting in a reduction of GFP levels. Thus, GFP intensity inversely correlates

with repeat size and fluorescence can be easily measured by flow cytometry. Repeat size variations can then be determined by single cell sorting of different population based on GFP intensity and measured by sequencing. This method has a straightforward readout, since within 5 days it is possible to measure the effect of a treatment on repeat instability. Santillan et al. were able to detect only repeat contraction events (B. A. Santillan et al. 2014). However, in our study, we show that both repeat expansions and contractions can be detected after treating this GFP$(CAG)_{101}$ cell line with engineered nucleases (Cinesi et al. 2016). These results confirmed the GFP reporter as the first chromosomal mammalian assay able to detect contractions and expansions in a CAG/CTG repeat tract within 5 days. The GFP$(CAG)_x$ cell lines were used in Chapter 2 to determine the ability of different treatments to induce repeat contractions.

I.III Genome editing

Genome editing consists of using engineered nucleases to target specific genomic sites and to trigger DNA sequence mutations (Chen et al. 2007). These nucleases induce DNA modifications, such as deletions, insertions, or replacements (Figure I.III.1). After specific site recognition, they cause a double-stranded break (DSB) that induces the activation of endogenous DNA repair mechanisms, such as non-homologous end joining (NHEJ) and homologous recombination (HR). NHEJ involves the joining of the DNA ends of the DSB without a homologous template to direct the repair. This process is often error-prone and can induce deletions and frameshifts. HR, on the other hand, uses a homologous sequence to regenerate the missing DNA sequence for HR and is usually error-free. Providing an ectopic template can be used to introduce specific mutations to an endogenous locus.

Genome editing has been optimized and used more and more during the last 30 years. ZFNs, Transcription Activator-like Effector Nuclease (TALEN) and the CRISPR-Cas9 are the main tools used in genome editing (H. Kim and Kim 2014).

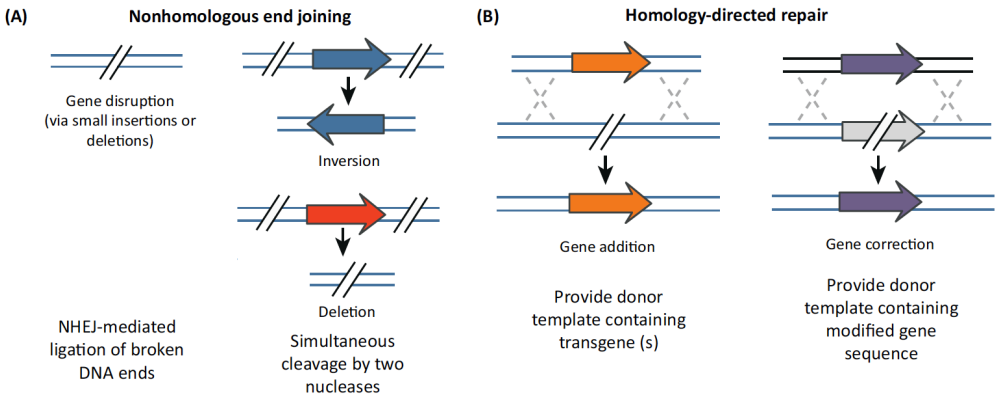

Figure I.III.1 Genome editing induced by engineered nucleases.
A) Activation of NHEJ mechanism induced by presence of DSB leads to 3 different possible results. Generation of a DSB can result in deletions or small insertions at the damaged locus leading to the disruption of the target gene. Alternatively, generations of two DSBs proximal to each other can result in either inversion of the excised sequence or deletion of it. B) HR is activated in presence of a donor double stranded DNA carrying a homologous sequence. Addition of a sequence or correction of a possible mutation are the possible results (Gaj, Gersbach, and Barbas 2013).

Zinc Finger Nucleases

ZFNs constitute the first generation of customizable DNA binding domains fused to a nuclease harnessed for the manipulation of animal and plant genomes (Y.-G. Kim, Cha, and Chandrasegaran 1996). They are composed of two different domains: the DNA-binding domain (DBD) and the DNA-cleavage domain (Figure I.III.2). The DBD has generally three zinc fingers that recognize the target site in the genome, binding a specific DNA sequence. Every zinc finger recognizes and binds 3 nucleotides. For increased sequence specificity, multiple zinc fingers are linked to each other for a recognition sequence of generally 9 to12 bp (Figure I.III.2) (Segal et al. 1999). The catalytic domain is a restriction enzyme, FokI, that induces a DSB at the target locus (Dana Carroll 2008; Cathomen and Joung 2008a). To trigger the nuclease activity at a specific locus, two ZFN arms have to recognize and bind to their complementary sequences. This allows FokI dimerization, thereby creating a DSB within a 5 bp spacer sequence (Christian et al. 2010; Dana Carroll 2008; Cathomen and Joung 2008a).

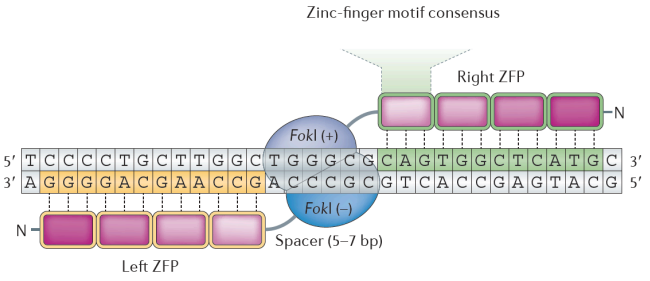

Figure I.III.2 Representation of ZFNs heterodimerization (H. Kim and Kim 2014).

ZFNs have been tested to correct and treat specific genetic disorders. For instance, their application has shown potential in preventing AIDS (Perez et al. 2008a). A deletion in a chemokine receptor gene, CCR5, is associated with HIV infection resistance (Perez et al. 2008b). Perez et al. were able to target the ZFNs to the human CCR5 gene with the use of adenovirus, and induce a deletion at this locus with a frequency of 50% in human $CD4^+$ T cells. Furthermore, with the use of a DNA donor, ZFN-mediated editing can lead to the insertion of a specific sequence, through the activation of HR (Moehle et al. 2007).

Even if ZFNs can efficiently target a specific locus, this method has a major limitation: off-target activity. Caused to the presence of repetitive sequences in the whole genome similar to the targeted one, ZFNs induced a high frequency of off-target mutations (D Carroll 2008; Cathomen and Joung 2008b). This is a significant risk factor when applied to clinical attempts. In fact, off-target events can generate additional mutations and clinical side effects (Pattanayak et al. 2011). Variable quantities of ZFNs can also induce off-target events since strong presence of this molecule reduces the cleavage specificity (Mussolino and Cathomen 2011; Pattanayak et al. 2011; Gabriel et al. 2011). Further optimizations of different variables of ZFN mechanism of action and administration are necessary to achieve a safe and precise standard for clinical use.

ZFNs have previously been designed and tested on CAG/CTG repeats (Mittelman et al. 2009b). Mittelman et al. used *APRT* and *HPRT* selection assays. Transfection of ZFNs showed increase in contractions in human and CHO cells. Long repeat tracts appeared also to be a better target for ZFN binding and cutting resulting in activity with higher rates of contractions, 7-10 fold increase, compared to shorter repeat tract, 2 fold increase (Mittelman et al. 2009b). Thus, ZFNs showed specificity in inducing DSBs and contraction events for expanded repeat sizes, such as patient mutant alleles, compared to WT allele sizes. Thus, ZFNs induced repeat contractions in human and CHO cells, but their contribution to expansions was unknown.

The role of ZFNs in inducing repeat contractions was successively confirmed in GFP reporter described above (B. A. Santillan et al. 2014). Transfection of ZFNs into this system showed a 10-fold increase in the number of cells with contracted repeats. However, only contraction and deletion events were observed (B. A. Santillan et al. 2014). Mittelman et al. and Santillan et. al. detected only repeat contractions, not measuring other events induced by ZFN activity. We optimized the GFP assay and observed that ZFN transfection induced repeat instability,

resulting in both contractions and expansions. These results are shown in Chapter II (Cinesi et al. 2016).

TALEN

A second family of engineered nucleases, broadly used in many different organisms, is TALEN. Similar to ZFNs, TALENs are formed by a DNA-cleavage domain, FokI.

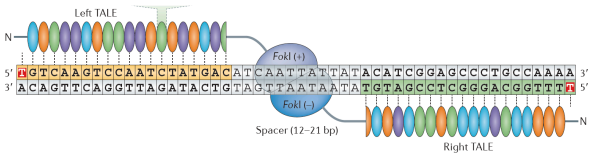

Figure I.III.3 Representation of TALEN dimerization and binding on a target DNA (H. Kim and Kim 2014)

However, the DNA binding domain specifically designed to recognize the target locus, is based on transcription activator-like effectors (TALEs), originally from the plant pathogen *Xanthomonas* bacterium (Cermak et al. 2011). They are constituted of a tandem of repeats of 33 to 35 amino acids. The specificity for the target site is established by two amino acids in position 12 and 13 that allow the recognition of a specific base-pair (Boch et al. 2009; Moscou and Bogdanove 2009). The heterodimerization of the two complementary monomers is necessary to induce the formation of DSBs (Figure I.III.3) (Beumer et al. 2013).

CAG repeat contractions with TALENs were observed in yeast (G.-F. Richard et al. 2014b; Mosbach et al. 2018). In this genomic assay, the intron present within the SUP4 gene has been replaced by 30-75 CAG/CTG repeats. The effect of TALENs designed to recognize and induce DSBs within the repeat sequence was tested. In homozygous yeast diploid cells, TALEN activity resulted in repeat contractions below the pathogenic threshold with 100% efficacy (G.-F. Richard et al. 2014b). Moreover, deep-sequencing of surviving yeast colonies revealed no off target mutations induced by TALENs (G.-F. Richard et al. 2014a). These results are promising as they could form the basis for new therapeutic treatment against TNR disorders.

Compared to ZFNs, TALENs have several advantages: longer recognition site for higher specificity, easier construction, less toxicity-related cell death, and higher on-target success

rate (Beumer et al. 2013). However, a new engineered nuclease has been developed in the last 5 years, with more promising results and an easy-to-design system: CRISPR-Cas9.

CRISPR-Cas9

CRISPR-Cas9 is the most recently developed and widely used engineered nuclease. CRISPR system was firstly discovered and described by Nataka and his team in 1987 as 30 bp palindromic repeats divided by 36 bp spacer genomic sequences present in *E.coli* (Ishino et al. 1987). In 2002, due to its repetitive structure it has been named clustered regularly interspaced short palindromic repeats (Jansen et al. 2002). These sequences were successively recognized as being of viral origin and were described as the bacterial and Archaea's immune system against viral infection (Mojica et al. 2005). In 2008, John Van Der Oost and colleagues described this adaptive immune system as composed by a Cas9 nuclease and a small RNA (crRNA) complementary to the viral DNA sequence, necessary to target the invader genome (Figure I.III.4) (Brouns et al. 2008). Once the organism survived a bacteriophage infection, bacteria store part of the foreign DNA in protospacers that will be subsequently transcribed into RNA and used to recognize and cleave invader DNA with the help of the cas endonuclease protein. In addition to the crRNA, a second RNA molecule is necessary for the CRISPR system to be efficient: the trans-activating CRISPR RNA (tracrRNA) (Deltcheva et al. 2011). The two RNA components can be fused in one single synthetic guide RNA (gRNA) as shown successively by Charpentier and Doudna, thereby simplifying the system (Jinek et al. 2012b). In 2013, CRISPR-Cas9 was shown to efficiently edit human and mouse genomes thanks to the optimized design developed by Zhang and his team (Cong et al. 2013; Mali et al. 2013). This engineered nuclease is an efficient and versatile tool for genome editing for any target DNA sequence.

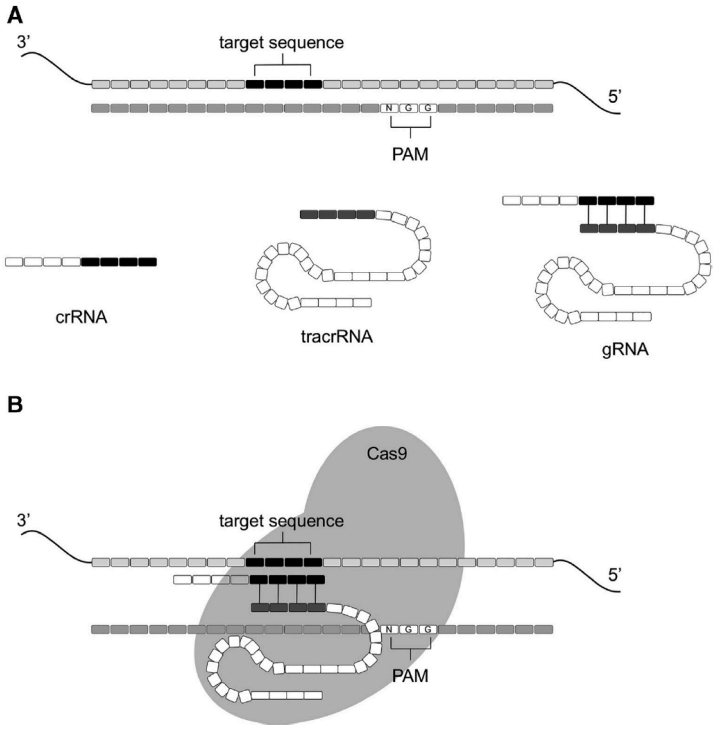

Figure I.III.4 The CRISPR-Cas9 targeting system.
CRISPR-Cas9 targets a nucleotide sequence present in the genome. On the conplementary strand upstream of the target, a specific PAM sequence needs to be present in order to activate Cas9 cleavage. gRNA is originally composed by 2 RNAs: crRNA and tracrRNA. The union of the two RNA form a gRNA that allowed the binding of Cas9 to the target DNA and DSBs induction (Memi, Ntokou, and Papangeli 2018).

Since its discovery, the CRISPR-Cas9 has been optimized to use a gRNA that recognizes and binds the complementary sequence forming a DNA-RNA hybrid. The specific binding recruits the Cas9 nuclease to the locus and induces a DSB (Jiang et al. 2013; Jinek et al. 2012a). The Cas9 protein needs the presence of a specific sequence downstream of the binding site defined as protospacer adjacent motif (PAM). For *Streptococcus pyogenes* Cas9, the PAM is usually 5'-NGG-3', that can vary, albeit with a reduced efficiency (Zhang et al. 2014).

Different successful studies are aimed to optimize this engineered nuclease efficiency and develop variations in CRISPR-Cas9 function. By mutating part of the nuclease domain, an inactivated form of CRISPR-Cas9 (dCas9) was developed. dCas9 binds to the target locus and can prevents transcription or protein interaction (Pinto et al. 2017). The fusion of dCas9 to specific protein can also be used to induce epigenetic variation at specific genomic sites.

By catalytically inactivating one of the two nuclease domains via point mutations, it was possible to turn the CRISPR-Cas9 nuclease into a DNA nickase (Cas9 nickase) (Cong et al. 2013). This Cas9 mutant is able to cleave only one of the two DNA strands, thus forming single-strand breaks. The Cas9 nickase used in this study carries an aspartate-to-alanine mutation (D10A) in its RuvC catalytic domain. Being formed by two separated genes, the Cas9 and the gRNA, allows easy adaptation and application for different designs. By simple cloning techniques, the Cas9 can be easily optimized for new purposes. Low costs and easy manipulation make the CRISPR-Cas9 a faster and better tool compared to the previous engineered nucleases (Gaj, Gersbach, and Barbas 2013).

CRISPR-Cas9 off targets

Engineered nucleases are known to induce off-target effects, and the Cas9 showed similar outcomes (Fu et al. 2013). Even if some studies confirmed undetectable off-targets induced by Cas9 activity (Cinesi et al. 2016; van Agtmaal et al. 2017; Monteys et al. 2017; S. Yang et al. 2017; Merienne et al. 2017), care should be taken before starting Cas9 clinical attempts. In fact, 20 nucleotides used to target the cleavage component to the locus, is an extreme small dimension and similar sequences can be found multiple times over the wide size of the eukaryotic genome, especially when targeted to repeat sequences. Even more, Cas9 binding tolerates a few mismatches in the target and PAM sequence, giving rise to possible off-target bindings (Fu et al. 2013). The off-target events constitute one of the major limitations for engineered nuclease for application in clinical treatments. In fact, the induction of additional random unwanted mutations can lead to the development of side effects and worse clinical condition, such as oncogenesis.

Prediction of possible off-target effects in gene editing is still challenging. Different techniques and designs can reduce the probability of off-target mutations. At the moment, online softwares

help the discovery of potential sites and the optimization of Cas9 gRNAs (Yee 2016, 20). By the use of genome databases, the sequence homology with the target is evaluated. The ranking based on the number of mismatches and the relative position evaluates possible alternative bindings. Increased specificity can be also achieved by combination of two gRNAs (Kolli et al. 2017; Ran et al. 2013). In fact, inducing double nicks with two gRNAs targeted upstream and downstream can efficiently excise the targeted locus. The induction of off-target nicks can be easily repair without mutation induced and avoid the generation of unspecific DSBs. (Kolli et al. 2017; Ran et al. 2013). Moreover, optimized form of Cas9 with reduced off-target events can be obtained by structural changes of this protein. In fact, in 2016 Kleinstiver et al. developed an optimized High Fidelity Cas9 generated by aminoacidic variations in the Cas9 sequence at Cas9-DNA contact points. The High Fidelity Cas9 showed similar on-target efficiency and eliminated off-target activity at undetectable levels *in vitro* (Kleinstiver et al. 2016).

Another approach that can be taken into consideration with the aim of reducing Cas9 unspecific bindings is a time limited expression of this editing tool. The modulation of Cas9 activity can be achieved in different ways. Preventing binding and editing after a time window can be done by specific protein inhibitors. Indeed, in 2017 Rauch et al. discovered 4 bacteriophage proteins able to regulate and inhibit Cas9 activity in *Listeria Monocytogenes* (Rauch et al. 2017). In addition, the blockade of Cas9 expression can be obtained by self-inactivation (Merienne et al. 2017; A. Li et al. 2019). In fact, providing a gRNA complementary to Cas9 sequence leads to generation of mutations and silencing of the Cas9 gene itself (Merienne et al. 2017). Merienne et al. provided in addition to the Cas9 and a gRNA, a second gRNA targeted to the ATG starting site of the Cas9 sequence, in order to disrupt its expression. HD-iPSC-derived neurons were treated with self-inactivating KamiCas9 system and strong reduction in KamiCas9 protein level was observed due to the 58% indels events happened in the Cas9 sequence over 4 weeks.

Comparison of regular Cas9 and KamiCas9 system did not show any difference in gene editing efficiency. Thus, progressively reduced activity of Cas9 is an efficient and specific solution that reduces potential off-target events. Determining the efficiency of Cas9 in inducing the correct mutation is relevant and essential for therapeutic attempts.

CRISPR-Cas9 delivery

The Cas9 nickase is an attractive way to induce genome modification *in vivo* and many genome editing studies have proved its efficiency. Delivery of the Cas9 to the affected tissues can be established and over the years, different approaches have been developed and optimized to deliver the CRISPR-Cas9 to cells.

Firstly, the CRISPR-Cas9 and the gRNA can be in different physical forms: DNA sequence-based, mRNA or ribonucleoprotein complexes (RNPs). The RNPs showed numerous advantages compared to the plasmid-based Cas9, from lower toxicity to fast and efficient action, including reduced off-targets and costs (S. Kim et al. 2014; Liang et al. 2015; Staahl et al. 2017; Kouranova et al. 2016; Zuris et al. 2015; M. Wang et al. 2016). By skipping the expression and the protein synthesis, Cas9 RNPs show a faster activity and consequently decay. However, transfection of RNP Cas9 into embryonic stem cells still induced mutations with a higher frequency, 23%, compared to plasmid transfection, 10%, with no detectable off-target events (S. Kim et al. 2014). No off-target resulting from Cas9 RNPs can be explained by the reduced time activity that this form offers compared to plasmid. However, the DNA-based Cas9 still remain the most common used form due to high delivery efficiency and widespread transgene expression (Koike-Yusa et al. 2014; Zincarelli et al. 2008).

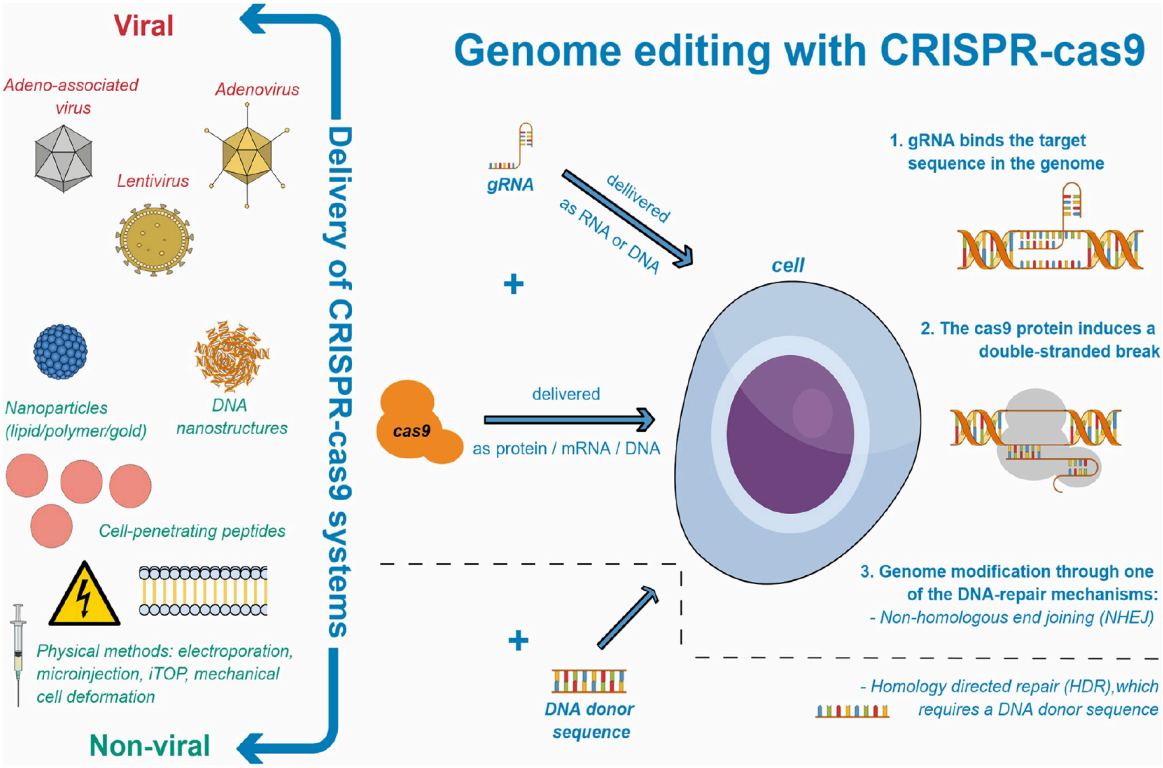

Figure I.III.5 Cas9 genome editing with the CRISPR-Cas9 and delivery system.
Different delivery approaches can be used to shuttle Cas9 to the target cells and allow its expression and activity: viral, non-viral and mechanical systems (left). Protein, RNA and DNA are the three different options to be delivered for Cas9 and the gRNA. An additional DNA donor sequence can be added in order to induce homologous recombination at the target locus (center). The gRNA recognizes the target sequence and recruits the Cas9 protein at the locus. The induction of DSB triggers the DNA repair and genome modification is achieved by the activation of either non-homologous end joining or homologous directed repair (right) *(Babačić et al. 2019)*.

Engineered nucleases can be delivered in three different ways: physical delivery, viral, and non-viral carriers (Figure I.III.5). Microinjection and electroporation are the most known techniques to mechanically introduce CRISPR-Cas9 into cells (Horii et al. 2014; H. Yang et al. 2013; Hashimoto and Takemoto 2015; Ousterout et al. 2015). Both approaches deliver protein and nucleic acids into mammalian cells with efficiency close to 100% (Horii et al. 2014). Microinjections and electroporation are efficient delivery techniques for single cell transfection, for *in vitro* and *ex vivo* work. However, due to really precise localization delivery and strong stressed induced, they are not suitable for *in vivo* studies.

In the non-viral carriers, lipid nanoparticles, polymer nanoparticles, cell-penetration peptides, and gold nanoparticles have also been used efficiently (Kang et al. 2017; Suresh, Ramakrishna,

and Kim 2017; Finn et al. 2018). These techniques are perfectly suitable for CRISPR-Cas9 gene editing in cells and mouse models. However, they do not fit good standards for *in vivo* experiments and clinical approaches due to low delivery efficacy compared to viral systems. In fact, viral approaches have been used and optimized for DNA-based tools since a long time. Although viral delivery approaches often result in unwanted mutations, they have proved to be the most efficient in vector distribution and extensive transgene expression, especially in central nervous system (Deverman et al. 2016; Choudhury, Harris, et al. 2016; Choudhury, Fitzpatrick, et al. 2016; Zincarelli et al. 2008). Viral delivery can be established by the use of lentiviruses, adenoviruses and adeno-associated viruses (AAVs). For our studies, we selected lentiviruses and AAVs to deliver the Cas9 nickase in patient-derived cells and mouse models, respectively. These viral shuttles will be described in detail in the following section.

CRISPR-Cas9 in expanded TNR disorders

Many studies have focused their attention on Cas9 induced gene editing in order to ultimately reverse the pathogenic phenotype in expanded TNR disorders. The optimization of Cas9 in different forms led to similar readouts and proved the feasibility of this technique in improving pathogenic symptoms.

Taking advantage of the epigenome potential of the Cas9, reduced toxicity and alleviation of cellular phenotype can be achieved. Targeting dCas9 to hypermethylated regions can induce chromatin changes and reactivate the transcription. In fact, the induction of demethylation at the CGG repeats present in *FMR1* gene is possible with the use of dCas9-Tet1 (Liu et al. 2018). Normal levels of FMR1 were observed after switching to an active chromatin state at the promoter and the open reading frame (ORF) in FXS iPSCs and neurons.

Excision of different expanded repeats leads to phenotypic amelioration. Pribadi et al. designed two gRNAs in order to cut the hexanucleotide repeats in *C9orf72* gene. The excision of the

entire expanded repeat sequence by Cas9 activity reduced foci formation and the hypermethylation of the allele in patient-derived iPSCs (Pribadi et al. 2016). Cas9 activity was also able to restore FMR1 expression in FXS iPSCs (Park et al. 2015). Deletion of CGG repeats in *FMR1* gene with DSB right upstream the repeat tract resulted in reactivation of gene expression. Moreover, this study demonstrated the possibility of inducing repeat excision with only one DSB (Park et al. 2015).

Deletion of the full CTGs repeat tract with part of flanking sequences showed improvements in cellular morphology, ribonucleoprotein foci formation and splicing alteration in DM1 patient-derived cells and DM1 mouse models (van Agtmaal et al. 2017; Provenzano et al. 2017; Scrudato et al. 2017; Dastidar et al. 2018; Y. Wang et al. 2018). Reversion of RNA foci and splicing defects was observed in DM1 patient myoblasts and fibroblasts when expanded CTG repeat were deleted by Cas9 activity combined with two gRNAs (van Agtmaal et al. 2017; Provenzano et al. 2017).

Cas9 can also select, cut and silence the mutant *HTT* gene by detection of SNPs characterizing the specific mutant allele (Dabrowska et al. 2018; Monteys et al. 2017; Shin et al. 2016; Merienne et al. 2017). The recognition of mutant allele by SNP presence and excision of promoter and part of ORF in *HTT* prevented generation of mutant *HTT* mRNA. Repeat excision consequently reversed of pathogenic phenotype in HD patient-derived fibroblasts (Shin et al. 2016). Selection of mutant allele by SNP detection has also been proposed by Monteys et al. where two gRNAs selected and cut part of the expanded allele in HD fibroblast cell line (Monteys et al. 2017). The silencing of the mutant allele led to phenotypic improvements. This approach showed also to be efficient in another TNR disorder context: FRDA. Increased *FXN* expression was observed when two ZFNs targeted upstream and downstream the expanded GAA repeat tract in fibroblasts (Y. Li et al. 2015). Similarly, *FXN* expression and protein level were restored when the GAA repeats were excised by the use of the Cas9 combined with two

gRNA in mouse model (Ouellet et al. 2017). The use of two gRNAs has shown to be a successful approach for targeting the mutant allele.

Unfortunately, all of the techniques mentioned above are not ideal for therapeutic approaches where flanking sequences should be perturbed at the minimum level, especially when repeat are placed in translated regions. The ideal solution is to directly change repeat size maintaining the genomic context as normal as possible. Even more, the generation of DSBs into the DNA is a stressful condition that cells need to overcome, with the probability of resulting adverse mutations and side effects. However, the direct target of the repeat tract without concomitant flanking sequence variation can be a safer solution. The direct contraction in repeat size is possible by using the Cas9 nickase (Cinesi et al. 2016). The Cas9 nickase targeted to CAG/CTG repeats is able to predominantly induce repeat contractions in mammalian cells. Induction of multiple nicks constitute a safer and less dangerous damage compared to DSBs that can be easily repaired. This gene editing tool holds the promise of possible therapeutic cure for patient and additional studies need to verify its efficiency at higher levels.

I.IV Gene therapy

Gene therapy has been defined by the US Food and Drugs Administration (FDA) as a technique that manipulate an individual's genome by replacing or inactivating disease-causing genes, or introducing new modified genes to cure a disease (FDA). By taking advantage of virus ability to detect and infect target cells, it is possible to induce genomic corrections to ameliorate and treat genetic disorders in patients, via either *in vivo* or *ex vivo* approach. This approach has been tested and optimized over the last 30 years for different purposes.

In the late '80s, this technique was considered particularly suitable for monogenic disorders. However, over the years different studies improved detailed understanding of this technique and gene therapy has shown to be efficient for other human disorders (Blaese et al. 1995; Gaspar et al. 2011; Ylä-Herttuala 2012; Maguire et al. 2008; Biagioni et al. 2018).

The first clinical attempt for gene therapy as a therapeutic approach was established by Blaese et al. in 1990. Two patients affected by a severe immunodeficiency, adenosine deaminase deficiency, took part in this clinical trial. Through an *ex vivo* approach, white blood cells of severe combined immune deficient patients were treated with retroviral vectors to express the normal adesine deaminase gene, and re-implanted into the patients (Blaese et al. 1995). The attempt had positive results but with temporary effects only. In the following years, retro- and adeno-viruses were also injected in human brains to treat cancer for the first time in an *in vivo* gene therapy treatment (Puumalainen et al. 1998). At the end of 20th century, the first case of death caused by gene therapy reduced the enthusiasm for such approaches. A high dose of adenovirus injected into the patient resulted in multiorgan failure and consequent death (Stolberg 1999). But in 2001 a successful gene therapy attempt, in a canine model for a congenital disorder, provided the proof-of-concept for the gene therapy approach, renewing the interest in the field (Acland et al. 2001). Over the last 20 years the gene delivery systems,

especially the viral components, have improved significantly and several trials have been shown to help a wide array of disorders (Bennett et al. 2012; MacLaren et al. 2014; Maguire et al. 2008; Nathwani et al. 2014; Tardieu et al. 2014; Mendell et al. 2015). One notable example is the reversion of blindness in patients with leber congenital amaurosis with as few as two retinal adeno-associated virus injections (Sengillo et al. 2017).

Three gene therapy treatments have already been approved in the European market and demonstrate safety in using this approach. Glybera was the first gene therapy approved in Europe where delivery of lipoprotein lipase gene (*LPL*) is done via AAV (Ylä-Herttuala 2012; European Medicines Agency 2012). Lipoprotein lipase deficient patients carry a defective *LPL* gene. Delivery of correct *LPL* restores protein levels and results in normalized fat metabolism reversing the symptoms (Ylä-Herttuala 2012; Stroes et al. 2008; Ross et al. 2004).

In 2016, an *ex vivo* gene therapy for Adenosine deaminase severe combined immune deficiency (ADA-SCID) has been approved in Europe: Strimvelis (Aiuti, Roncarolo, and Naldini 2017). Patient affected by ADA-SCID show impaired immune reactions and lymphocyte development caused by silenced mutated *ADA* gene. Hemapoietic Stem cells are treated with retrovirus carrying *ADA* gene and re-administered to patients (Aiuti et al. 2002, 2009). During clinical trials patients showed, improved immune functions and lower toxic metabolites, demonstrating Strimvelis as able to alleviate ADA-SCID symptoms. Several expectations are hold by gene therapy approach for curing cancer. One gene therapy treatment already present in the European market that demonstrate its efficiency against melanoma is Imlygic (European Medicines Agency 2015). This lentivirus carries a granulocyte macrophage colony stimulating factor that induces systemic antitumor response in patients. This oncolytic immunotherapy showed benefits in tumor lysis and boost in immune reaction in metastatic melanoma (Andtbacka et al. 2015). Gene therapy is the new generation therapeutic avenue for many different genetic disorders.

A major factor important for the success of the gene therapy approach is the choice of the delivery shuttle. Recombinant lentiviruses, adenoviruses, retroviruses, and others are the vectors used to vehicle the DNA treatment. Differences in the composition of the viral particles confer specific characteristics, such as tissue tropism, genomic integration. Thus, selection of the virus is important for the success of the treatment.

Lentiviruses

Lentiviruses belongs to the retroviral family and they originally cause chronic disorders in mammalian species, including humans. The most famous lentivirus is the human immunodeficiency virus (HIV). They are characterized by a RNA genome that is retro-transcribed into DNA by the reverse transcriptase enzyme once the host cell has been infected. The viral DNA is then integrated in the host genome, generally in coding regions (Lewinski et al. 2006). In 1996, Naldini et al. developed the first engineered lentivirus from HIV and efficiently delivered it in humans (Naldini et al. 1996). In the following years, steps have been taken to improve safety and reduce virulence and oncogenic potential of lentiviruses (Dull et al. 1998). These include the removal of accessory genes, self-inactivating mutations, and division in multiple plasmids during viral production (Modlich et al. 2006; Salmon and Trono 2007). With the scope of reducing genotoxicity, self-inactivation can be achieved by deleting one of the two long terminal repeats that triggers gene expression, reducing possibility of inducing or silencing gene expression in the surrounding area of integration (Modlich et al. 2006). Recombination events can potentially occur during the viral production, generating viruses able to replicate and leading to an increased mutagenesis frequency in the host genome. Thus, the genes necessary for recombinant lentivirus production were distributed in different plasmids to reduce as much as possible the probability of producing replication competent viruses (Salmon and Trono 2007). Lentiviruses tend to integrate viral genes into transcribed

regions of active genes, giving rise to potential dangerous gene mutations (G. P. Wang et al. 2009; Mitchell et al. 2004; Schröder et al. 2002). Nevertheless, host genomic insertions tend to happen in 5' regions of active genes and differently from other retroviruses, lentivirus showed to not integrate in tumor growth genes reducing possibility of oncogenesis (Montini et al. 2006). They elicit a stronger immune reaction in mouse models compared to other viruses (Nienhuis, Dunbar, and Sorrentino 2006; High 2011). However, lentiviruses showed to be a safer delivery shuttle for clinical gene therapy than other retroviruses (Cattoglio et al. 2010; Lewinski et al. 2006). The limitation in being neutralized and inactivated by human serum make lentiviruses not an optimal delivery system for *in vivo* gene therapy (DePolo et al. 2000). Nevertheless, they have shown to efficiently transduce hematopoietic stem cells in *ex vivo* experiment. In a successful clinical trial, hematopoietic stem cells have been treated with ß-globin SIN lentivirus (Cavazzana-Calvo et al. 2010). In patients affected by ß-thalassemia, a mutation in the ß-globin gene induces silencing and consequent absence of this protein. The restoration of normal blood hemoglobin levels can be achieved by re-administration of hemopoietic stem cells transduced by ß-globin SIN lentivirus (Cavazzana-Calvo et al. 2010). *Ex vivo* lentivirus gene therapy showed few successes in different disorders (Aiuti, Roncarolo, and Naldini 2017; Andtbacka et al. 2015).

Adeno-associated viruses

More promising results and ongoing clinical trials in gene therapy have been obtained using AAV-based vectors (clinicaltrials.org). AAVs are non-pathogenic parvoviruses able to infect dividing and non-dividing cells. They contain a single stranded DNA genome and host genome integration happens rarely. AAV genome integration has been observed in clinical trials (Kaeppel et al. 2013). Even though, it showed a low integration frequency without toxicity observed. Once released in the cell, viral DNA tends to remain in extrachromosomal circular

form (Xiao, Li, and Samulski 1996). This allows viral gene expression in a certain time window. Recombinant AAVs have been developed to limit the immune reaction, bringing this vector to a safer level compared to others (Nayak & Herzog 2010). However, the packaging capacity of AAV-mediated delivery limits its use. Inserts longer than 4 kb strongly reduce the production efficiency of AAVs (Wu, Yang, and Colosi 2010). Despite *Streptococcus pyogenes* Cas9 being 4'140 bps in length, its functionality when packed into an AAV has been well demonstrated in a HD mouse models (Monteys et al. 2017; S. Yang et al. 2017). AAV virion is constituted of capsid proteins whose aminoacid sequences determine the viral interactions and specificity for target cells and transduction efficiency. Based on capsid composition, AAVs are categorized in 11 serotypes that show specific tropism (Wu, Asokan, and Samulski 2006; Schmidt and Grimm 2015). AAV1 is well suited for delivery gene expression in brain (Monteys et al. 2017; Swiech et al. 2015). Muscles and liver are the prominent targets for AAV8 (Nelson et al. 2016; Ran et al. 2015; Y. Yang et al. 2016). Differently, AAV9 can efficiently drive the gene editing to wide range of tissues, including skeletal muscles, heart and brain (Bisset et al. 2015; Dufour et al. 2014; Tabebordbar et al. 2016; Kemaladewi et al. 2017; Johansen et al. 2017; Chow et al. 2017; Zincarelli et al. 2008). Even more, generation of new hybrid AAVs with modified tropism and increased transduction efficiency is possible by combination of structural capsid components from different serotypes (Tervo et al. 2016; Murlidharan et al. 2016). For these reasons, AAVs are considered one of the most suitable delivery vectors for gene therapy, leading us to the choice of AAVs to target the specific affected cell types in DM1 and HD mouse models.

Unfortunately, for expanded TNR disorders no gene therapy treatment is available for the moment. Nevertheless, many pre-clinical studies showed successful results in delivering treatments via a viral vector, the Cas9 included. The efficiency of AAV-Cas9 delivery in DM1

mouse model was demonstrated. The dSaCas9 was targeted on CTG repeats in HSA^{LR} mice muscles, which carry an expanded CUG repeat within the final untranslated exon of the human skeletal actin. The dSaCas9 activity inhibited repeat expression, rescued RNA foci formation and missplicing events in muscle fibers (Pinto et al. 2017). In HD knock-in mice, AAV expressing the Cas9 and 2 gRNAs, efficiently transduced striatal cells and allowed Cas9 components expression. This successfully led to permanent excision of the CAG repeats, consequent depletion of Huntingtin aggregates and alleviation of motor deficits, such as muscular strength and motor coordination (S. Yang et al. 2017). Differently, recombinant AAV expressing Cas9 showed ability in infecting brain cells in HD mouse models. Reduced level of human *HTT* mRNA confirmed excision of the repeat tract induced by Cas9 and the efficient treatment approach (Monteys et al. 2017).

In conclusion, AAV vector and gene therapy approach is a good technique to delivery Cas9 nickase to affected tissues.

The goal of this project is to design a gene editing approach capable of specifically inducing repeat contraction to be used as a novel therapeutic avenue for expanded CAG/CTG repeat disorders. In Chapter II, I demonstrate the ability of the CRISPR-Cas9 nickase to induce repeat contractions predominantly, using a mammalian system. Lipofectamine transfection of the Cas9 nickase induced repeat contractions in GFP$(CAG)_{101}$ cells, with a rate of 30% over the total alleles in only 5 days (Cinesi et al. 2016). In chapter III, with a gene therapy approach, patient-derived cells and DM1 and HD mouse models have been treated with the Cas9 nickase AAV and targeted to the CAG/CTG repeat tract. Repeat instability at the mutated loci was measured by SP-PCR and sequencing. Results from this project will shed the light on the Cas9 nickase gene therapy approach as a possible cure for expanded TNR disorders.

Chapter II

Contracting CAG/CTG repeats using the CRISPR-Cas9 nickase

nature COMMUNICATIONS

ARTICLE

Received 15 Jun 2016 | Accepted 12 Sep 2016 | Published 9 Nov 2016

DOI: 10.1038/ncomms13272 OPEN

Contracting CAG/CTG repeats using the CRISPR-Cas9 nickase

Cinzia Cinesi[1], Lorène Aeschbach[1], Bin Yang[1] & Vincent Dion[1]

CAG/CTG repeat expansions cause over 13 neurological diseases that remain without a cure. Because longer tracts cause more severe phenotypes, contracting them may provide a therapeutic avenue. No currently known agent can specifically generate contractions. Using a GFP-based chromosomal reporter that monitors expansions and contractions in the same cell population, here we find that inducing double-strand breaks within the repeat tract causes instability in both directions. In contrast, the CRISPR-Cas9 D10A nickase induces mainly contractions independently of single-strand break repair. Nickase-induced contractions depend on the DNA damage response kinase ATM, whereas ATR inhibition increases both expansions and contractions in a MSH2- and XPA-dependent manner. We propose that DNA gaps lead to contractions and that the type of DNA damage present within the repeat tract dictates the levels and the direction of CAG repeat instability. Our study paves the way towards deliberate induction of CAG/CTG repeat contractions *in vivo*.

[1] Center for Integrative Genomics, University of Lausanne, 1015 Lausanne, Switzerland. Correspondence and requests for materials should be addressed to V.D. (email: Vincent.dion@unil.ch).

Repetitive DNA sequences are hotspots for genome instability because they pose a particular challenge to the DNA repair and replication machineries. Their mutation often leads to disease[1]. For example, tracts of CAG/CTG triplets (henceforth referred to as CAG repeats) longer than about 35 units cause at least 14 different currently incurable neurological and neuromuscular diseases[2]. In addition, when CAG repeats expand to pathological lengths, they become highly dynamic and their length changes at high frequencies in both somatic and germ cells throughout the lifetime of an individual[3–6].

The molecular mechanisms governing CAG repeat instability revolve around the ability of these sequences to fold into non-B-DNA structures when exposed as single-stranded DNA[7–9]. These unusual structures are mistaken for damaged DNA whether or not they contain lesions. The subsequent repair is error-prone due to the repetitive nature of the sequences and their structure-forming ability[3]. Another non-mutually exclusive model suggests that DNA damage within the repeat tract triggers repair, which is, in turn, error-prone due to secondary structures formed by these sequences[5]. In support of these models, several DNA repair pathways promote the instability of expanded CAG repeats, including mismatch repair[10], double-strand break (DSB) repair[11–14], transcription-coupled nucleotide excision repair[15,16], base excision repair (BER)[17,18], as well as DNA replication[19]. In contrast, single-strand break (SSB) repair (SSBR)[20] and signalling via the DNA damage response (DDR)[21] antagonize CAG repeat instability. Therefore, changes in repeat length provide an opportunity to understand the interaction and interdependence of several different DNA repair pathways at naturally occurring sequences.

Importantly, repeat length determines in large part the severity of the diseases caused by expanded repeats[4]. It has therefore been proposed that contracting the repeat tract would be beneficial in reducing phenotype expression. Repeat expansion, on the other hand, would further exacerbate the disease symptoms[4,22,23]. Currently, there is no treatment that specifically shrinks CAG repeats. This is, in part, because the assays used to measure repeat instability are tedious, slow and/or can only survey instability in one direction. Consequently, the understanding of the mechanism of CAG repeat instability remains poor. Elucidating how contractions can be induced, without also provoking expansions, is critical in designing therapeutic avenues.

Here we present a green fluorescent protein (GFP)-based chromosomal reporter assay that can monitor both CAG repeat expansions and contractions in the same human cell population. We combined this assay with gene-editing tools, namely zinc finger nucleases (ZFNs) and the CRISPR-Cas9 technology. We found that DSBs induced within the expanded repeat tract either by the Cas9 nuclease or a ZFN led to both expansions and contractions. Remarkably, the Cas9 D10A mutant (referred to as the Cas9 nickase) induces instability with a marked bias towards contractions and no detectable off-target mutations. We implicate the DDR kinases ataxia telangiectasia mutated (ATM) and ataxia telangiectasia and Rad3 related (ATR) in promoting contractions and preventing instability, respectively. Moreover, it is not dependent on the SSBR factors XRCC1 and PARylation. Cas9 nickase-induced repeat contraction appears to occur via a pathway different from SSBR- or BER-induced instability. We propose that DNA gaps may be the crucial mutagenic intermediate during nickase-induced contractions. Our results have important implications for gene editing in expanded trinucleotide repeat diseases.

Results

A GFP-based assay to detect CAG repeat instability. We made use of a recently described GFP-based assay capable of detecting contractions in human cells[24] (Fig. 1a). In this assay, CAG repeats within the intron of a GFP mini-gene interfere with splicing in a repeat length-dependent manner, with longer repeats diminishing GFP production. Thus, GFP intensities, measured by flow cytometry, serve as a proxy for the length of the repeat tract (Supplementary Fig. 1A,B). The reporter is present as a single copy integrated in the genome of human HEK293 T-Rex Flp-In cells. Its transcription is driven by a doxycycline (dox)-inducible promoter. A second isogenic cell line, GFP$(CAG)_0$, harbours the same reporter at the same genomic location but is devoid of a CAG repeat. Santillan *et al.*[24] validated the assay by expressing a ZFN that cuts the CAG repeat tract. This treatment increased the number of cells with higher GFP intensities (GFP^+) in a reporter cell line with 89 repeats (GFP$(CAG)_{89}$) by about 3.5-folds, suggesting that the ZFN treatment induced contractions. They did not report testing for expansions.

To determine whether we could monitor expansions using this assay, we sorted GFP^- and GFP^+ cells from a population of GFP$(CAG)_{101}$ cells using fluorescence-activated cell sorting (FACS). We defined GFP^- cells as those within the 1% of the cells in the population expressing the least amount of GFP. Similarly, GFP^+ cells are the brightest 1% in the population. From the GFP^- population, we isolated 19 clones with expansions reaching up to 258 CAGs (Supplementary Fig. 1C). Of the 12 GFP^+ clones isolated, 11 had contractions, the largest of which shrank the repeat tract down to 33 CAGs. The allele sizes in GFP^- and GFP^+ cells were significantly different ($P = 1.0 \times 10^{-5}$, using a Wilcoxon *U*-test), demonstrating that repeat size differences can be detected with this assay. Sequencing the region flanking the CAG repeats also uncovered deletions in five single clones with contractions (Supplementary Fig. 1D). With the exception of one clone that contained a complex rearrangement, the clones with deletions included 2 bp of microhomology at the junction, suggesting that a minor CAG repeat instability pathway is due to an error-prone alternative end-joining mechanism, as suggested recently[25]. Similar results were obtained after sorting cells from populations that were kept in culture for 6 months with or without dox (Supplementary Fig. 1E–H). These results demonstrate that the assay can detect contractions as well as expansions that nearly triple the size of the repeat tract.

DSBs induce both contractions and expansions. To determine whether ZFN-induced expansions in addition to the contractions reported by Santillan *et al.*[24], we first repeated the same experiment. Here we defined GFP^- and GFP^+ cells as those with GFP intensities in the brightest and dimmest 1% after transfection with the control vector, (Supplementary Fig. 2A—see Methods). We reproduced their results: ZFN expression increased the frequency of GFP^+ cells by 3.2-folds, but had no effect on the number of GFP^- cells (Fig. 1b). While optimizing the assay, we noted that GFP intensities increased on the addition of dox for 72 h before reaching a steady-state level (Supplementary Fig. 2B). This is in contrast to the 24 h previously reported[24]. Increasing the time of GFP induction raised the overall apparent average intensity of GFP and unmasked an additional GFP^- cell population only in the sample transfected with both ZFN arms (Fig. 1c). This approach revealed 2.5- and 3.9-fold increases in the proportion of GFP^- and GFP^+ cells, respectively, on expression of both ZFN arms compared with transfecting an empty vector control (Fig. 1d). Expressing either ZFN arm individually led to only small changes in GFP levels: between 1.3- and 1.4-fold increases in the number of GFP^- cells and between 0.9- and 1.5-fold for GFP^+ cells (Fig. 1d). Expressing both ZFN arms in the GFP$(CAG)_0$ cell line had no effect on GFP intensities (Supplementary Fig. 2C), confirming

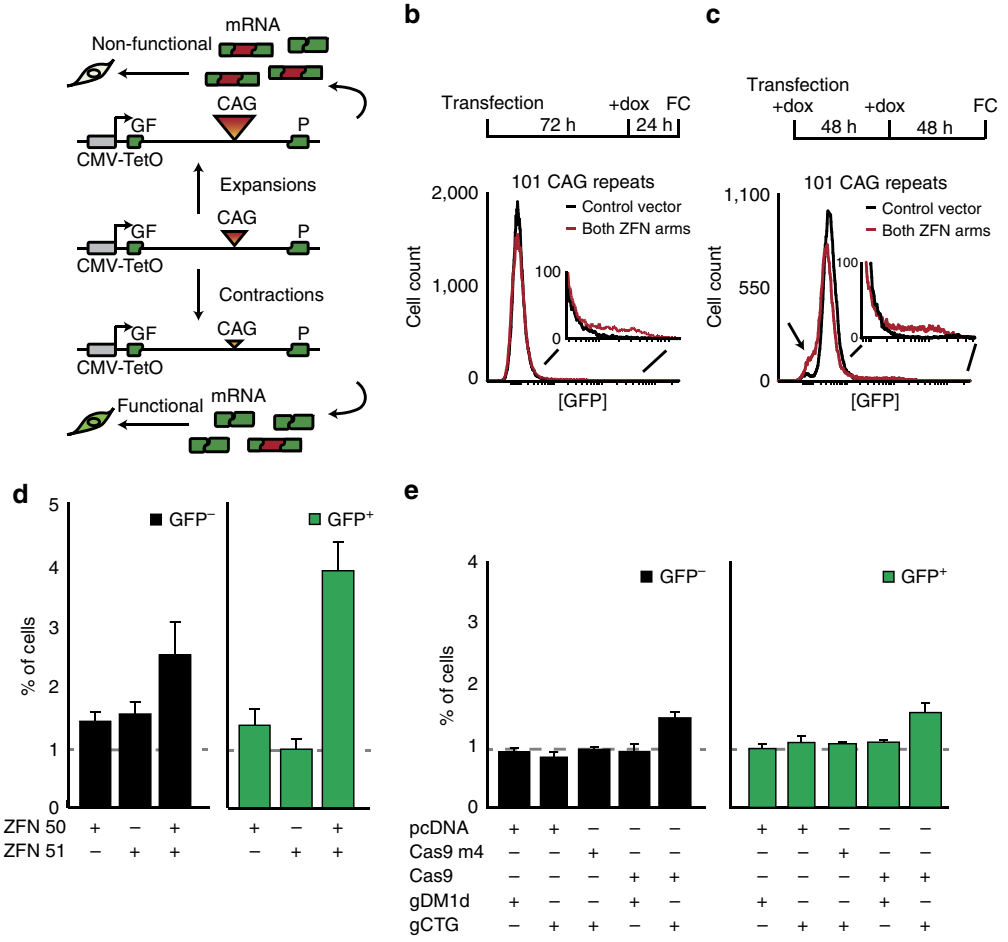

Figure 1 | DSBs within CAG repeats lead to expansions and contractions. (**a**) GFP-based assay to detect changes in repeat length. (**b**) Representative flow cytometry profiles after expression of a ZFN in GFP(CAG)$_{101}$ using the protocol from ref. 24. (**c**) Representative flow cytometry profiles with increased dox induction time uncovering an increase in GFP$^-$ cells on ZFN expression in GFP(CAG)$_{101}$ cells (arrow). (**d**) Quantification of the ZFN experiments in **c** revealed that ZFN induces the appearance of GFP$^-$ and GFP$^+$ cells. ZFNs are composed of two different ZFN arms, each fused to a FokI nuclease that must dimerize to be active. ZFN 50 and ZFN 51 are individual ZFN arms[24]. The dashed line represents the number of cells present in gates set to include the dimmest (GFP$^-$) or brightest (GFP$^+$) 1% of the cells when a control vector, pcDNA3.1 Zeo, is transfected. Error bars are s.e.m. from 15 replicates for experiments with both ZFN arms, 12 for the single ZFN transfections. (**e**) Quantification of GFP$^-$ and GFP$^+$ cells obtained after expression of the indicated vectors. Dashed line: dimmest (GFP$^-$) or brightest (GFP$^+$) 1% of the cells transfected with the Cas9 nuclease vector and the empty gRNA plasmid, pPN10. The error bars are s.e.m. Number of replicates per treatment: pcDNA + gDM1d, $n = 3$; pcDNA + gCTG, $n = 5$; Cas9 m4 + gCTG, $n = 4$; Cas9 + gDM1d, $n = 3$; Cas9 + gCTG, $n = 7$. FC, flow cytometry; dox, doxycycline.

that the presence of the repeat tract is necessary. We confirmed that GFP$^-$ cells contained expansions and GFP$^+$ cells harboured contractions by sorting cells exposed to both ZFN arms. Of the 9 GFP$^-$ clones analysed, 8 revealed an expansion (Supplementary Fig. 2D,E). None of them contained deletions and were therefore not GFP$^-$ because they had lost the GFP reporter. Of the 13 GFP$^+$ clones, 11 had contractions. Of those, 3 had deletions in the flanking sequences, which is similar to the findings of a previous study constrained to measuring only contractions and using a different ZFN[26]. Here again, the size of GFP$^-$ and GFP$^+$ cells in the recovered clones were significantly different ($P = 5 \times 10^{-4}$, using a Wilcoxon U-test). These results demonstrate that GFP$^-$ and GFP$^+$ cells accurately reflect the presence of expansions and contractions, making this assay especially well suited to detect expansions and contractions quickly within a chromosomal environment.

To confirm that DSBs within the repeat tract lead to both expansions and contractions, we used a second type of programmable nuclease: CRISPR-Cas9. This bacterial nuclease is guided to virtually any sequence of interest by a guide RNA (gRNA) molecule, where it induces blunt-ended DSBs, making it a highly effective gene-editing tool[27–29]. Transfection of a vector expressing a gRNA that targets the unrelated *DMPK* locus (gDM1d) together with Cas9 did not affect GFP expression (Fig. 1e). Similarly, expressing a gRNA containing six CTGs as the target sequence (gCTG) alone, expressing the Cas9 nuclease plus the gCTG in GFP(CAG)$_0$ cells, or the gCTG together with a catalytically inactive version of Cas9 (Cas9m4) did not change GFP expression significantly (Fig. 1e and Supplementary Fig. 2F). However, expressing the Cas9 nuclease together with gCTG resulted in a meek 1.4- and 1.5-fold induction of GFP$^-$ and GFP$^+$ cells, respectively, compared with co-transfecting the Cas9 expression vector with the empty gRNA vector (Fig. 1e). This low efficiency may reflect that the protospacer adjacent motif next to the target sequence of gCTG is not the canonical NGG. We conclude that DSBs induced within the repeat tract by a ZFN or the Cas9 nuclease provoke nearly as many expansions as contractions.

The Cas9 nickase induces mainly CAG repeat contractions. The use of the Cas9 enzyme allowed us to test whether the type of DNA damage present within the repeat tract influences CAG repeat instability. The Cas9 D10A mutant can be used with the same gRNA to introduce DNA nicks on the strand complementary to the gRNA[30]. DNA nicks are important intermediates in repeat instability *in vitro*[31,32]. We therefore asked whether inducing DNA nicks with the Cas9 nickase could influence CAG repeat instability.

We found that expressing the Cas9 nickase together with gCTG in GFP$(CAG)_{101}$ cells increased the number of GFP^- cells by 1.6-fold and GFP^+ cells by 3.2-folds compared with cells expressing only the nickase (Fig. 2a). Transfecting the Cas9 nickase with gCAG, which cuts the opposite strand compared with gCTG, had a similar effect, leading to increases of 1.4- and 3.7-folds in GFP^- and GFP^+ cells, respectively (Fig. 2a). To control for potential indirect effects on GFP expression, we expressed the Cas9 nickase along with gDM1d. This had no effect on GFP expression (Fig. 2a). In addition, the gCTG alone did not increase either GFP^- or GFP^+ cells, similar to expressing the gCTG together with the Cas9m4 mutant (Fig. 1e), suggesting that the activity of the nickase is necessary. Increasing the number of transfections to three in the span of 12 days further increased the number of GFP^+ cells to 6.2-folds, without a concomitant change in GFP^- cells (Fig. 2b and Supplementary Fig. 2G,H; $P = 0.32$ and 0.001 for GFP^- and GFP^+ cells, respectively, using a Wilcoxon *U*-test). The Cas9 nickase did not increase the number of dead cells, which could skew the quantification of GFP^- and GFP^+ cells (Supplementary Table 1). Also, the difference in the number of GFP^+ cells induced between the nuclease and the nickase was not due to differences in expression levels of the Cas9 enzyme (Supplementary Fig. 3A,B). We further confirmed that the way we quantified the data did not induce a bias against expansions (Supplementary Fig. 3C,D). These observations suggest that the Cas9 nickase leads to instability with a bias towards contractions.

To confirm this effect using an assay that is independent of the GFP reporter, we isolated DNA after expressing the Cas9 nickase and gCTG together and performed small-pool PCR (SP-PCR). This method bypasses the inherant advantage in amplification efficiency that smaller alleles have by setting up a larger number of reactions, each with only a few genomes as templates[33]. Using samples treated according to our 12-day regimen, we could detect larger and more frequent contractions in cells exposed to both the

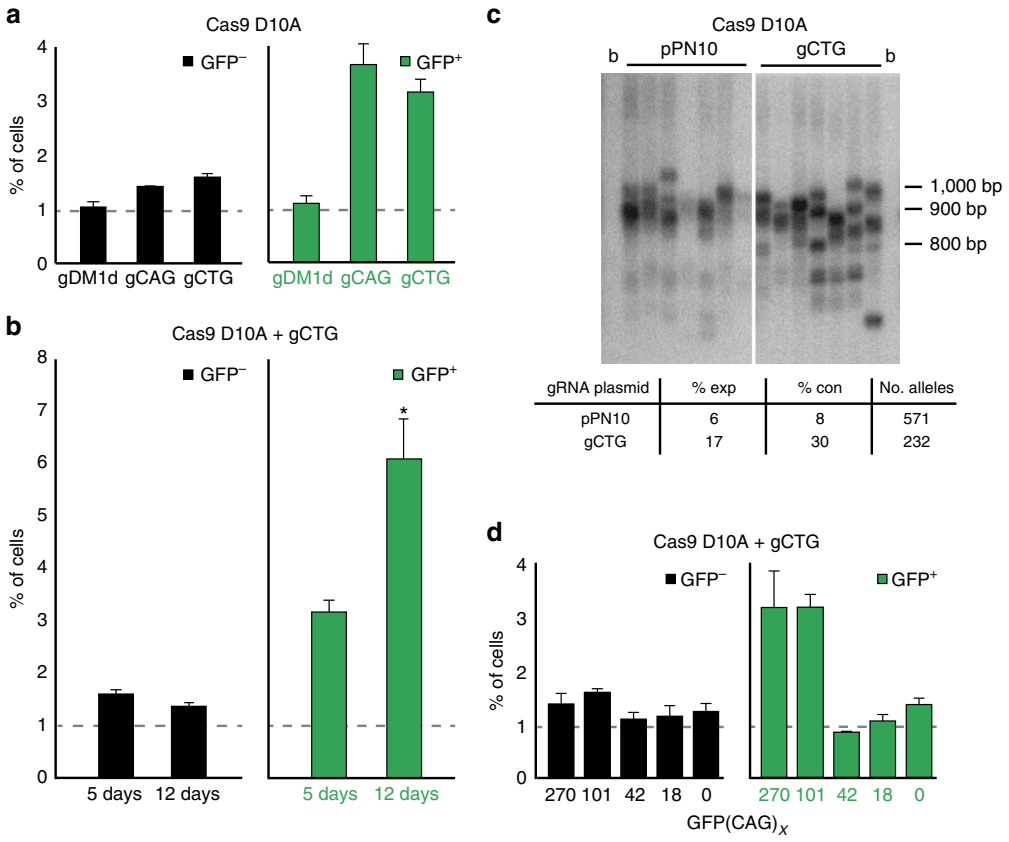

Figure 2 | The Cas9 nickase causes CAG repeat contraction. (**a**) Quantification of the effect of Cas9 nickase expression in GFP$(CAG)_{101}$ cells. Number of replicates per treatment: gCTG, $n = 37$; gCAG, $n = 3$; gDM1d, $n = 3$. Quantification of gCTG experiments also include results from Cas9 nickase expression treated with DMSO and siRNAs against vimentin. Dashed line: dimmest (GFP^-) or brightest (GFP^+) 1% of the cells transfected with the Cas9 nickase vector and the empty gRNA plasmid. (**b**) Quantification of GFP^- and GFP^+ cells after 5 days (1 transfection) or 12 days (3 transfections) of expressing the Cas9 nickase along with gCTG in GFP$(CAG)_{101}$ cells. Number of replicates per treatment: 5 days, $n = 37$ (same as in **a**); 12 days, $n = 4$ (*$P = 0.001$, using a Wilcoxon *U*-test, compared with 5-day treatment). Dashed line: dimmest (GFP^-) or brightest (GFP^+) 1% of the cells transfected with the Cas9 nickase vector and the empty gRNA plasmid over the indicated period of time. (**c**) SP-PCR (top) and its quantification (bottom) of DNA isolated from GFP$(CAG)_{101}$ cells after Cas9 nickase expression with or without gCTG (shown: 100 pg DNA per PCR) or pPN10 (50 pg DNA per PCR) for 12 days. b, no DNA blank. (**d**) The ability of the Cas9 nickase to induce contractions is repeat-length dependent. Dashed line: dimmest (GFP^-) or brightest (GFP^+) 1% of the cells transfected with the Cas9 nickase vector and the empty gRNA plasmid in the indicated cell line. For each cell line the 1% threshold is determined independently. The error bars are s.e.m. Number of replicates per treatment: GFP$(CAG)_{270}$, $n = 3$; GFP$(CAG)_{101}$, $n = 37$ (same as in **a**); GFP$(CAG)_{42}$, $n = 3$; GFP$(CAG)_{18}$, $n = 2$; GFP$(CAG)_0$, $n = 13$.

Table 1 | Effect of the Cas9 nickase targeted by gCTG at CAG/CTG sites in the genome.

Locus	No. of repeats*		No. of alleles sequenced	No. with changes
	Allele 1	Allele 2		
AR	20 + 5	21 + 5	18	0
ATN1	15	16	18	0
ATXN1	12 + 11	12 + 12	18	0
DMPK	5	5	18	0
PPP2R2B	10	10	18	0
TBP	9 + 18	9 + 19	18	0
TCF4	14	17	18	0

See Supplementary Table 1 for sequence composition at these loci.
*Alleles from GFP^+ cells sorted from $GFP(CAG)_{101}$ cells transfected with the Cas9 nickase and gCTG expressing plasmids.

nickase and gCTG (Fig. 2c). The number of contractions accounted for nearly a third of the total alleles compared with only 8% when cells were transfected with the Cas9 nickase-expressing vector alone (Fig. 2c, $P<0.0001$, using a Fisher's exact test). On nickase expression there was also an increase in the number of expansions, but there were fewer of them and the changes in size were smaller than for the contractions. We conclude that the Cas9 nickase targeted by gCAG or gCTG leads to a marked bias towards contractions, which is in sharp contrast to the results we obtained with the ZFN and the Cas9 nuclease.

We next examined the effect of repeat length on Cas9 nickase-induced contractions. To do so, we used $GFP(CAG)_x$ cell lines with repeat sizes ranging from 0 to 270 CAGs. We detected slight increases of 1.2- to 1.6-fold in GFP^- cells on expression of both the Cas9 nickase and gCTG. This effect was largely independent of the repeat size, suggesting that this slight increase in GFP^- cells seen in $GFP(CAG)_{101}$ is only partly caused by changes in repeat length (Fig. 2d). By contrast, the same treatment increased the proportion of GFP^+ cells in $GFP(CAG)_{270}$ and $GFP(CAG)_{101}$ cells, but not in $GFP(CAG)_{42}$, $GFP(CAG)_{18}$ nor $GFP(CAG)_0$ (Fig. 2d). These observations suggest that normal-length repeats are not prone to instability on action of the Cas9-nickase. We further substantiated this claim by examining the extent of the Cas9-induced changes at seven different loci in the genome harbouring repeats of normal sizes (Supplementary Table 2). We used nine GFP^+ clones with contractions within the GFP reporter caused by the action of the Cas9 nickase guided by gCTG. Of the 126 alleles sequenced, we found that they all remained mutation-free (Table 1), suggesting that the frequency of off-target mutations caused by the nickase is low. Together, these results argue that expanded CAG repeats are targets of the Cas9 nickase, leading predominantly to contractions.

SSBR is not involved in Cas9 nickase-induced contractions. Our results suggest that the type of damage induced within the repeat tract influences instability. It was therefore important to confirm the mutagenic intermediate created by the Cas9 nickase. The simplest hypothesis is that DNA nicks are themselves mutagenic. We therefore tested the effect of X-Ray Repair Cross-Complementing Protein 1 (XRCC1) and Poly (ADP-ribose) polymerase (PARP) activities on nickase-induced instability. The XRCC1–PARP1 complex works as a nick sensor and is involved in their repair[34]. In addition, XRCC1 interacts with a number of DNA glycosylases and is required for the repair of single-nucleotide gaps, i.e., SSBs that arise during BER[35]. This is highly relevant because BER causes expansion in a Huntington disease mouse model[17,18], and both XRCC1 and PARP1 protect against contractions in a mammalian-based assay that is blind to expansions[20]. Therefore, the prediction was that the knockdown of *XRCC1* or the inhibition of PARP using Oliparib would significantly affect the contraction frequencies caused by the Cas9 nickase if DNA nicks or SSBs are mutagenic. This prediction was not confirmed: neither the knockdown of *XRCC1* nor the chemical inhibition of PARP activity changed the frequency of GFP^+ cells compared with controls (Fig. 3a,b and Supplementary Fig. 4A,B). We confirmed that the XRCC1 protein levels were substantially reduced and that the Oliparib concentration used led to an accumulation of cells in G2 and that it inhibited PARylation in response to Zeocin assault (Supplementary Table 3 and Fig. 3a,b). These observations suggest that the mutagenic intermediate is neither a DNA nick nor a SSB, and imply that nickase-induced contractions occur through a mechanism that is distinct from spontaneous and BER-dependent CAG repeat instability. We posit instead that DNA gaps larger than a single nucleotide may lead to nickase-induced contractions.

ATR and ATM in Cas9 nickase-induced CAG repeat instability. DNA gaps, for example, those induced by ultraviolet light during G1 of the cell cycle, activate ATR[36]. We therefore tested the effect of inhibiting this DDR kinase on nickase-induced instability using the small molecule VE-821 (ref. 37). We found that this inhibitor led to a 3.1- and 5.9-fold increase in GFP^- and GFP^+ cells, respectively, when used in combination with the Cas9-nickase and gCTG (Fig. 4a, $P=0.03$ compared with dimethylsulphoxide (DMSO) treated cells, using a Wilcoxon U-test). This treatment did not affect GFP expression in $GFP(CAG)_0$ (Supplementary Fig. 4B), confirming that the effect depends on the Cas9 nickase activity within the expanded repeat tract. These data suggest that ATR prevents CAG repeat instability at Cas9 nickase-induced damage.

ATM is a related DDR kinase that is partially redundant with ATR[38]. Thus, we wanted to know what effect ATM might have on nickase-induced contractions. KU60019, a specific inhibitor of ATM[39], led to a nearly two-fold reduction in the frequency of GFP^+ cells compared to DMSO-treated cells (Fig. 4a, $P=0.01$, using a Wilcoxon *U*-test). To test whether the effect of ATR was dependent on the activity of ATM, we treated the cells with both inhibitors simultaneously. This double treatment reduced the number of contractions induced by the Cas9 nickase compared with DMSO-treated cells ($P=0.03$, using a Wilcoxon *U*-test), to a level similar to using the ATM inhibitor alone (Fig. 4a, $P=0.57$, using a Wilcoxon *U*-test). These observations suggest that the activity of ATM is required to cause nickase-induced instability in the absence of ATR.

A role for MSH2 and XPA in the absence of ATR activity. We next aimed to further define how the Cas9 nickase leads to a contraction bias. A central player in CAG repeat instability is MutS Homolog 2 (MSH2), which is essential for mismatch repair. *MSH2* knockout in mouse models and its knockdown in human cell-based assays nearly eliminates expansions[10,40,41]. Its role in

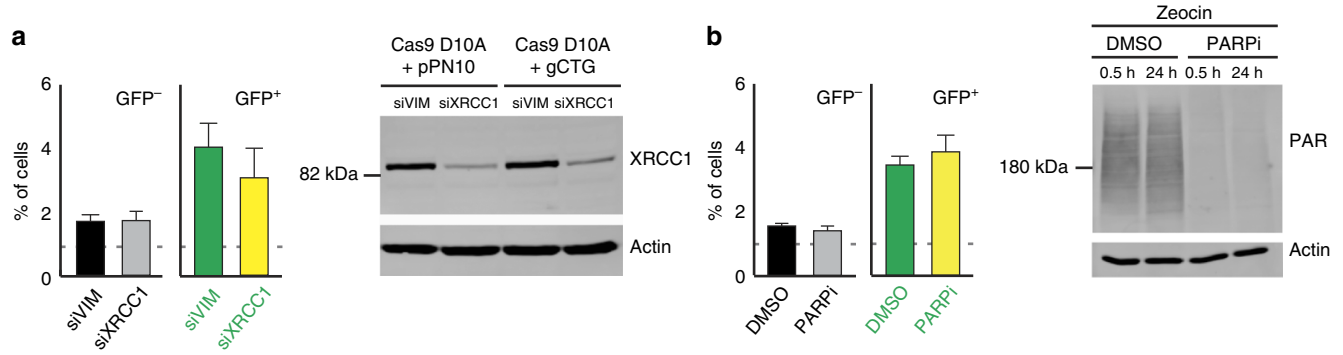

Figure 3 | SSB repair is not involved in Cas9-nickase-induced repeat instability. (**a**) Left: XRCC1 knockdown ($n=4$) did not affect the GFP expression in GFP$(CAG)_{101}$ cells ($P=0.7$ for both GFP$^-$ and GFP$^+$ cells, using a Wilcoxon U-test). Dashed line: dimmest (GFP$^-$) or brightest (GFP$^+$) 1% of the cells transfected with the Cas9 nickase vector; the empty gRNA plasmid; and the indicated siRNAs. Right: western blot showing knockdown efficiency. (**b**) Left: same as **a**, but cells treated with the PARP inhibitor Oliparib ($n=4$, $P=0.5$ for GFP$^-$ cells and $P=0.4$ for GFP$^+$ cells compared with DMSO-treated cells, using a Wilcoxon U-test). Dashed line: dimmest (GFP$^-$) or brightest (GFP$^+$) 1% of the cells transfected with the Cas9 nickase vector together with the empty gRNA plasmid, and treated with either DMSO or Oliparib. Right: PAR levels 30 min and 24 h after treatment with 100 μg ml^{-1} of Zeocin. The error bars represent the s.e.m.

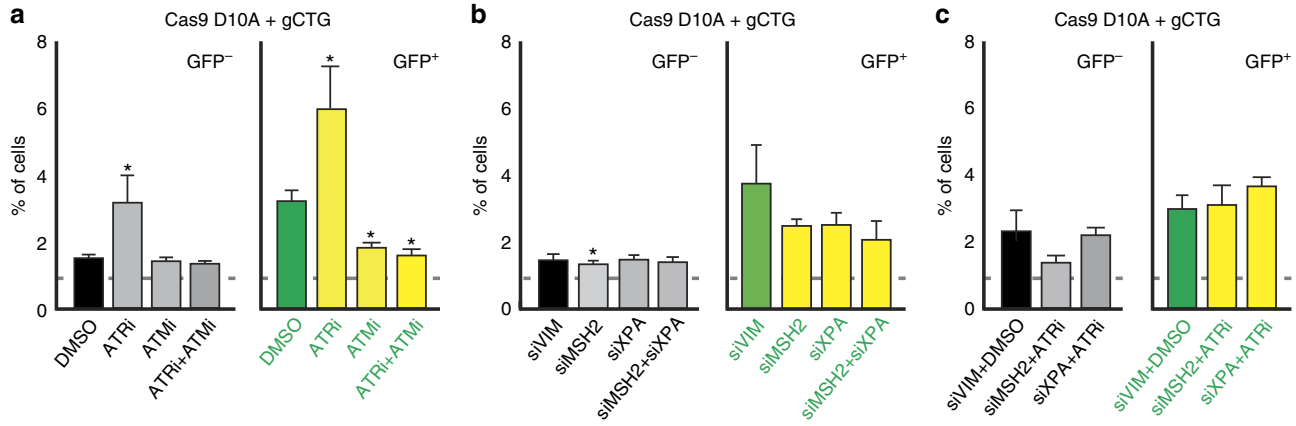

Figure 4 | Mechanism of Cas9-nickase-induced repeat instability. (**a**) Quantification of GFP$^-$ and GFP$^+$ cells on treatment with DMSO ($n=20$, which includes the amount of DMSO for treatment with one or two inhibitors in GFP$(CAG)_{101}$ cells; these controls were indistinguishable from each other), an ATR inhibitor (VE-821, $n=5$), or an ATM inhibitor (KU60019, $n=5$), or both ($n=3$). Dashed line: dimmest (GFP$^-$) or brightest (GFP$^+$) 1% of the cells transfected with the Cas9 nickase vector together with the empty gRNA plasmid and treated with the DMSO or the indicated inhibitor. (**b**) Quantification of the GFP$^-$ and GFP$^+$ cells on knockdown with siRNAs (siVIM, $n=13$; siMSH2, $n=14$; siXPA, $n=9$; siMSH2 + siXPA, $n=4$). siVIM quantifications include results from knockdown of vimentin with both 10 and 20 nM of siRNAs as the results were indistinguishable from each other. Dashed line: dimmest (GFP$^-$) or brightest (GFP$^+$) 1% of the cells transfected with the Cas9 nickase vector; the empty gRNA plasmid; and the indicated siRNAs. (**c**) Quantification of the GFP$^-$ and GFP$^+$ cells on combinatorial knockdown of the indicated siRNAs and the ATR inhibitor VE-821 (siVIM + DMSO, $n=6$; siMSH2 + ATRi, $n=3$; siXPA + ATRi, $n=6$). Dashed line: dimmest (GFP$^-$) or brightest (GFP$^+$) 1% of the cells transfected with the Cas9 nickase vector together with the empty gRNA plasmid, and treated with the indicated inhibitors and siRNAs The error bars are s.e.m. *$P\leq0.05$.

contraction, however, is more controversial. In mouse models, knocking out *MSH2* either promoted or had no effect on contractions[10]. In human cells *MSH2* downregulation promotes contractions or instability in both directions, depending on the model system used[15,40,42,43]. We found that *MSH2* knockdown did not consistently reduce the number of Cas9 nickase-induced GFP$^+$ cells compared with a control knockdown of vimentin (Fig. 4b, $P=0.14$, using a Wilcoxon U-test). MSH2 promotes CAG repeat contractions together with the NER factor, Xeroderma Pigmentosum, Complementation Group A (XPA)[15], in a human cell-based assay. XPA is also required for CAG repeat instability in mouse neuronal tissues[44] and for contractions in a human cell-based assay[15]. It was therefore not surprising that the knockdown of *XPA* alone or in combination with *MSH2* knockdown did not significantly reduce the frequency of nickase-induced GFP$^+$ cells (Fig. 4b, $P=0.18$, using a Wilcoxon U-test, for comparing *XPA* and vimentin (*VIM*) knockdowns; and $P=0.07$, using a Wilcoxon U-test, when comparing double knockdown to vimentin knockdown). These results argue that neither MSH2 nor XPA are involved in generating contractions at Cas9 nickase-induced lesions.

We reasoned that ATR inhibition may be increasing the number of expansions and contractions because DSB intermediates may form under these conditions. We therefore tested whether the NER pathway, which is known to generate DSBs on ultraviolet damage[45] and at short inverted repeats[46], could contribute to repeat instability in the absence of ATR activity. Knockdown of *XPA* in cells treated with VE-821 led to results indistinguishable from those obtained when treating cells with DMSO together with a control siRNA (Fig. 4c, $P=0.70$, using a Wilcoxon U-test). Similarly, the effect of VE-821 treatment was suppressed by *MSH2* knockdown (Fig. 4c, $P=0.71$ compared

with control DMSO and vimentin siRNA treatments, using a Wilcoxon *U*-test). These results suggest that expansions and contractions induced by the inhibition of ATR occur because of a XPA- and MSH2-dependent activity that may eventually generates DSBs.

Discussion

Many assays have been used with great success to dissect the mechanisms of repeat instability. Unfortunately, they are often slow, labour-intensive and/or cannot probe both expansions and contractions at once[15,24,33,47–49]. Here we have adapted a chromosomal-based reporter assay such that it can monitor instability in both directions within only 5 days. We show that the assay can be coupled to pharmaceutical treatments, siRNAs and cDNA overexpression, making it highly versatile and well suited for screening.

DNA nicks appear to be repaired by distinct and still poorly understood mechanisms. For example, they stimulate homology-directed repair in a human cell-based assay[50]. Intriguingly, this process is suppressed by RAD51 and BRCA2, which are required for homologous recombination at DSBs[50]. PARP inhibition also stimulates nick-induced homology-directed repair[51]. Our observation that the same PARP inhibitor has no effect on nickase-induced contraction is suggestive of a different pathway being used at CAG repeats and that DNA nicks are not the mutagenic intermediates leading to nickase-induced contractions. Furthermore, the lack of an effect when knocking down XRCC1 or inhibiting PARP1 implies that the Cas9 nickase leads to contraction via a pathway different from that of BER-generated SSBs. We cannot rule out that DNA nicks lead to contractions independently of the known pathways leading to spontaneous instability. Instead, however, we offer a model (Fig. 5) whereby the Cas9 nickase induces several nicks on the same strand within the repeat tract, thereby generating DNA gaps. This hypothesis is attractive because it provides an explanation for the repeat-length dependency of nickase-induced contractions: shorter repeats have fewer gCTG-binding sites and thus DNA gaps are not created as readily, leading to a stable tract. Together, these observations suggest that different types of DNA lesions found within the repeat tract are repaired by different pathways, which may dictate the direction of repeat instability.

DNA gaps are important intermediates in CAG repeat instability in model systems as varied as yeast and mice[52–54]. How they lead to contraction, however, has remained unclear. In our model (Fig. 5), we propose that DNA gaps caused by the Cas9 nickase are converted to contractions via an ATM-dependent mechanism—perhaps by promoting ligation of single-stranded DNA ends across a hairpin. This intermediate could be further processed or simply replicated in the following cell cycle to create a contraction. DNA gap filling, promoted by ATR, would prevent the involvement of ATM, providing an explanation for the apparent role of ATR in antagonizing ATM. When ATR signalling is compromised, an intermediate, possibly stabilized by MSH2 (ref. 55) and/or XPA[56], lingers and is processed more often by an XPA-dependent recruitment of downstream nucleases. The resulting DSB is further repaired via the same error-prone pathway that processes ZFN and Cas9-induced DSBs.

The yeast homologue of ATR, Mec1, prevents the appearance of contractions, most likely by preventing DSB formation at expanded CAG repeats[21]. Tel1, the ATM homologue, had no effect on CAG repeat instability[14]. Admittedly, budding yeast displays a bias towards contractions in wild-type cells and may therefore process CAG repeats differently than human cells. Nevertheless, it is unclear why the roles that we have uncovered here should be different than the ones uncovered in yeast. One possibility is that the mutagenic intermediates that Mec1 and Tel1 are sensing in the yeast studies were different than those involved here.

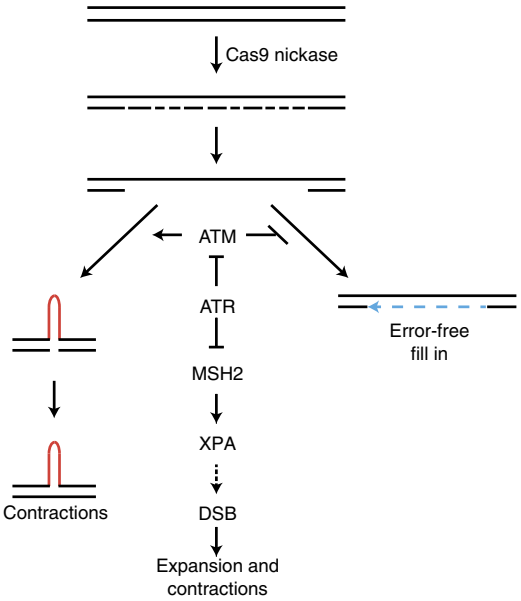

Figure 5 | Model for Cas9-nickase-induced repeat contraction.

ATR and ATM heterozygosities also have distinct effects on the instability of CGG/CCG repeats in mice. In agreement with data presented here, ATR prevents the expansion of CGG/CCG repeats both in somatic tissues as well as in non-replicating prophase I-arrested mouse oocytes[57]. The effect of ATR on contractions was not reported. *Atm*$^{+/-}$ animals, by contrast, did not display an overt somatic instability phenotype. Instead, they showed markedly increased frequencies of expansions in the male germlines[58]. The effect on contractions was not reported. The reason for these differences is currently unclear but may include the very different nature of the trinucleotide repeats studied (CAG/CTG versus CGG/CCG), and/or the difference between the human cells used here and the *in vivo* mouse model used in both previous studies. More work is required to resolve this issue.

Our results have profound implications for somatic gene editing of expanded CAG diseases. Programmable nucleases were proposed to provide a tool to shorten repeat tracts and a much needed cure[59]. Some attempts have been made to test this hypothesis using ZFNs or TALENs[24,26,60,61]. Our data caution that inducing DSBs within the repeat tract in an attempt to shrink them would also lead to repeat expansion. This would be a problem because the expansions are likely to exacerbate the disease phenotype[22,23]. An alternative may be to induce two DSBs in regions immediately flanking, but not within, the repeat tract. This approach would be prone to off target effects[62–64], may lead to the mutation of the wild-type allele, and gRNAs would have to be designed and tested for each disease locus. Our approach would be simpler, using a single gRNA that could target any of the disease loci. In addition, our data argue that only longer, pathogenic, repeat tracts are targeted for contractions; an ideal scenario as it leaves the normal allele intact.

For CAG repeat contraction to be a viable therapeutic avenue, the disease phenotypes must be reversible. There is some evidence that this is the case. Indeed, the myotonia and cardiac symptoms of a myotonic dystrophy mouse model were reversible on shutting off the expression of the pathogenic transgene[65]. Similarly, halting the expression of a spinocerebellar ataxia type 1 allele with 82 CAGs markedly improved the pathological

phenotype of Purkinje cells and reversed motor dysfunction[66]. Homology-directed replacement of an expanded CAG repeat in induced pluripotent stem cells (iPSC) derived from Huntington disease patients improved suceptibility to cell death and mitochondrial defects[67]. Removing a CGG/CCG repeat tract along with flanking sequences from the *FMR1* gene with CRISPR-Cas9 nuclease reactivated the expression of FMRP in a few iPSC clones[68]. Finally, excising expanded GAA/TTC repeats in Friedreich Ataxia fibroblasts reactivated the expression of frataxin, improved the activity of the Fe-S-containing Aconitase, and increased cellular ATP levels[69]. Together with our results, these studies offer great hope that Cas9 nickase-mediated shrinkage of expanded repeat tracts in somatic tissues may alleviate disease symptoms in patients.

Methods

Cell culture. The GFP$(CAG)_0$ and GFP$(CAG)_{101}$ cells lines were a kind gift from John H. Wilson[24]. The cells tested negative for mycoplasma using the MycoAlert detection kit (Lonza) at the start of our experiments and during the revisions of this manuscript. The GFP$(CAG)_{15}$, GFP$(CAG)_{18}$, GFP$(CAG)_{42}$, GFP$(CAG)_{50}$ and GFP$(CAG)_{270}$ were isolated from populations grown for 6 months unperturbed or after transfection with the ZFN. They did not contain mutations in the region flanking the repeat tract. The cells were maintained at 37 °C with 5% CO_2 in Dulbecco's modified Eagle's medium (DMEM) glutamax, supplemented with 10% fetal bovine serum (FBS), 100 U ml^{-1} penicillin (pen), 100 µg ml^{-1} streptomycin (strep), 15 µg ml^{-1} blasticidine and 150 µg ml^{-1} hygromycin. When the cells were destined for flow cytometry, they were kept in DMEM glutamax, with 10% of dialysed calf serum, along with pen–strep. During the long-term culturing, the unstransfected and unperturbed cells were split one to five twice a week, and the medium was supplemented with blasticidine and hygromycin to ensure continued expression of the TetR and GFP transgenes.

Plasmids and siRNA transfections. The plasmids used in this study are found in Supplementary Table 4. They are available on request. cDNA transfections were performed using 6×10^5 cells per well in 12-well plates using a total of 1 µg of DNA and Lipofectamine 2000 (Life Technologies) per well. The culture medium was replaced 6 h after transfection and 2 µg ml^{-1} of dox, diluted in DMSO, was added. Controls without dox were treated with DMSO alone. Forty-eight hours later, the medium was replaced and dox was freshly added. Flow cytometry, protein extraction and/or DNA extraction were performed after another 48 h of incubation.

The siRNAs used in this study are found in Supplementary Table 5. When transfecting with both a cDNA and a siRNA, 8×10^5 cells per well were used along with 1 µg of DNA and 20 nM of siRNAs using Lipofectamine 2000. The medium was replaced 6 h later and dox was added. Forty-eight hours after the first transfection, we performed a second siRNA transfection with RNAiMax (Life Technologies) using half of the cells present and 20 nM of siRNA. We collected the cells to assess knockdown efficiency or GFP fluorescence analysis 48 h later. When transfecting two siRNAs, we used a final siRNA concentration of 40 nM, where 20 nM of each individual siRNA were used. We found that single knockdowns at 20 nM were no different from those also containing 20 nM of the vimentin siRNA and were pooled for the statistical analyses and in the presented figures.

Pharmacological inhibitors. When using small-molecule inhibitors (Supplementary Table 6), the cells were treated as above. The medium, along with the dox and the inhibitors, was replaced after 48 h and for another 48 h of treatment. Cell cycle analysis was performed after 96 h of treatment. Briefly, the cells were fixed with 100% ethanol and treated with RNAseA (50 µg ml^{-1}) before adding propidium iodine (50 µg ml^{-1}). Flow cytometry analysis was performed as described below.

Flow cytometer and cell sorting. In preparation for flow cytometry analysis, cells were re-suspended in phosphate-buffered saline (PBS) with 1 mM EDTA to a concentration of about 10^6 cells per ml. For each condition, we measured at least 2×10^5 events using a LSRII from BD. Data analysis was done using Flowing II. FACS was performed using a FACS Aria II (BD) or MoFlo Astrios (Beckman Coulter). For single-clone analyses, we re-suspended the cells to a concentration of 2×10^6 cells per ml and sorted the GFP$^-$ and GFP$^+$ cells. The cells were then expanded in DMEM glutamax supplemented with pen–strep, blasticidine, hygromycin, 5% FBS and 5% dialysed calf serum. For viability tests, cells were treated as described above except that 96 h after the first transfection they were collected in PBS with 1 mM EDTA, and 1 µM of TO-PRO-3 was added as a dead cell marker.

Quantification of GFP$^-$ and GFP$^+$ cells. To quantify the fold increase in the number of GFP$^-$ or GFP$^+$ cells, we first established gates that contained the top or bottom 1% of GFP-expressing cells in the control treatment, for example, the nickase plasmid transfected together with an empty gRNA vector (pPN10). For each treatment or cell line, therefore, the top and bottom 1% were adjusted to take any shift in GFP expression into account. In some cases, we adjusted the voltage of the flow cytometer laser to accommodate samples with very high or very low GFP expression. This adjustment did not interfere with the quantification (Supplementary Fig. 3C,D). Once the GFP gates were established, we calculated the percentage of cells from the test population (for example, expressing both the Cas9 nickase and the gCTG) falling within these same gates. In cases where inhibitors or siRNAs were used, the control population expressed the Cas9 nickase, pPN10 and the inhibitor or siRNA. The 1% cutoffs were used to keep a balance between having enough cells for robust statistics and detecting significant fold changes[24]. This method probably underestimates the frequencies of change compared with SP-PCR (Fig. 2).

Repeat length determination and SP-PCR. To determine the repeat length of each sorted clone, we isolated DNA using the PeqGold MicroSpin Tissue DNA kit (PeqLab). The DNA was then amplified with primers oVIN-0437 and oVIN-0459 (Supplementary Table 7). Several PCR reactions were set-up with MangoTaq and the products were gel-extracted, pooled and sent for sequencing with the same primers used for the amplification. The repeat size was determined from at least two different amplification and sequencing reactions. The longest repeat size determined was used in the rare cases where the repeat length was not identical between the runs. SP-PCR was done based on the protocol described in ref. 70. Briefly, primers oVIN-0459 and oVIN-0460 were used for the amplification along with between 50 and 100 pg of genomic DNA per PCR. The products were then run on an agarose gel and transferred into a membrane. The probe was derived from a PCR product amplified with the same primers from a plasmid containing 40 repeats. The primers used to amplify the off-target loci are found in Supplementary Table 7.

Antibodies and western blotting. Protein extraction was done using RIPA buffer and proteinase inhibitor cocktail tablets (Roche, Germany) and at least 10 µg of proteins were loaded onto 6 or 10% Tris/glycine SDS polyacrylamide gels and transferred onto nitrocellulose membranes. The antibodies used in this study are found in Supplementary Table 8. An Odyssey Infrared Imager (Licor) was used for signal detection. All uncropped western blots are found in Supplementary Fig. 5.

Statistics. When determining whether there were differences in the frequency of GFP$^-$ and GFP$^+$ cells between treatments, we were unable to guarantee that the data were normally distributed using a two-tailed Kolmogorov–Smirnov test. We therefore used a two-tailed Wilcoxon *U*-test as it is non-parametric. We also performed two-tailed Student's *t*-tests, which gave similar results as the *U*-tests. The same was true when comparing length of the repeat tracts in clones sorted from different populations. We used a Poisson distribution to evaluate the total number of alleles amplified in our SP-PCR experiments based on the proportion of PCRs that did not yield a detectable product. Fisher's exact tests were used to determine whether there were changes in the number of contractions and expansions seen in the SP-PCR experiment. All statistical analyses were done using R Studio version 0.99.441. We concluded that a significant difference existed when $P < 0.05$.

Data availability. The data presented in this study are available from the corresponding author.

References

1. Wang, G. & Vasquez, K. M. Impact of alternative DNA structures on DNA damage, DNA repair, and genetic instability. *DNA Repair (Amst.)* **19,** 143–151 (2014).
2. Orr, H. T. & Zoghbi, H. Y. Trinucleotide repeat disorders. *Annu. Rev. Neurosci.* **30,** 575–621 (2007).
3. Dion, V. Tissue specificity in DNA repair: lessons from trinucleotide repeat instability. *Trends Genet.* **30,** 220–229 (2014).
4. Lopez Castel, A., Cleary, J. D. & Pearson, C. E. Repeat instability as the basis for human diseases and as a potential target for therapy. *Nat. Rev. Mol. Cell Biol.* **11,** 165–170 (2010).
5. McMurray, C. T. Mechanisms of trinucleotide repeat instability during human development. *Nat. Rev. Genet.* **11,** 786–799 (2010).
6. Usdin, K., House, N. C. & Freudenreich, C. H. Repeat instability during DNA repair: insights from model systems. *Crit. Rev. Biochem. Mol. Biol.* **50,** 142–167 (2015).
7. Lee, D. Y. & McMurray, C. T. Trinucleotide expansion in disease: why is there a length threshold? *Curr. Opin. Genet. Dev.* **26,** 131–140 (2014).
8. Mirkin, S. M. Expandable DNA repeats and human disease. *Nature* **447,** 932–940 (2007).
9. Axford, M. M. *et al.* Detection of slipped-DNAs at the trinucleotide repeats of the myotonic dystrophy type I disease locus in patient tissues. *PLoS Genet.* **9,** e1003866 (2013).
10. Schmidt, M. H. & Pearson, C. E. Disease-associated repeat instability and mismatch repair. *DNA Repair (Amst)* **38,** 117–126 (2016).

11. Su, X. A., Dion, V., Gasser, S. M. & Freudenreich, C. H. Regulation of recombination at yeast nuclear pores controls repair and triplet repeat stability. *Genes Dev.* **29,** 1006–1017 (2015).
12. Marcadier, J. L. & Pearson, C. E. Fidelity of primate cell repair of a double-strand break within a (CTG).(CAG) tract. Effect of slipped DNA structures. *J. Biol. Chem.* **278,** 33848–33856 (2003).
13. Richard, G. F., Dujon, B. & Haber, J. E. Double-strand break repair can lead to high frequencies of deletions within short CAG/CTG trinucleotide repeats. *Mol. Gen. Genet.* **261,** 871–882 (1999).
14. Sundararajan, R., Gellon, L., Zunder, R. M. & Freudenreich, C. H. Double-strand break repair pathways protect against CAG/CTG repeat expansions, contractions and repeat-mediated chromosomal fragility in Saccharomyces cerevisiae. *Genetics* **184,** 65–77 (2010).
15. Lin, Y., Dion, V. & Wilson, J. H. Transcription promotes contraction of CAG repeat tracts in human cells. *Nat. Struct. Mol. Biol.* **13,** 179–180 (2006).
16. Jung, J. & Bonini, N. CREB-binding protein modulates repeat instability in a Drosophila model for polyQ disease. *Science* **315,** 1857–1859 (2007).
17. Kovtun, I. V. *et al.* OGG1 initiates age-dependent CAG trinucleotide expansion in somatic cells. *Nature* **447,** 447–452 (2007).
18. Mollersen, L. *et al.* Neil1 is a genetic modifier of somatic and germline CAG trinucleotide repeat instability in R6/1 mice. *Hum. Mol. Genet.* **21,** 4939–4947 (2012).
19. Yang, Z., Lau, R., Marcadier, J. L., Chitayat, D. & Pearson, C. E. Replication inhibitors modulate instability of an expanded trinucleotide repeat at the myotonic dystrophy type 1 disease locus in human cells. *Am. J. Hum. Genet.* **73,** 1092–1105 (2003).
20. Hubert, Jr L., Lin, Y., Dion, V. & Wilson, J. H. Topoisomerase 1 and single-strand break repair modulate transcription-induced CAG repeat contraction in human cells. *Mol. Cell. Biol.* **31,** 3105–3112 (2011).
21. Lahiri, M., Gustafson, T. L., Majors, E. R. & Freudenreich, C. H. Expanded CAG repeats activate the DNA damage checkpoint pathway. *Mol. Cell* **15,** 287–293 (2004).
22. Budworth, H. *et al.* Suppression of somatic expansion delays the onset of pathophysiology in a mouse model of Huntington's disease. *PLoS Genet.* **11,** e1005267 (2015).
23. Wheeler, V. C. *et al.* Mismatch repair gene Msh2 modifies the timing of early disease in Hdh(Q111) striatum. *Hum. Mol. Genet.* **12,** 273–281 (2003).
24. Santillan, B. A., Moye, C., Mittelman, D. & Wilson, J. H. GFP-based fluorescence assay for CAG repeat instability in cultured human cells. *PLoS ONE* **9,** e113952 (2014).
25. Chatterjee, N., Lin, Y., Yotnda, P. & Wilson, J. H. Environmental stress induces trinucleotide repeat mutagenesis in human cells by Alt-nonhomologous end joining repair. *J. Mol. Biol.* **428,** 2978–2980 (2016).
26. Mittelman, D. *et al.* Zinc-finger directed double-strand breaks within CAG repeat tracts promote repeat instability in human cells. *Proc. Natl Acad. Sci. USA* **106,** 9607–9612 (2009).
27. Jinek, M. *et al.* A programmable dual-RNA-guided DNA endonuclease in adaptive bacterial immunity. *Science* **337,** 816–821 (2012).
28. Sternberg, S. H. & Doudna, J. A. Expanding the biologist's toolkit with CRISPR-Cas9. *Mol. Cell* **58,** 568–574 (2015).
29. Mali, P. *et al.* RNA-guided human genome engineering via Cas9. *Science* **339,** 823–826 (2013).
30. Cong, L. *et al.* Multiplex genome engineering using CRISPR/Cas systems. *Science* **339,** 819–823 (2013).
31. Panigrahi, G. B., Lau, R., Montgomery, S. E., Leonard, M. R. & Pearson, C. E. Slipped (CTG)*(CAG) repeats can be correctly repaired, escape repair or undergo error-prone repair. *Nat. Struct. Mol. Biol.* **12,** 654–662 (2005).
32. Hou, C., Chan, N. L., Gu, L. & Li, G. M. Incision-dependent and error-free repair of (CAG)(n)/(CTG)(n) hairpins in human cell extracts. *Nat. Struct. Mol. Biol.* **16,** 869–875 (2009).
33. Monckton, D. G., Wong, L. J., Ashizawa, T. & Caskey, C. T. Somatic mosaicism, germline expansions, germline reversions and intergenerational reductions in myotonic dystrophy males: small pool PCR analyses. *Hum. Mol. Genet.* **4,** 1–8 (1995).
34. Caldecott, K. W., Aoufouchi, S., Johnson, P. & Shall, S. XRCC1 polypeptide interacts with DNA polymerase beta and possibly poly (ADP-ribose) polymerase, and DNA ligase III is a novel molecular 'nick-sensor' in vitro. *Nucleic Acids Res.* **24,** 4387–4394 (1996).
35. Horton, J. K. *et al.* XRCC1 and DNA polymerase beta in cellular protection against cytotoxic DNA single-strand breaks. *Cell Res.* **18,** 48–63 (2008).
36. Costanzo, V. *et al.* An ATR- and Cdc7-dependent DNA damage checkpoint that inhibits initiation of DNA replication. *Mol. Cell* **11,** 203–213 (2003).
37. Prevo, R. *et al.* The novel ATR inhibitor VE-821 increases sensitivity of pancreatic cancer cells to radiation and chemotherapy. *Cancer Biol. Ther.* **13,** 1072–1081 (2012).
38. Marechal, A. & Zou, L. DNA damage sensing by the ATM and ATR kinases. *Cold Spring Harb. Perspect. Biol.* **5,** a012716 (2013).
39. Golding, S. E. *et al.* Improved ATM kinase inhibitor KU-60019 radiosensitizes glioma cells, compromises insulin, AKT and ERK prosurvival signaling, and inhibits migration and invasion. *Mol. Cancer Ther.* **8,** 2894–2902 (2009).
40. Du, J., Campau, E., Soragni, E., Jespersen, C. & Gottesfeld, J. M. Length-dependent CTG.CAG triplet-repeat expansion in myotonic dystrophy patient-derived induced pluripotent stem cells. *Hum. Mol. Genet.* **22,** 5276–5287 (2013).
41. Manley, K., Shirley, T. L., Flaherty, L. & Messer, A. Msh2 deficiency prevents in vivo somatic instability of the CAG repeat in Huntington disease transgenic mice. *Nat. Genet.* **23,** 471–473 (1999).
42. Nakatani, R., Nakamori, M., Fujimura, H., Mochizuki, H. & Takahashi, M. P. Large expansion of CTG*CAG repeats is exacerbated by MutSbeta in human cells. *Sci. Rep.* **5,** 11020 (2015).
43. Seriola, A. *et al.* Huntington's and myotonic dystrophy hESCs: down-regulated trinucleotide repeat instability and mismatch repair machinery expression upon differentiation. *Hum. Mol. Genet.* **20,** 176–185 (2011).
44. Hubert, Jr L., Lin, Y., Dion, V. & Wilson, J. H. Xpa deficiency reduces CAG trinucleotide repeat instability in neuronal tissues in a mouse model of SCA1. *Hum. Mol. Genet.* **20,** 4822–4830 (2011).
45. Bradley, M. O. & Taylor, V. I. DNA double-strand breaks induced in normal human cells during the repair of ultraviolet light damage. *Proc. Natl Acad. Sci. USA* **78,** 3619–3623 (1981).
46. Lu, S. *et al.* Short inverted repeats are hotspots for genetic instability: relevance to cancer genomes. *Cell Rep.* **10,** 1674–1680 (2015).
47. Cleary, J. D., Nichol, K., Wang, Y. H. & Pearson, C. E. Evidence of cis-acting factors in replication-mediated trinucleotide repeat instability in primate cells. *Nat. Genet.* **31,** 37–46 (2002).
48. Claassen, D. A. & Lahue, R. S. Expansions of CAG.CTG repeats in immortalized human astrocytes. *Hum. Mol. Genet.* **16,** 3088–3096 (2007).
49. Pelletier, R., Farrell, B. T., Miret, J. J. & Lahue, R. S. Mechanistic features of CAG*CTG repeat contractions in cultured cells revealed by a novel genetic assay. *Nucleic Acids Res.* **33,** 5667–5676 (2005).
50. Davis, L. & Maizels, N. Homology-directed repair of DNA nicks via pathways distinct from canonical double-strand break repair. *Proc. Natl Acad. Sci. USA* **111,** E924–E932 (2014).
51. Metzger, M. J., Stoddard, B. L. & Monnat, Jr R. J. PARP-mediated repair, homologous recombination, and back-up non-homologous end joining-like repair of single-strand nicks. *DNA Repair (Amst.)* **12,** 529–534 (2013).
52. House, N. C., Yang, J. H., Walsh, S. C., Moy, J. M. & Freudenreich, C. H. NuA4 initiates dynamic histone H4 acetylation to promote high-fidelity sister chromatid recombination at postreplication gaps. *Mol. Cell* **55,** 818–828 (2014).
53. Daee, D. L., Mertz, T. & Lahue, R. S. Postreplication repair inhibits CAG.CTG repeat expansions in *Saccharomyces cerevisiae*. *Mol. Cell. Biol.* **27,** 102–110 (2007).
54. Kovtun, I. V. & McMurray, C. T. Trinucleotide expansion in haploid germ cells by gap repair. *Nat. Genet.* **27,** 407–411 (2001).
55. Pearson, C. E., Ewel, A., Acharya, S., Fishel, R. A. & Sinden, R. R. Human MSH2 binds to trinucleotide repeat DNA structures associated with neurodegenerative diseases. *Hum. Mol. Genet.* **6,** 1117–1123 (1997).
56. Lin, Y. & Wilson, J. H. Nucleotide excision repair, mismatch repair, and R-loops modulate convergent transcription-induced cell death and repeat instability. *PLoS ONE* **7,** e46807 (2012).
57. Entezam, A. & Usdin, K. ATR protects the genome against CGG.CCG-repeat expansion in Fragile X premutation mice. *Nucleic Acids Res* **36,** 1050–1056 (2008).
58. Entezam, A. & Usdin, K. ATM and ATR protect the genome against two different types of tandem repeat instability in Fragile X premutation mice. *Nucleic Acids Res.* **37,** 6371–6377 (2009).
59. Richard, G. F. Shortening trinucleotide repeats using highly specific endonucleases: a possible approach to gene therapy? *Trends Genet.* **31,** 177–186 (2015).
60. Liu, G., Chen, X., Bissler, J. J., Sinden, R. R. & Leffak, M. Replication-dependent instability at (CTG) x (CAG) repeat hairpins in human cells. *Nat. Chem. Biol.* **6,** 652–659 (2010).
61. Richard, G. F. *et al.* Highly specific contractions of a single CAG/CTG trinucleotide repeat by TALEN in yeast. *PLoS ONE* **9,** e95611 (2014).
62. Cho, S. W. *et al.* Analysis of off-target effects of CRISPR/Cas-derived RNA-guided endonucleases and nickases. *Genome Res.* **24,** 132–141 (2014).
63. Kuscu, C., Arslan, S., Singh, R., Thorpe, J. & Adli, M. Genome-wide analysis reveals characteristics of off-target sites bound by the Cas9 endonuclease. *Nat. Biotechnol.* **32,** 677–683 (2014).
64. Tsai, S. Q. *et al.* GUIDE-seq enables genome-wide profiling of off-target cleavage by CRISPR-Cas nucleases. *Nat. Biotechnol.* **33,** 187–197 (2015).
65. Mahadevan, M. S. *et al.* Reversible model of RNA toxicity and cardiac conduction defects in myotonic dystrophy. *Nat. Genet.* **38,** 1066–1070 (2006).

66. Zu, T. *et al.* Recovery from polyglutamine-induced neurodegeneration in conditional SCA1 transgenic mice. *J. Neurosci.* **24,** 8853–8861 (2004).
67. An, M. C. *et al.* Genetic correction of Huntington's disease phenotypes in induced pluripotent stem cells. *Cell Stem Cell* **11,** 253–263 (2012).
68. Park, C. Y. *et al.* Reversion of FMR1 methylation and silencing by editing the triplet repeats in fragile X iPSC-derived neurons. *Cell Rep.* **13,** 234–241 (2015).
69. Li, Y. *et al.* Excision of expanded gaa repeats alleviates the molecular phenotype of Friedreich's ataxia. *Mol. Ther.* **23,** 1055–1065 (2015).
70. Dion, V., Lin, Y., Hubert, Jr L., Waterland, R. A. & Wilson, J. H. Dnmt1 deficiency promotes CAG repeat expansion in the mouse germline. *Hum. Mol. Genet.* **17,** 1306–1317 (2008).

Acknowledgements

We thank F. Hamaratoglu, J.H. Wilson and members of the Dion laboratory for helpful discussions. H. Ferreira, G. Gourdon, F. Hamaratoglu, J. E. Martin, M. Op, A. Orioli and G.-F. Richard critically read the manuscript. We thank J.H. Wilson and J. Lingner for reagents; P. Nunes and A. Feola for cloning some of the gRNA vectors; and O. Rodriguez Lima for blindly quantifying the SP-PCR blots. This work is supported by a Swiss National Science Foundation professorship (#144789) and by Gebert Rüf Stiftung and UNISCIENTIA STIFTUNG within the programme «Rare Diseases – New Approaches» (GRS-060/14) to V.D.

Author contributions

Everyone contributed to performing the experiments and analysing the results. C.C. and V.D. designed the experiments and wrote the paper.

Additional information

Supplementary Information accompanies this paper at http://www.nature.com/naturecommunications

Competing financial interests: Procedure ongoing for European Patent application number EP16165203.7.

Reprints and permission information is available online at http://npg.nature.com/reprintsandpermissions/

How to cite this article: Cinesi, C. *et al.* Contracting CAG/CTG repeats using the CRISPR-Cas9 nickase. *Nat. Commun.* **7**, 13272 doi: 10.1038/ncomms13272 (2016).

Publisher's note: Springer Nature remains neutral with regard to jurisdictional claims in published maps and institutional affiliations.

This work is licensed under a Creative Commons Attribution 4.0 International License. The images or other third party material in this article are included in the article's Creative Commons license, unless indicated otherwise in the credit line; if the material is not included under the Creative Commons license, users will need to obtain permission from the license holder to reproduce the material. To view a copy of this license, visit http://creativecommons.org/licenses/by/4.0/

© The Author(s) 2016

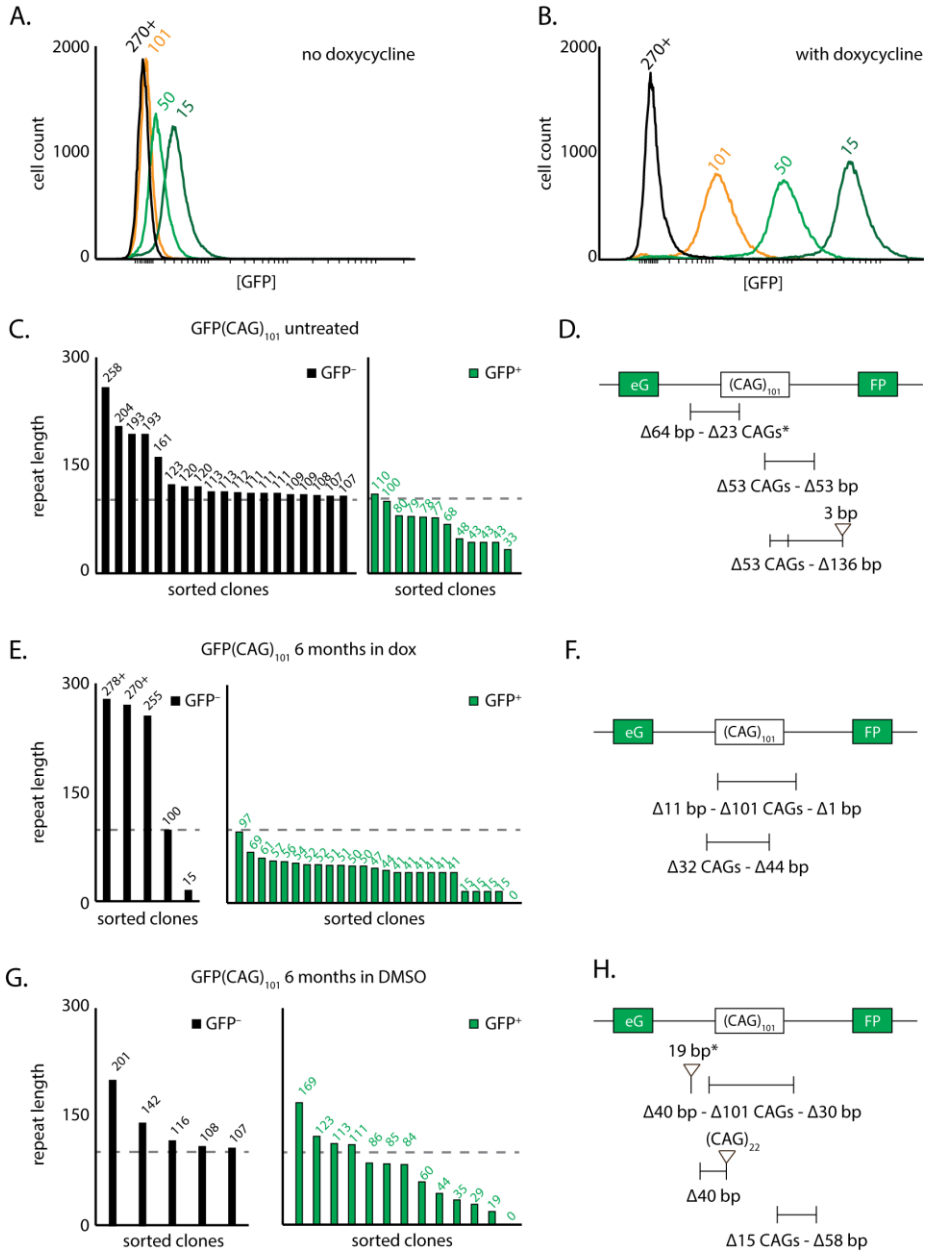

Supplementary Fig. 1: *Characterization of the GFP reporter assay and GFP⁻ and GFP⁺ cells isolated from GFP(CAG)$_{101}$.* A) Profile of GFP intensity in three cell lines isolated by FACS after six months of culturing compared to the starting population of GFP(CAG)$_{101}$. The repeat length in each clone is marked above the flow cytometry profiles. B) Same as A, but in the presence of 2µg/ml dox for 5 days. C) Repeat length for clones isolated from the GFP⁻ and GFP⁺ populations from GFP(CAG)$_{101}$ cells. The distributions of repeat lengths between GFP⁻ and GFP⁺ cells were significantly different (P=1x10^{-5}). D) Schematic representation of clones from C with mutations in the flanking sequences. *: Three different clones were isolated with the same deletion, two with 78 repeats, one with 77. E) Same as C, but with clones cultured in the presence of dox for 6 months. The distributions of repeat lengths between GFP⁻ and GFP⁺ cells were significantly different (P=0.025). F) Schematic representation of the deletions found after 6 months of culturing in the presence of dox. G) Same as E, except that the cells were exposed to DMSO. The distributions of repeat lengths between GFP⁻ and GFP⁺ cells were significantly different (P=0.035). H) Same as F, but for clones cultured in DMSO. *: The 19bp insertion is a direct repeat of the 19bp immediately found before the insertion.

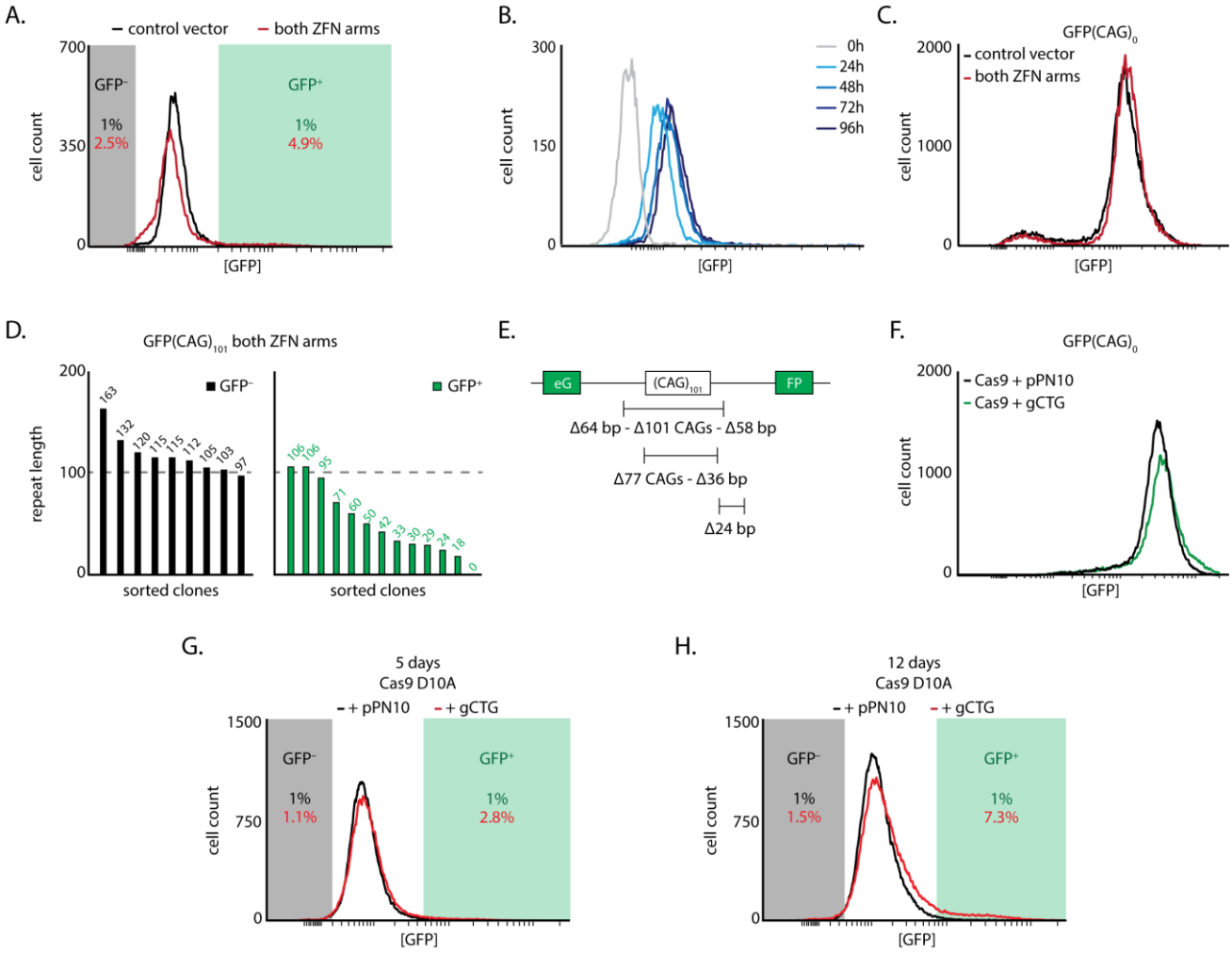

Supplementary Fig. 2: *Assay optimization, the effect of ZFN and Cas9 nuclease on GFP(CAG)$_0$ and analysis of GFP$^-$ and GFP$^+$ clones collected after ZFN treatment.* A) Example of data quantification. The GFP$^-$ and GFP$^+$ gates are set as the top or bottom 1% of the control population, in this case transfected with pcDNA3.1. The same gates are then used to determine the proportion of cells from the treated population that falls within these set gates have changed expression. B) Flow cytometry profile of cells treated with dox for an increasing amount of time. C) One of 10 flow cytometry experiments of GFP(CAG)$_0$ cells transfected with vectors expressing both ZFN arms or with a control vector (pcDNA3.1 Zeo). D) Repeat tract lengths in GFP$^-$ and GFP$^+$ clones after treatment of GFP(CAG)$_{101}$ cells with both ZFN arms. Dashed grey bars: repeat size in the starting population: 101 CAG repeats. The distributions of repeat lengths between GFP$^-$ and GFP$^+$ cells were significantly different ($P=5x10^{-4}$) E) Schematic representation of clones with deletions in the sequences surrounding the CAG repeat. F) One of two flow cytometry experiments comparing cells expressing the Cas9 nuclease and the gCTG or transfected with an empty gRNA vector (pPN10). G and H) Representative flow cytometry profiles showing that the number of GFP$^+$ cells increases after two more transfections over a total period of 12 days compared to our standard 5-day treatment.

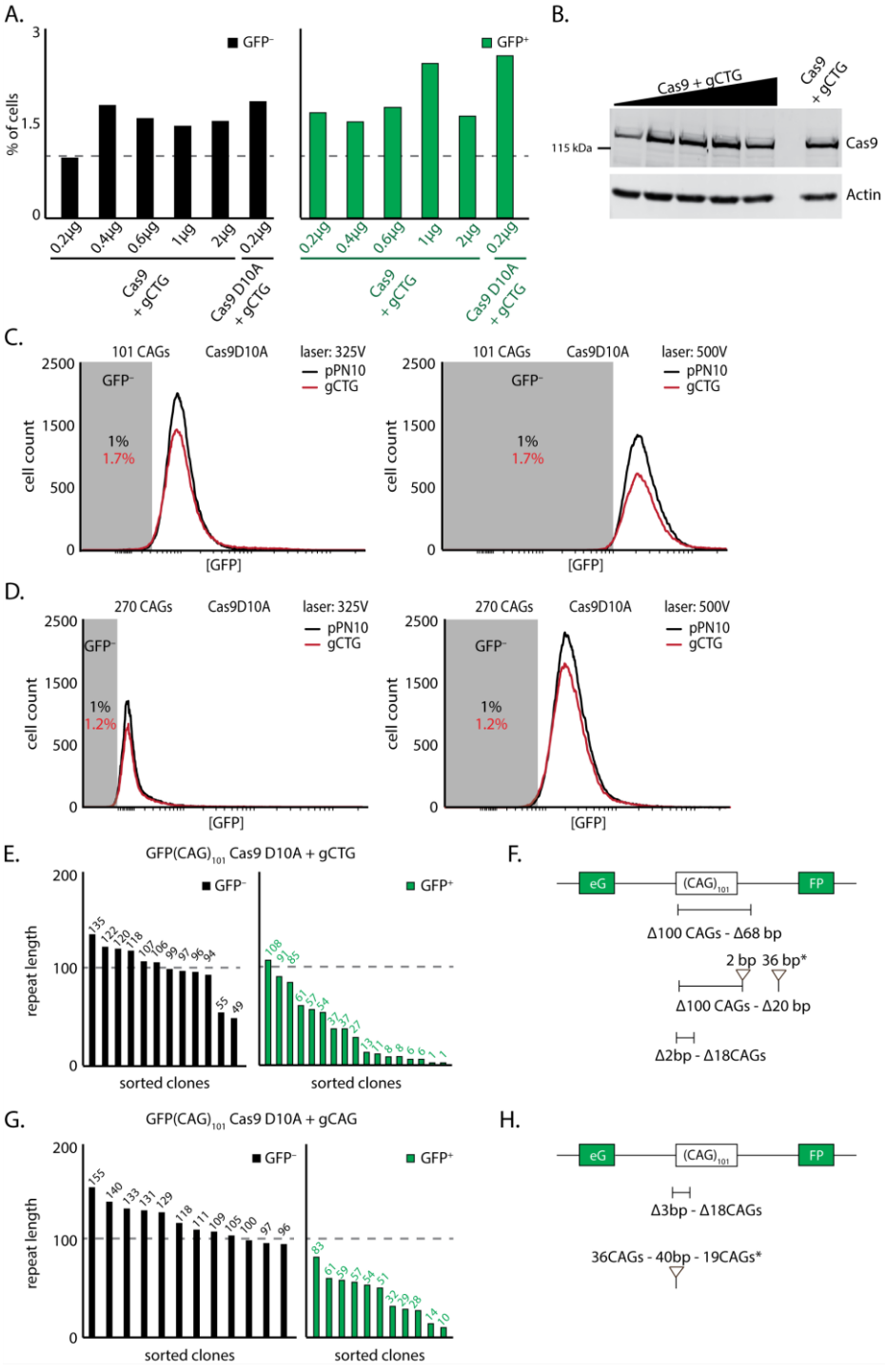

Supplementary Fig. 3: *Cas9 nickase induces repeat instability with a bias towards contractions.* A) Expression levels of the Cas9 nuclease and Cas9 nickase do not account for the different effects of these two enzymes on the number of GFP$^-$ and GFP$^+$ generated. Dashed line: dimmest (GFP$^-$) or brightest (GFP$^+$) 1% of the cells transfected with the indicated amount of the Cas9 nickase or nuclease vector together with the empty gRNA plasmid. B) Western of Cas9 levels for the experiment presented in (A). C) Flow cytometry data results from GFP$(CAG)_{101}$ cells transfected with the Cas9 nickase and with either pPN10 or gCTG-expressing vector showing that changing the laser intensity, and thus the apparent GFP expression, does not change the results of the quantifications. D) As in (C) but with GFP$(CAG)_{270}$. E) Size of repeat in clones isolated from GFP$(CAG)_{101}$ cells transfected with the gCTG and the Cas9-nickase expressing vectors. The distributions of repeat lengths between GFP$^-$ and GFP$^+$ cells were significantly different ($P=2x10^{-4}$). F) Schematic of the rearrangements from in 3 GFP$^+$ clones from (E). *: This clone contained a complex rearrangement with the 36bp insertion that includes a 10bp insertion followed by two direct repeats of 13bp corresponding to the last 13bp prior to the insertion. G) Same as in E, but with cells transfected with the Cas9 nickase together with gCAG. The distributions of repeat lengths between GFP$^-$ and GFP$^+$ cells were significantly different ($P=1.5x10^{-6}$). H) Schematic of the clones from (G) that had changes in the sequences flanking the repeat. *: This clone had a 19 CAG repeat expansions downstream of a duplication that included the 40bp immediately upstream of the repeat tract and 36 more CAGs.

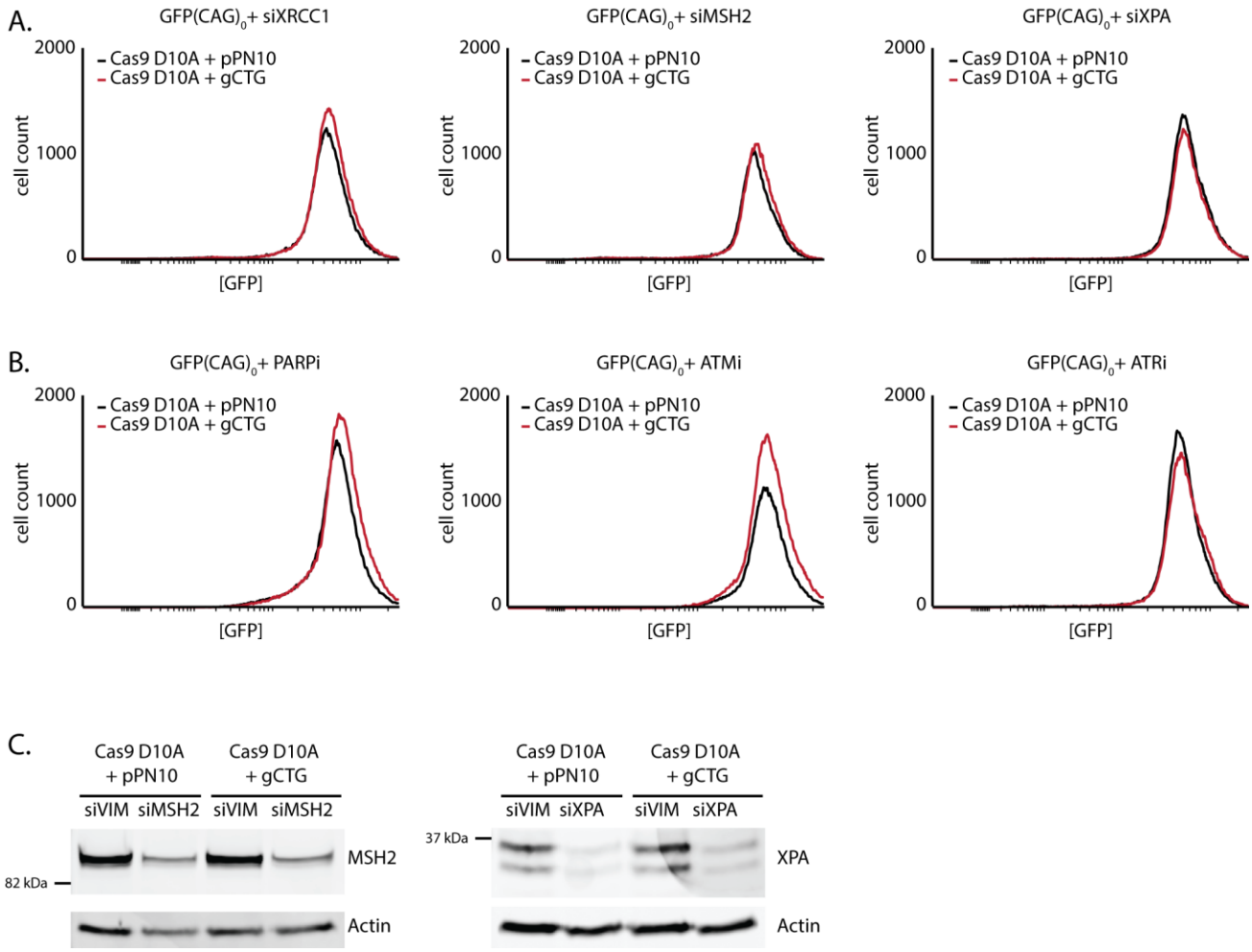

Supplementary Fig. 4: *Effect of siRNA and inhibitor treatments on GFP(CAG)$_0$ cells and knockdown efficiency*. A) Representative flow cytometry plots from siRNA knockdown experiments (*MSH2*: n=6; *XPA*: n=6; *XRCC1*: n=4). B) Representative flow cytometry results for inhibitor experiments (ATMi: n=5; ATRi: n=5; PARPi: n=4). C) Western blot showing knockdown efficiency by the *MSH2* and XPA siRNAs.

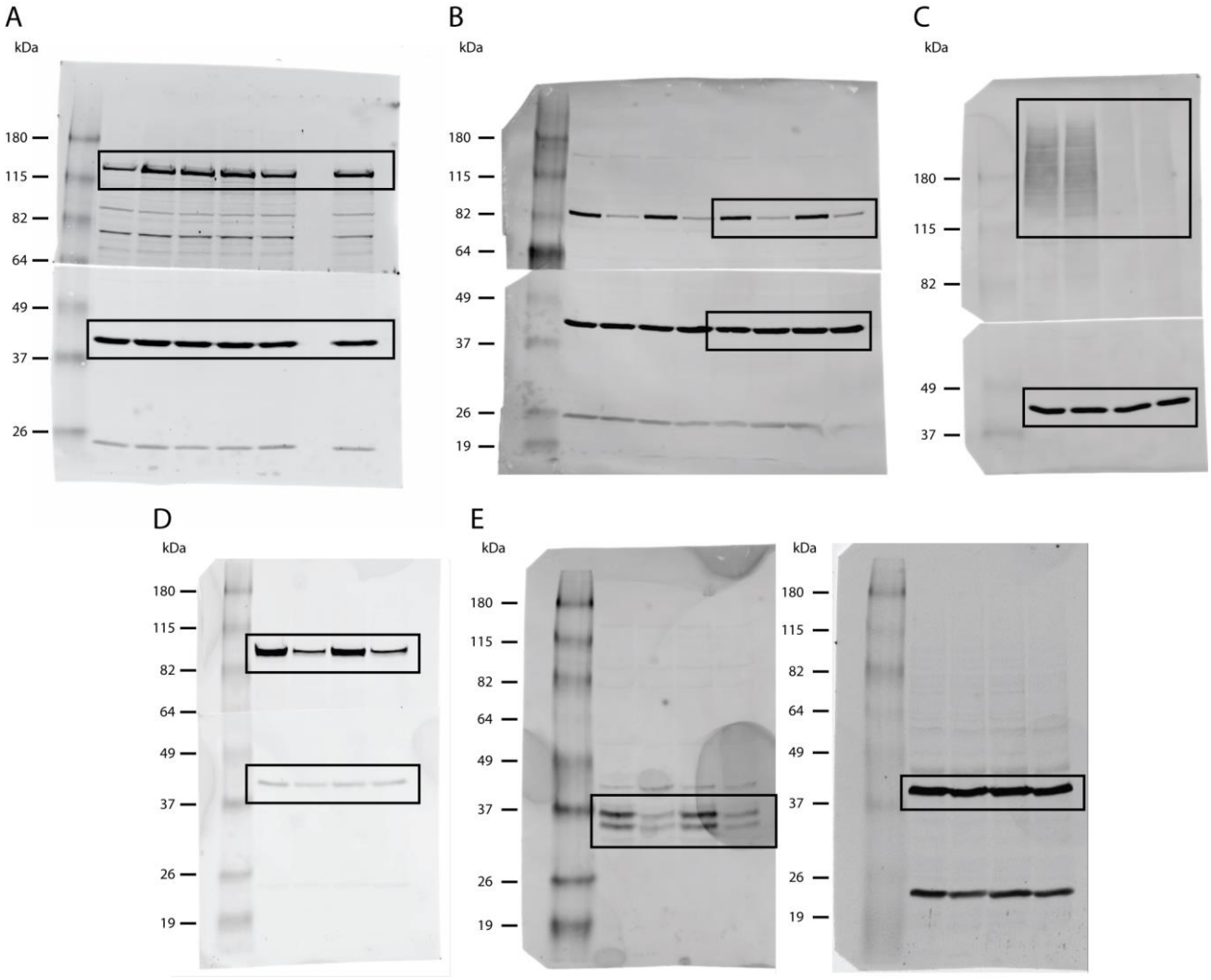

Supplementary Fig. 5: *Full size western blots.* A) Cas9 (top) and ACTIN (bottom) immunoblots from Supplementary Fig. 3B. B) XRCC1 (top) and ACTIN (bottom) blots from Fig. 3A. C) PARP (top) and ACTIN (bottom) western blots from Fig. 3B. D) MSH2 (top) and ACTIN (bottom) immunoblots from Fig. 4C. E) XPA (left) and ACTIN (right) immunoblots from Supplementary Fig. 4C. Boxes indicate the bands that were cropped.

Supplementary Tables

Treatment		Viability %*
pcDNA		76.6
ZFN 50		81.6
ZFN 51		79.8
ZFNs		75
Cas9 + pPN10		76.9
Cas9 + gDM1d		76.1
Cas9 + gCTG		85.4
Cas9 D10A + pPN10		77.3
Cas9 D10A + gDM1d		75.8
Cas9 D10A + gCTG	DMSO	81
	ATRi	82.6
	ATMi	77.2
	PARPi	75.9

Supplementary Table 1: Cell viability after transfection with the indicated plasmids and treatments.
*: derived from three experiments.

Locus	Sequence
AR	$(CAG)_{20\text{-}21}$-CAA GAG ACT AGC CCC AGG $(CAG)_5$
ATN1	CAG-CAA-CAG-CAA-$(CAG)_{15\text{-}16}$
ATXN1	$(CAG)_{12}$-CAT-CAG-CAT-$(CAG)_{11\text{-}12}$
DMPK	$(CTG)_5$
PPP2R2B	$(CAG)_{10}$
TBP	$(CAG)_3$-$(CAA)_3$-$(CAG)_9$-CAA-CAG-CAA-$(CAG)_{18\text{-}19}$-CAA-CAG
TCF4	$(CTG)_{14\text{-}17}$-$(CTC)_6$

Supplementary Table 2: Sequences of loci with CAG/CTG repeats in GFP$(CAG)_{101}$. Pure stretches are designated with parenthesis with the number of repeat as subscript. When two numbers are present, they refer to the number of repeats present on each allele.

Treatment	inhibitor	<2n	G1	S	G2	>4n
Cas9 D10A	DMSO	4.3 ± 0.5*	50.0 ± 1.1	18.8 ± 0.7	20.2 ± 1.4	6.2 ± 0.8
	ATMi	7.5 ± 0.8	34.9 ± 1.6	15.3 ± 1.7	37.2 ± 1.6	4.9 ± 1
	ATRi	2.0 ± 0.1	41.4 ± 1.4	20.9 ± 2.5	25.4 ± 2.2	10.3 ± 3
	PARPi	5.0 ± 0.4	40.7 ± 1.9	19.0 ± 2.2	30.0 ± 4.9	5.3 ± 1

Supplementary Table 3: Cell cycle analysis upon inhibitor treatment and Cas9 D10A transfection.
*: n=4 for each treatment. Average % of cells ± standard deviation.

Name	Content	Source
pcDNA3.1 Zeo	Empty vector	Life Technologies
pcDNA3.3-TOPO - Cas9_D10A	Cas9 D10A	[1] via Addgene
pcDNA3.3-TOPO hCas9	human Cas9	[1] via Addgene
pPN10	Empty gRNA	This study
pPN10-gCAG	pPN10 with $(CAG)_6$ gRNA – PAM: CAG	This study
pPN10-gCTG	pPN10 with $(CTG)_6$ gRNA – PAM: CTG	This study
pPN10-gDM1d	pPN10 with gRNA against the 3' UTR of the *DMPK* gene target: TGCGAACCAACGATAGGTG PAM: GGG	This study
pZFN50	Single ZFN arm: 50	[2]
pZFN51	Single ZFN arm: 51	[2]

Supplementary Table 4: Plasmids using in this study. All plasmids created here are available upon request.

siRNA	Target	Sequence	Reference
siVIN-0001	*VIM*	GAAUGGUACAAAUCCAAGU	[3]
siVIN-0002	*MSH2*	UCUGCAGAGUGUUGUGCUU	[3]
siVIN-0003	*XPA*	GCUACUGGAGGCAUGGCUA	[3]
siVIN-0062	*XRCC1*	CAGUUUGUGAUCACAGCACAGGAAU	[4]

Supplementary Table 5: siRNAs used in this study.

Name inhibitor	Target	Concentration
Oliparib	PARP1/2	1 µM
KU60019	ATM	1 µM
VE-821	ATR	1 µM

Supplementary Table 6: Inhibitors used, their known target, and the concentration used in our experiments.

Primer	Locus	Sequence
oVIN-0437	Pem1 intron in the GFP cassette	TACCAGGACAGCAGTGGTCA
oVIN-0459	Pem1 intron in the GFP cassette	AAGAGCTTCCCTTTACACAACG
oVIN-0460	Pem1 intron in the GFP cassette	TCTGCAAATTCAGTGATGC
oVIN-1251	DMPK	GAGCGTGGGTCTCCGCCCAG
oVIN-1252	DMPK	CACTTTGCGAACCAACGATA
oVIN-1255	ATN1	ACTCAGCCTTCTCTCCCATC
oVIN-1256	ATN1	TGTAGGACACCTGGCTGTGA
oVIN-1257	AR	TAGGGCTGGGAAGGGTCTAC
oVIN-1258	AR	CTCTGGGACGCAACCTCTCT
oVIN-1259	ATXN1	TTCCAGTTCATTGGGTCCTC
oVIN-1260	ATXN1	GTGTGTGGGATCATCGTCTG
oVIN-1269	TBP	TTCTCCTTGCTTTCCACAGG
oVIN-1270	TBP	GGGGAGGGATACAGTGGAGT
oVIN-1273	PPP2R2B	GCAGCAAAGAGCAGCCGCAG
oVIN-1274	PPP2R2B	CTGGTCCCACGGGAGGGCGG

Supplementary Table 7: Primers used here with the locus targeted.

Antibody	Species	Dilution	Source	Reference
Anti-Actin	Rabbit	1:2000	Sigma-Aldrich	A2066-.2ML
Anti-CRISPR-Cas9	Rabbit	1:1000	Abcam	ab204448
Anti-MSH2 [3A2B8C]	Mouse	1:2000	Abcam	ab52266
Anti-PAR	Mouse	1:1000	Amsbio	4335-AMC-050
Anti-XPA [5F12]	Mouse	1:2000	Abnova	MAB6747
Anti-XRCC1 [33-2-5]	Mouse	1:1000	Abcam	ab1838

Supplementary Table 8: List of antibodies used, the dilution that we used for western blotting, the source and reference number.

Supplementary references

1. Mali, P. et al. RNA-guided human genome engineering via Cas9. *Science* **339**, 823-6 (2013).
2. Santillan, B.A., Moye, C., Mittelman, D. & Wilson, J.H. GFP-based fluorescence assay for CAG repeat instability in cultured human cells. *PLoS One* **9**, e113952 (2014).
3. Lin, Y., Dion, V. & Wilson, J.H. Transcription promotes contraction of CAG repeat tracts in human cells. *Nat Struct Mol Biol* **13**, 179-80 (2006).
4. Hubert, L., Jr., Lin, Y., Dion, V. & Wilson, J.H. Topoisomerase 1 and single-strand break repair modulate transcription-induced CAG repeat contraction in human cells. *Mol Cell Biol* **31**, 3105-12 (2011).

Chapter III

Cas9 nickase effect in patient-derived cells and *in vivo*

III.I Introduction

We previously showed that the Cas9 nickase can induce contractions in a cell line carrying 100 repeats. Although useful to uncover the basic mechanism of repeat instability, the system used was not a disease model. Thus, we tested the effect of the Cas9 nickase on expanded CAG repeat tracts in patient sizes. The use of DM1 and HD patient derived cells will determine the activity of Cas9 nickase on longer repeats. Since a viral infection technique showed a stronger efficiency in integrating exogenous DNA into the genome compared to transfection methods, the Cas9 nickase coding sequence can be packed into lentiviral vectors. This experiment would determine whether the Cas9 nickase is effective in contracting expanded repeats in *DMPK* and *HTT* loci.

For therapeutic purposes, it is fundamental to determine whether the Cas9 nickase can be used to improve pathogenic symptoms *in vivo* and be delivered via a gene therapy approach. The efficiency of the Cas9 nickase in inducing repeat contractions and reversing the pathogenic phenotype in specific affected tissues are essential steps that need to be investigated. To test a gene therapy approach and the activity of Cas9 nickase *in vivo*, DM1 and HD mouse models were injected with AAV expressing Cas9 nickase and gRNA. This experiment would determine the feasibility of the Cas9 nickase in curing expanded TNR patients with a gene therapy approach.

Plasmids and cloning

Plasmids and primers used in this study are listed in Table III.II.1 and Table III.II.2.

The lentiviral vector expressing the Cas9 nickase for viral production was obtained from Addgene (Addgene plasmid #63593; http://n2t.net/addgene:63593; RRID:Addgene_63593), here referred as bVIN-478. To produce the lentiviral vector containing gCTG (bVIN-418), the gRNA sequence was cloned into pLenti X1 Puro DEST (694-6), (Addgene plasmid #17297; http://n2t.net/addgene:17297; RRID:Addgene_17297) vector by the use of Gateway®Technology (Invitrogen, Carlsbad, CA), for 3rd generation lentivirus packaging system (Campeau et al. 2009). The U6 promoter linked to gCTG sequence was amplified with primers oVIN-1374 and oVIN-1375, and flanked by the attB-sites. A BP reaction was then performed to generate an entry clone, which was successively cloned into the destination vector using LR Clonase (Invitrogen, Carlsbad, CA).

Table III.II.1 List of plasmids used in this study.

Name	Alias	Content	Description	Reference
bVIN-235	pDONR221	ChlR, ccdB	Donor plasmid for entry clone	Addgene plasmid #2394
bVIN-321	pPN10-gCTG	gRNA target to (CTG)6	gCTG expressing vector under U6 promoter	(Cinesi et al. 2016)
bVIN-374	pMD2.G	pMD2.G + VSV-G	3rd generation lentiviral packaging plasmid	(Dull et al. 1998)
bVIN-375	pRSV-Rev	pRSV-Rev	3rd generation lentiviral packaging plasmid	(Dull et al. 1998)
bVIN-376	pMDLg/pRRE	pMD + GAG/POL	3rd generation lentiviral packaging plasmid	(Dull et al. 1998)
bVIN-387	pLenti X1 Puro DEST	Empty vector	3rd gen Empty vector for Lentiviral production	(Campeau et al. 2009)
bVIN-418	pLenti-Puro-gCTG	U6 promoter and gCTG	3rd gen Lenti-gCTG production	This study
bVIN-478	pLenti-Cas9(D10A)-Blast	Cas9 D10A	3rd gen Lenti-Cas9-D10A production	(Sanjana, Shalem, and Zhang 2014)

Table III.II.2 Primer list used in this study

Name	Structure	Fragment amplified	Sequence	Reference
oVIN-100	10 CAG repeats	SP-PCR probe	AGCAGCAGCAGCAGCAGCAGCAGCAGC	(Dion et al. 2008)
oVIN-1663	For: Gag	*GAG* gene	GGAGCTAGAACGATTCGCAGTTA	(Salmon and Trono 2007)
oVIN-1664	Rev: Gag		GGTGTAGCTGTCCCAGTATTTGTC	
oVIN-1665	For: WPRE	*WPRE* gene	GGCACTGACAATTCCGTGGT	(Salmon and Trono 2007)
oVIN-1666	Rev: WPRE		AGGGACGTAGCAGAAGGACG	
oVIN-2018	For: Albumin	*ALB* gene	GCTGTCATCTCTTGTGGGCTGT	(Salmon and Trono 2007)
oVIN-2019	Rev: Albumin		ACTCATGGGAGCTGCTGGTTC	
oVIN-1251	For: 3'UTR-Dmpk	human *DMPK* gene	GAGCGTGGGTCTCCGCCCAG	(Aeschbach and Dion 2017)
oVIN-1252	Rev: 3'UTR-Dmpk		CACTTTGCGAACCAACGATA	
oVIN-1333	For: exon1-Htt	Human *HTT* gene	CCGCTCAGGTTCTGCTTTTA	This study
oVIN-1334	Rev: exon1-Htt		CAGGCTGCAGGGTTACCG	
oVIN-2530	Rev: exon1-Htt	Murine *HTT* gene	TTCCCTAACTTCGCAAACTG	This study
oVIN-2548	For: exon1-Htt		CCACCTCATCCTCTTGCTT	
oVIN-1374	For: att site-U6 prom-gRNA	U6 prom-gRNA	CTGACCTAGGGGACAAGTTTGTACAAAAAAGCAGGCTAAGGTCGGGCAGGAAGAGGG	This study
oVIN-1375	Rev: att site-gRNA		CTGACCTAGGGGACCACTTTGTACAAGAAAGCTGGGTAAAAAGCACCGACTCGGTGC	
FAM6	For: exon1-Htt FAM labelled	Human *HTT* gene	ATGAAGGCCTTCGAGTCCCTCAAGTCCTTC	(Mangiarini et al. 1997, 3)
HU3	Rev: exon1-Htt		GGCGGCTGAGGAAGCTGAGGA	

Patient-derived cells

Patient-derived LCLs were obtained from the Coriell Institute Repository (Camden, New Jersey). In this study, we used GM14044 (an HD-derived LCL) and GM06077 (from a DM1 individual) (Table III.II.3). Cells were maintained in RPMI 1640 (Invitrogen, Carlsbad, CA) containing 15% FBS, 1% penicillin and streptomycin in 15 mL flasks. Cells were incubated at 37°C in a 5% CO_2 humidified atmosphere.

Table III.II.3 LCLs used in this study

Name	Disease	Repeat size allele 1	Repeat size allele 2	Age at onset	Symptoms	Reference
GM06077	DM1	NA	1600	2	Cognitive and motor symptoms	(Kalman et al. 2013)
GM14044	HD	19	750	2.5	Dementia and motor disfunctions	(Nance et al. 1999)

Lentiviral transduction was established by two subsequent and not concomitant transductions of the patient cells with the 2 lentiviruses. At D0 100'000 lymphoblastoid cells were plated in 12 well/plates with 2 mL of media. The following day, 5 µL of lentivirus was added directly into the media and incubated over 3 days. In order to select for transduced cells, specific selection markers were added into the medium: 15 µg/mL blasticidin for Lentivirus-Cas9-nickase and/or 1 µg/mL puromycin for Lentivirus-gCTG. Genomic DNA was extracted at different time points with NucleoSpin® Tissue kit (MACHEREY-NAGEL, Düren, Germany). Cells transduced with only Lenti-Cas9-D10A were used as control reference.

Lentivirus

Plasmids used to generate lentiviruses are listed in Table III.II.1. To produce 3rd generation lentiviruses, I followed the Trono lab protocol (Salmon and Trono 2007). $3x10^6$ HEK 293T cells were plated in four 20 cm/plates, in DMEM/glutamax (Invitrogen, Carlsbad, CA) supplemented with 10% fetal bovine serum (FBS) and incubated at 37°C in a 5% CO_2 humidified atmosphere for 56 hours. Two hours before the transfection, medium was replaced with 22.5 mL fresh medium. Cells were then transfected with CalPhos Mammalian Transfection kit (Takara, Clontech, Cat#631312). I added in each tube: 2.64 mL of TE Buffer 0.1X (final 0.06 X), 1.09 mL H_2O, 90 µg vector with gene of interest (either bVIN-418 or bVIN-478), 31.6 µL of pMD2G (conc. 1 µg/µL), 58.4 µL of pMDLg/pRRE (conc. 1 µg/µL),

24 µL of pRSV-Rev (conc. 1 µg/µL), 0.562 mL of $CaCl_2$ 2M (final 0.25 M). Successively, solution in the first tube was added to a second tube, containing 4.5 mL of HeBs 2x, drop-by-drop and vortex. The final mix was then incubated for 5 min at RT, and 2.25 ml was distributed into each of the four dishes. Transfection mix was incubated overnight, before the medium was replaced with a fresh 14 mL of medium. Eight hours later, the medium was collected and replaced. The same procedure was followed during the next day. On the 4th day, medium containing viruses was filtered with 0.22 µm Stericup filter (Millipore) and distributed equally into six conical tubes (#358126, BECKMAN COULTER, Indianapolis, IN). The medium was then ultracentrifuged in an Optima™ L-90K Ultracentrifuge (BECKMAN COULTER, Indianapolis, IN) for 2 hours at 14°C at 19500 rpm. The supernatant was removed and the pellet was collected in 200 µL of PBS. The viral solution was finally aliquoted and stored at -80°C.

AAV

Alejandro Monteys took care of AAV vector cloning and rAAV production. Two vectors containing either Cas9 nickase or gCTG were cloned. Cas9 nickase was under a CMV promoter (Figure III.II.1). The U6 promoter triggered the expression of gCTG linked to a CMV-eGFP sequence. Viruses were generated thanks to the Research Vector Core at the Raymond G Perelman Center for Cellular and Molecular Therapeutics at The Children's Hospital of Philadelphia.

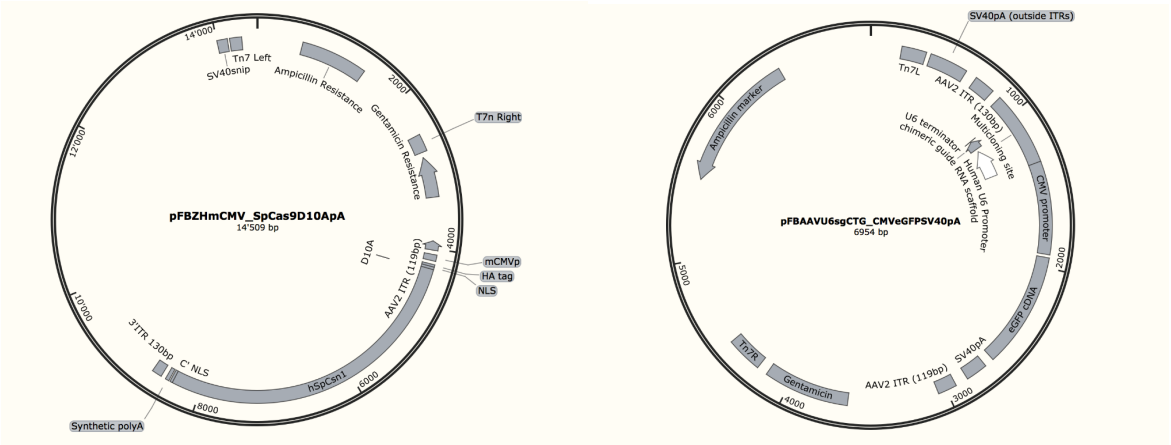

Figure III.II.1 Plasmids used to generate AAV-Cas9-D10A and AAV-gCTG
Left) PFBZHmCMV_SpCas9D10AApA contains Cas9 nickase gene under CMV promoter. Cas9 D10A is HA tagged and it is flanked by ITR sequences necessary for integration into the viral genome. Right) gCTG sequence is under the U6 promoter necessary for its expression and is linked to eGFP for visual expression localization through fluorescence. gCTG and eGFP are flanked by the ITR sequences.

Mouse models and viral injections

In collaboration with Geneviève Gourdon and her team, DM250 and DMSXL mice (Seznec et al. 2000a; Huguet et al. 2012) were housed at the Animal facility, Institute Imagine, Paris. Housing and handling of mice were performed in accordance with the guideline established by French Council on animal care "Guide for the Care and Use of Laboratory Animals": EEC86/609 Council Directive -Decree 2001-131. These transgenic mice have been generated by the integration of 45 kb long fragment derived from patient LCLs into B6D2/F1 mouse embryos as described in (Geneviève Gourdon et al. 1997; Seznec et al. 2000b; Huguet et al. 2012). This fragment contains dystrophia myotonica WD repeat-containing gene (*DMWD*), *DMPK* and *SIX5*. DM250 mouse carries 250 CTG repeats and shows repeat genomic instability similar to human and motor disfunctions (Panaite et al. 2008). Stronger phenotype is observed in DMSXL mice, which carries over 1000 CTG repeats, from repeat instability, RNA foci formation to motor symptoms (Huguet et al. 2012). DM250 and DMSXL mice were injected by Aline Huguet-Lachon, Imagine Institute, Paris. Different injection sites were used: tail vein, facial vein, or intraventricular at birth or in 2 months old mice (Table III.II.4). Three virus conditions were used: AAV9-Cas9-D10A+AAV9-gCTG, AAV9-Cas9-D10A, or AAV9-gCTG. Different quantities of viruses were injected based on the site of injection: tail vein: $3x10^{11}$ v.g. AAV9-Cas9-D10A + $3x10^{11}$ v.g. AAV9-gCTG; facial vein: $1x10^{11}$ v.g. AAV9-Cas9-D10A + $1x10^{11}$ v.g. AAV9-gCTG; intraventricular vein: $1x10^{11}$ v.g. AAV9-Cas9-D10A + $1x10^{11}$ v.g. AAV9-gCTG. I collected 15 different tissues from each mouse: frontal cortex, hippocampus, cerebellum, brainstem, diaphragm, heart, liver, pancreas, spleen, kidney, quadriceps, gastronemius, testis/ovaries, tail, skin. Tissues were frozen in liquid nitrogen and store at -80°C. Genomic DNA from mouse tissues was extracted with phenol/chloroform extraction protocol.

Table III.II.4 DM250 and DMSXL mice injected with Cas9 nickase.
Experimental details of DM250 and DMSXL mice injected with AAV9 Cas9 D10A and gCTG. P0: at birth; P1: at 1 day of age; mo: months; SAC: sacrifice; F: female; M: male; NA: not available.

Mouse	Line	N° repeats	Injection	Type of injection	Age at injection	Week after treatment	Age at SAC	Sex
347	DM250	250	No injection				4 mo	F
350							3.75 mo	M
278							5.75 mo	F
2349			AAV9-gCTG + AAV9-Cas9-D10A	Facial vein	P0	6	1.5 mo	F
2354					P0	6	1.5 mo	M
2356					P1	10	2.5 mo	M
2351				Intraventricular	P0	11	2.75 mo	F
2360					P0	6	1.5 mo	F
2359					P0	6	1.5 mo	F
2363					P1	10	2.5 mo	F
279				Tail vein	~2 mo	11	4.75 mo	NA
267					~2 mo	6	3.5 mo	NA
270					~2 mo	10	4.5 mo	NA
224					~2 mo	6	3.5 mo	NA
2378	DMSXL	1000/1600	AAV9-gCTG + AAV9-Cas9-D10A	Facial vein	P0	6	1.5 mo	M
2377					P0	10	2.5 mo	M
2381					P0	6	1.5 mo	F
2380					P0	11	2.75 mo	F
2413			AAV9-gCTG	Facial vein	P0	6	1.5 mo	M
2411					P0	11	2.75 mo	M
2382			AAV9-Cas9-D10A	Facial vein	P0	6	1.5 mo	F
2372			AAV9-gCTG + AAV9-Cas9-D10A	Intraventricular	P0	6	1.5 mo	F
2370					P0	6	1.5 mo	M
2376					P0	10	2.5 mo	F
2375					P0	11	2.75 mo	F
1962			AAV9-gCTG + AAV9-Cas9-D10A	Tail vein	~2 mo	10	4.5 mo	NA
1956					~2 mo	6	3.5 mo	NA
1961					~2 mo	6	3.5 mo	NA
1952					~2 mo	11	4.75 mo	NA

In collaboration with Vanessa Wheeler and her team, Hdh^{Q111} knock-in mice (White et al. 1997a; V. C. Wheeler et al. 1999) were tested and hosted at the Center for Comparative Medicine, MGH, Boston. Housing and handling of mice were performed in accordance with the recommendations in the Guide for the Care and Use of Laboratory Animals of the National Institutes of Health under and approved protocol of Massachusetts General Hospital Subcommittee on Research Animal Care. In this mouse model, part of the murine exon 1 and intron 1 of *HTT* gene (Hdh) have been replaced with the human homologue, carrying $(CAG)_{109}$CAACAG (White et al. 1997b; V. C. Wheeler et al. 1999). Hdh^{Q111} mouse shows cellular phenotype of HD already at 1 month old, such as nuclear mutant huntingtin aggregates in the striatum (Vanessa C. Wheeler et al. 2000, 200). Injections have been done by Ricardo Mouro Pinto, Center for Genomic Medicine, MGH, Boston, or Julieanne Brandolini from Center for Comparative Medicine, MGH, Boston. All Hdh^{Q111} knock-in mice received a tail vein injection with different AAV8 solutions: AAV8-Cas9-D10A+AAV8-gCTG, AAV8-Cas9-D10A, AAV8-gCTG, or PBS (Table III.II.5). Mice of 1 month of age received $1.5x10^{12}$ v.g. per virus and 6 months old mice received $3x10^{12}$ v.g. per virus. Four weeks after treatment, mice were sacrificed and 11 tissues per mouse collected: striatum, cortex cerebellum, heart, liver, kidney, spleen, quadricep, pancreas, testis/ovaries, tail. Tissues were frozen in liquid nitrogen and store at -80°C. Genomic DNA have been extracted from the different tissues with QIAamp DNA FFPE Tissue Kit (#56404, QIAGEN).

Table III.II.5 Hdh^{Q111} mice injected with AAV8 Cas9 nickase and gCTG
Experimental design of AAV Cas9 D10A + gCTG injection into HD mouse model. Mo: months; SAC: sacrifice; F: female; M: male.

Mouse	Line	N° repeats	Tail vein injection	Age at injection	Week after treatment	Age at SAC	Sex
G2128	Q111/+	107	AAV8-gCTG + AAV8 Cas9-D10A	1 mo	4	2 mo	M
G2129	Q111/+	111		1 mo	4	2 mo	M
G2130	Q111/+	110		1 mo	4	2 mo	M
F2336	Q111/+	114		6.25 mo	4	7.25 mo	F
M3605	Q111/+	109		1 mo	4	2 mo	M
G2380	Q111/+	113		1 mo	4	2 mo	M
F2334	Q111/+	113		6.25 mo	4	7.25 mo	F
F2330	Q111/+	115		6.25 mo	4	7.25 mo	M
G2132	Q111/+	111	AAV8-Cas9-D10A	1 mo	4	2 mo	M
F2332	Q111/+	114		6.25 mo	4	7.25 mo	M
G2133	Q111/+	110	AAV8-gCTG	1 mo	4	2 mo	M

zQ175 mouse experiment is the result of a collaboration with Francesca Cicchetti and Melanie Alpaugh, University of Laval, Quebec City. Melanie Alpaugh took care of the project design, mice housing, AAV injections, behavioral tests and tissues collections. The zQ175 knock-in mouse line carries a chimeric *Hdh:Htt* gene, mouse/human, in a C57BL/6J background and has been generated from natural expansion in CAG 140 mouse (Menalled et al. 2012, 2003). The human sequence has been integrated at the exon 1 of *Hdh* murine sequence, and constitutes of $(CAG)_{173}$CAACAG followed by 10 bp of the human intron 1 sequence. Homozygous mice showed motor deficits at 9 months of age, cognitive impairments and transcriptional abnormalities (Menalled et al. 2012, 201). All mice were injected into the cortex and striatum at 1 year of age and different combinations of viruses have been used: AAV8-Cas9-D10A+AAV8-gCTG, AAV8-Cas9-D10A alone or AAV8-gCTG alone (Table III.II.6). Mice received $1.5x10^{12}$ v.g. of each virus. Behavioral tests were performed at 14/30/60/90 days after injection and both cognitive and motor abilities were measured.

Cortex and striatum were collected at 90 days after injection. Tissues were frozen in liquid nitrogen and store at -80°C. Genomic DNA was extracted from striatum.

Table III.II.6 zQ175 mice injected with AAV8-Cas9-D10A + AAV8-gCTG
WT and zQ175 mice have been injected with Cas9 nickase and gCTG viruses or only one of the two. WT: wild-type; mo: months; w: weeks; F: female; M: male.

Mouse	Line	N° repeats	Intraventricular injection	Age at injection	Weeks after treatment	Age at SAC	Sex
8919	WT		AAV9-Cas9-D10A + AAV9-gCTG	12 mo	6 w	14 mo	M
8920				12 mo	6 w	14 mo	M
8936				12 mo	6 w	14 mo	M
8942				12 mo	6 w	14 mo	M
9024				12 mo	6 w	14 mo	M
9038				12 mo	6 w	14 mo	M
8921			AAV9-Cas9-D10A	12 mo	6 w	14 mo	M
8922				12 mo	6 w	14 mo	M
8928				12 mo	6 w	14 mo	M
8941				12 mo	6 w	14 mo	M
9044				12 mo	6 w	14 mo	M
8930	zQ175	175	AAV9-Cas9-D10A + AAV9-gCTG	12 mo	6 w	14 mo	M
8937				12 mo	6 w	14 mo	M
8940				12 mo	6 w	14 mo	M
9041				12 mo	6 w	14 mo	M
8929			AAV9-gCTG	12 mo	6 w	14 mo	M
8935				12 mo	6 w	14 mo	M
9039				12 mo	6 w	14 mo	M
8943			AAV9-Cas9-D10A	12 mo	6 w	14 mo	M
9040				12 mo	6 w	14 mo	M
9042				12 mo	6 w	14 mo	M
9045				12 mo	6 w	14 mo	M

Sequencing

Repeat sequences from Hdh^{Q111} mice have been PCR amplified with conditions previously described (Mangiarini et al. 1997). Briefly, a forward primer was fluorescently labeled with 6-FAM (FAM6) (Perkin Elmer) coupled with the HU3 reverse primer. PCR conditions: 67 mM Tri-HCl pH 8.8, 16.6 mM NH_4SO_4, 2.0 mM $MgCl_2$, 0.17 mg/mL BSA, 10 mM 2-mercaptoethanol, 10% DMSO, 200 µM dNTPs, 8 ng/µL primers with 0.5 U/µL Taq polymerase. The PCR program was: 90 sec at 94°C, 25 cycles of 30 sec at 94°C, 30 sec at 65°C, 90 sec at 72°C followed by 10 min at 72°C. Sequences were obtained with ABI 3720 DNA analyzer (Applied Biosystems). GeneMapper v3.7 with GeneScan 500-LIZ as internal standard size was used as size reference. GeneMapper determines the repeat size based on the highest trace (J.-M. Lee et al. 2010).

SP-PCR

Genomic DNA was extracted from treated cells using NucleoSpin Tissue Kit (MACHEREY-NAGEL, Düren, Germany). Genomic DNA from mouse tissues was extracted with phenol/chloroform extraction protocol. SP-PCR was performed and adapted from previously described protocol (Dion et al. 2008).

One negative control per seven PCR reactions per sample were settled using MangoTaq polymerase (bioline) for both HD patient-derived LCLs and zQ175 mouse samples and MyFi™ DNA polymerase (bioline) for both DM1 patient-derived LCLs and DM250 mouse samples.

MyFi PCR conditions: 1X reaction buffer, 0.5µM oVIN-1251, 0.5µM oVIN-1252, MyFi™ DNA polymerase (bioline), from 0.2 to 20 ng of DNA and H_2O to 10µL. The PCR program used for MyFi reaction consists in 95°C for 1 min, followed by 32 cycles at 95°C for 15 sec, 60°C for 15 sec and 72°C for 2 min, at the end a final extension of 72°C for 10 min.

Mango Taq PCR conditions: 1X reaction buffer, 0.2mM dNTP mix, 1 mM $MgCl_2$, Forward primer 0.5 µM (oVIN-1333 for human *HTT*, oVIN-2548 for murine *HTT*), Reverse primer 0.5 µM (oVIN-1334 for human *HTT*, oVIN-2530 for murine *HTT*), 3% DMSO, 1U/µL Mango Taq, from 0.2 to 20 ng of DNA and H_2O to 10µL. The PCR program used for Mango Taq reaction consists in 95°C for 5 min, followed by 5 cycles at 95°C for 20 sec, 52°C for 20 sec and 72°C for 4 min, followed by 25 cycles at 95°C for 30 sec, 55°C for 30 sec and 72°C for 90 sec, at the end a final extension of 72°C for 10 min.

PCR products were subsequently loaded on a 2% agarose gels and run for 4 hours at 180 Volts. Gel was cut in function of PCR products sizes and washed twice in Alkaline Transfer Buffer (0.4M NaOH, 1M NaCl) for 20 min. DNA is successively transferred onto a nylon membrane (Fisher Scientific #NP0HYA0010) overnight by capillary action. The membrane was washed in Neutralization Buffer (1.5M NaCl, 0.5M Tris base, pH 7.4) for 5 min at RT. Successively, the membrane was incubated with Ultrahyb buffer (Thermo Scientific #AM8670) and Salmon Sperm DNA for 1 hour at 52 °C. The hybridization probe was generated by the activity of T4 PNK (New England BioLabs #M0201S), oVIN-100 oligonucleotide and radioactively marked ATPs with the following reaction: 1X Reaction buffer, 50 pmol of oVIN-100, 10mM [γ-^{32}P] ATP, 10U T4 PNK, and H_20 to 25 µL. After an incubation of 1 hour at 37°C, the probe was exposed to a temperature of 65 °C for 10 min. The probe was then added directly to the membrane and incubated at 52 °C for 2 hours. After two washes with Washing Buffer (0.5X SSC, 0.1% SDS) for 20 min, the membrane was exposed to a phosphoscreen from 2 to 24 hours, and revealed with a Typhoon scannersphoimager.

Lentivirus titration

Lentivirus titration was done using Trono's protocol (Salmon and Trono 2007).

HEK 293 cells were cultured at 37°C in a 5% CO_2 humidified atmosphere in DMEM/glutamax (Invitrogen, Carlsbad, CA) supplemented with 10% fetal bovine serum (FBS), 100 U/mL penicillin, 100 µg/mL streptomycin. On day 1, 100'000 cells were plated in 12 well/plates in seven wells. On day 2, one out of the seven wells was used to count the number of cells present. The other wells were transduced with the addition of the virus as following: no virus, 3 µL of virus, 2 µL of virus, 10 µL of dilution A (1/10 dilution of Virus in PBS), 10 µL of dilution B (1/10 dilution of A in PBS), 10 µL of dilution C (1/10 dilution of B in PBS). After 96 hours of incubation, the cells were harvested and their genomic DNA was extracted.

qPCR was performed with the FastStart Universal SYBR Green Master (Roche) using a 7900HT Fast Real-Time PCR System in a 384-Well Block Module (Applied Biosystems™). Primers used to detect virus copy number are: oVIN-1663 and oVIN-1664 for *GAG*, oVIN-1665 and oVIN-1666 for *WPRE*, oVIN-2018 and oVIN-2019 for *ALB*. PCR conditions are 50 cycles of 10 min at 95°C, 15 sec at 95°C and 1 min at 60°C. Copy numbers were obtained by comparison of specific viral gene with albumin values.

Protein extraction and Western Blot

Tissue proteins have been collected by the used of precellys 24 Tissue Homogenizer (Bertin Technologies). Tissue portions have been collected in TUBES and RIPA buffer was added. RIPA buffer was constituted of 50 mM TrisHCl pH 8.0, 150 mM NaCl, 1% TritonX-100, 0.1% SDS, 0.5% Na-deoxycholate, 1x Protease inhibitor (Roche). Samples were homogenized for 10 sec at 5000 rpm. The solution was successively collected and incubated on ice for 30 min, followed by 30 min of centrifugation at 20000 g at 4°C. The supernatant was then collected and stored at -20°C. The samples were boiled for 5 min in LSD sample Buffer 4x (Invitrogen, Carlsbad, CA). The protein extracts were run on a NuPAGE™ 3-8% Tris Acetate gel (#EA0375BOX, ThermoFisher Scientific) for 1.5 hour at 120 V. The proteins were then transferred to a nitrocellulose membrane for 1.5 hour at 100 V. The membrane was blocked with Blocking buffer for Fluorescent Western blotting (Bioconcept). The primary antibodies were incubated overnight at 4°C with specific dilution in PBS (anti-Cas9 1:1000, anti-HA 1:1000, anti-actin 1:2000). An Odyssey Infrared Imager (Licor) was used for signal development and detection.

III.III.I The Cas9 nickase readily contracts repeat tracts in patient-derived LCLs

The Cas9 nickase activity resulted in contraction events in the GFP$(CAG)_{101}$ cell line. The ability of this engineer nickase in inducing repeat contractions needs to be verified in a disease model, such as patient-derived cells. To determine whether the nickase can induce contractions in patient-derived cells, we used a DM1-derived LCL with one allele reaching 1600 CTGs and the other having normal length as well as a HD-derived LCL with 750 CAGs on allele and 19 on the other. We used lentiviral transduction to integrate the Cas9 nickase in the LCLs and selected for cells expressing the blasticidin resistance gene fused to Cas9. Then, we transduced these cells with viruses containing the gCTG expression cassette and took samples over 56 days. Repeat instability was successively measured by SP-PCR.

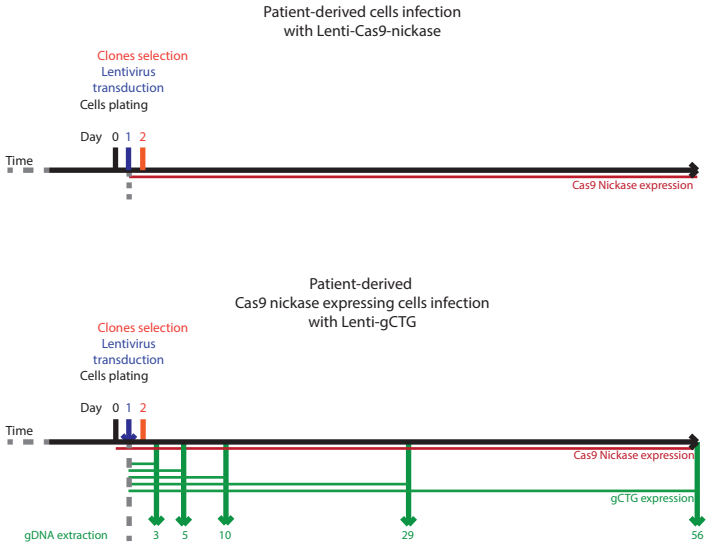

Figure III.III.1 Experimental design of Cas9 nickase viral transduction into DM1 and HD LCLs.
Cells were first exposed to Lenti-Cas9 nickase by direct addition into the medium and transduced clones were selected by blasticidin resistance (up). Cas9 nickase expressing cells were successively infected with Lenti-gCTG and selection marker was added. Genomic DNA was extracted at different time points (down).

SP-PCRs results show broadly a shortening of the repeats over time induced by Cas9 nickase activity compared to cells expressing only the Cas9 nickase (Figure III.III.2). A higher number of bands with shorter sizes is present in cells treated with both Cas9 nickase and gCTG, in both DM1 and HD cases. Already after three days of treatment increased the abundance of shorter bands. Unfortunately, results for longer than 3 days exposure of Cas9 nickase and gCTG in HD LCLs are not available yet. For the DM1 sample, shortening of the repeat tract is visible over the time course. After 5 days of treatment, the expanded band disappear, leaving space to a variety of shorter bands. At 29 days we observe only bands with WT repeat size almost without any presence of expanded repeats. However, 56 days of treatment shows variable sizes of expanded repeats above the WT ones. Quantification of shortening events and to which repeat size are yet to be performed. In conclusion, Cas9 nickase showed ability to induce repeat contractions in patient-derived LCLs for DM1 and HD within as little as 3 days of nicking the repeat tract.

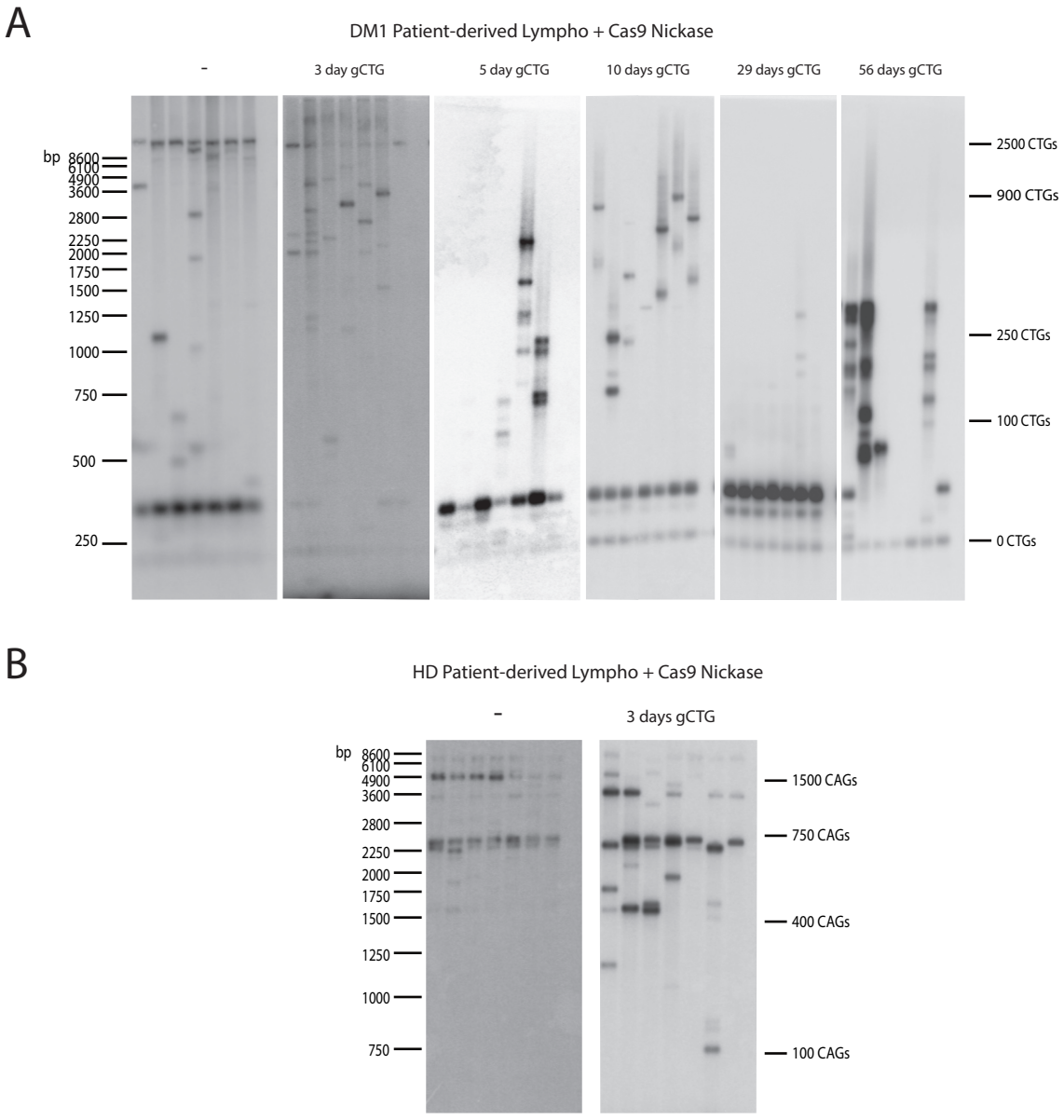

Figure III.III.2 Cas9 nickase transduction into DM1 and HD patient-derived LCLs showed repeat contraction events.
A) SP-PCR of DM1 patient-derived cells treated with Cas9 nickase and gCTG. B) SP-PCR of HD LCLs treated with Lenti-Cas9-nickase and Lenti-gCTG.

III.III.II Cas9 nickase gene therapy in expanded TNR mouse models

Cas9 nickase demonstrated, in the previous experiments, its ability to induce repeat contraction in a repeat tract of pathogenic length. To test whether the Cas9 nickase could induce repeat contractions in a more physiological and systemic level, we selected 1 mouse model for DM1, DM250 and DMSXL, and 2 mouse models for HD, Hdh^{Q111} and zQ175. A viral transduction of Cas9 nickase into mouse models can reveal the efficiency of a gene therapy approach in delivering this treatment into affected patients. To do so, mice have been injected with 2 AAVs expressing Cas9 nickase or gCTG. Mouse tissues have been collected at different time windows for Cas9 activity. Repeat instability was then measured by either SP-PCR or GeneScan sequencing.

Cas9 nickase + gCTG did not show an increase in CAG/CTG instability in DM250 and DMSXL mice

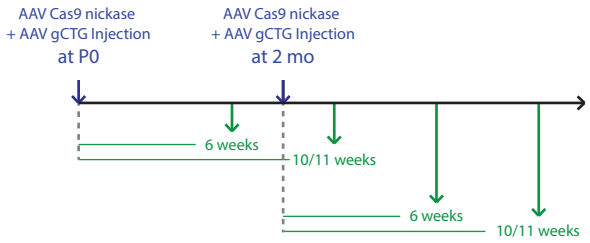

Figure III.III.3 Time line of AAV9 injections in DM250 and DMSXL mice.
Mice have been injected with both AAV9-Cas9-D10A and AAV9-gCTG at two different time points: at birth (P0) or at 2 months old (2 mo). Tissues have been collected either at 6 weeks or at 10/11 weeks after injections and genomic DNA was extracted.

To measure repeat instability induced by the engineered nickase in DM250 injected mice, I performed a SP-PCR on quadricep genomic DNAs. SP-PCR results did not reveal any effect specifically induced by Cas9 nickase activity (Figure III.III.4). In all the membranes, a strong signal for 250 CTG repeat band was present as expected. Distribution of additional band was very similar over the different samples, not injected sample included. We observed unexpected smeary bands for many reactions, that hide possible results. It is, in fact, difficult to visualize whether large discrete contractions are present. It is also notable the irreproducibility of results within the same sample. Sample 278, for example, showed different distribution patterns in two distinct membranes. This variability makes comparison between control non-injected and injected not possible. Quantification of band distributions revealed a variable percentage of contracted alleles over the total number in mouse transduced with Cas9 nickase and gCTG (Table III.III.1). This high variability and the low number of alleles measured did not allow me to draw conclusions. No significant difference was observed between injected and non-injected mice. I conclude that if an increase in contractions is present in these samples, they are masked

by the high variability found in our not-injected controls. More samples will need to be analyzed to resolve the matter.

Table III.III.1 SP-PCR quantification of contracted alleles of quadricep genomic DNAs isolated from Cas9 nickase treated and untreated DM250 mice.

Sample	Injection	% contracted alleles	total alleles
278 - DM250	-	2	823
224 - DM250	Cas9-D10A + gCTG	2.7	725
267 - DM250	Cas9-D10A + gCTG	0.91	659
279 - DM250	Cas9-D10A + gCTG	5.9	152

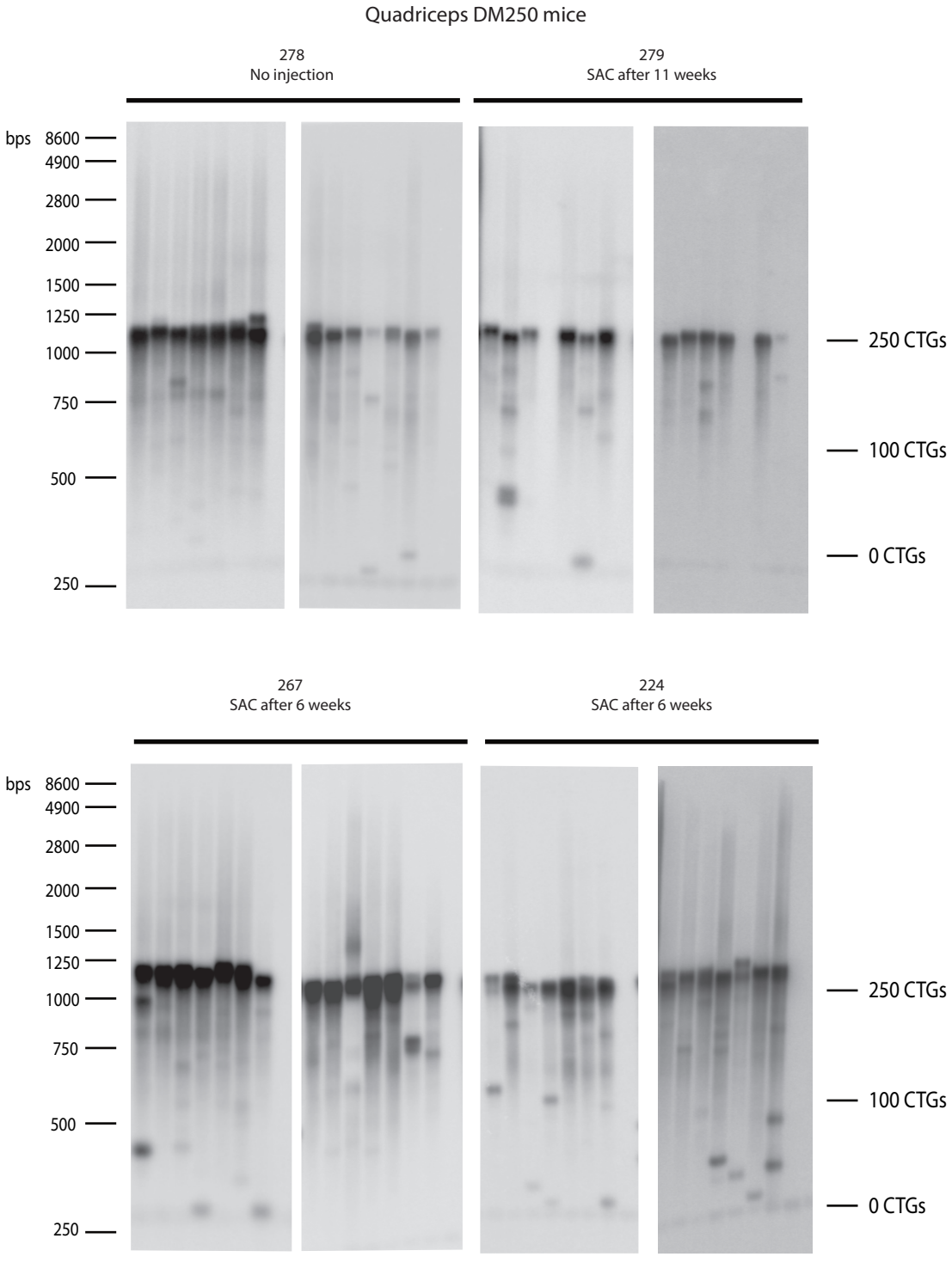

Figure III.III.4 CTG repeat instability after 6 or 11 weeks of Cas9 nickase in DM250 mice quadriceps did not show any difference compared to untreated DM250 mice.
SP-PCRs have been performed on genomic DNA from quadriceps of AAV9-Cas9-D10A and AAV9-gCTG injected DM250 mice. Amplification of CTG repeat tract in the *DMPK* gene did not reveal repeat instability induced by the treatment. Two different membranes of each sample are presented in this figure. SAC: sacrificed.

To determine whether the infection and gene expression was efficient, we decided to do WB experiment to detect Cas9 in liver protein extracts. WB was performed by Lorène Aeschabch. The Cas9 levels were measured by the use of Cas9 nickase and HA antibodies (Figure III.III.5). Cas9 sequence carried by AAVs was HA-tagged. Cas9 nickase protein was not detectable in liver protein extracts of AAV9-Cas9-D10A injected mice. No one of the 4 mouse samples selected showed the presence of this protein. However, a strong signal is observed in GFP$(CAG)_{101}$ cells transfected with a plasmid expressing the Cas9 nickase. It is not clear the nature of the small band observed in mice samples, but its presence in non-injected mouse excludes relation with the engineered nickase. Moreover, a second antibody, anti-HA, confirmed the absence of Cas9. The Cas9 nickase is not detectable in DM250 mouse liver infected with AAV9-Cas9-D10A. Thus, whether the AAV-based delivery of the Cas9 nickase leads to contractions in the DM250 mice remains an open question.

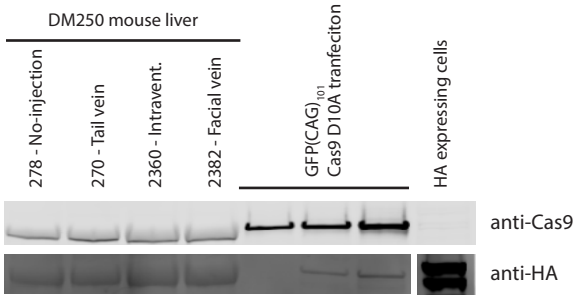

Figure III.III.5 Cas9 nickase protein was not present at detectable levels in DM250 mouse livers.
WB with anti-Cas9 and anti-HA did not show presence of Cas9 nickase protein in DM250 mouse liver compared to GFP$(CAG)_{101}$ cells transfected with increasing amount of Cas9 nickase.

Cas9 nickase activity did not induce detectable repeat size variation in Hdh^{Q111} mice

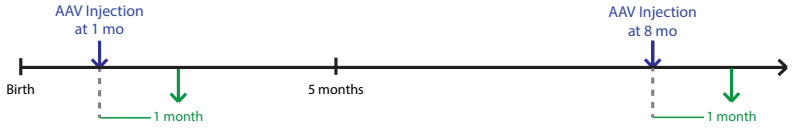

Figure III.III.6 Time line of AAV8 injections in Hdh^{Q111} mice.
Mice have been injected with both AAV8-Cas9-D10A and AAV8-gCTG at either 1 month old (1 mo) or at 8 months old (8 mo). Mice have been sacrificed and tissues collected 1 month after injections.

Repeat sizes measured by GeneScan sequencing (Figure III.III.7) remained stable over the 4 weeks of treatment compared to the original size (Table III.III.2). We observed 1 to 3 repeat units differences and no strong repeat size variations have been observed after sequencing. Results lead us to the possible conclusion that the Cas9 nickase activity does not result in repeat instability in Hdh^{Q111} mice.

Table III.III.2 No variation in repeat size has been detected by GeneScan sequencing of CAG at Hdh from different tissues after Cas9 nickase injection.
Genomic DNA was extracted from different tissues of treated mice. However, ear punch genomic DNA has been collected at the day of injection. Numbers correspond to repeat unit at the *Hdh* locus.

Sample	**Ear punch**	**Heart**	**Kidney**	**Pancreas**	**Spleen**	**Tail**	**Testis/ ovaris**	**Original size**
G2128	107	107	108	108	108	107	-	107
G2129	-	-	112	-	110	110	-	111
G2130	-	-	-	111	111	111	-	110
G2132	111	-	-	-	-	110	111	111
G2133	-	-	110	109	112	109	-	110
F2330	-	-	-	118	116	116	-	115
F2332	-	-	-	-	114	115	-	114
F2334	-	-	113	-	115	115	113	113
F2336	-	-	-	119	115	114	118	114

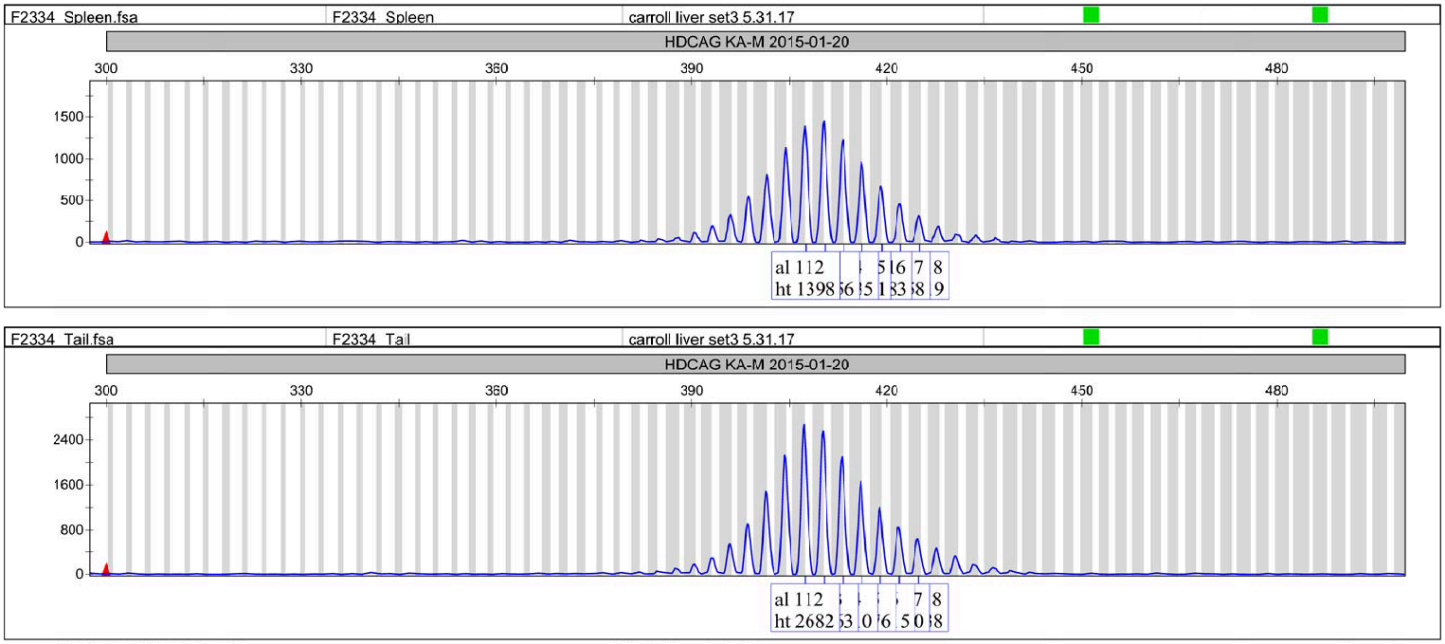

Figure III.III.7 Representative GeneMapper histogram of Hdh^{Q111} mouse samples.
Up) Histogram representation of GeneScan sequencing of CAG repeat sizes at *Hdh* locus of spleen genomic DNA from AAV-Cas9-D10A + AAV-gCTG injected mouse. Different repeat sizes were clustered in different peaks. Down) Same as up, GeneMapper result from tail genomic DNA of same mouse.

To understand whether the Cas9 nickase was expressed *in vivo*, Cas9 protein levels were determined by WB in liver cells (Figure III.III.8) 1 month after injections. Neither Cas9 nor HA-tag antibodies detected Cas9 nickase protein in mouse liver extracts. We included a positive control in which GFP(CAG)$_{101}$ cells were transfected with the Cas9 nickase, not HA-tagged. I conclude that Cas9 nickase protein was absent in liver extract of treated mice explaining the undetected CAG repeat instability.

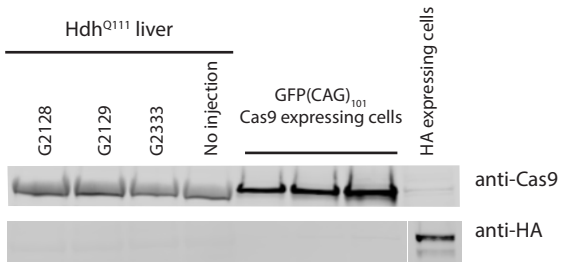

Figure III.III.8 Cas9 nickase protein was not detected in treated mouse livers.
Liver protein extracts from Hdh^{Q111} mice did not reveal presence of the Cas9 protein with both Cas9 and HA antibodies by WB. However, protein form GFP(CAG)$_{101}$ cells lipofectamine transfected with Cas9 nickase presented a strong presence of this protein.

AAV8-Cas9-D10A + AAV8-gCTG have been injected into zQ175 mouse model

From promising preliminary data where Cas9 nickase improved motor functions in zQ175 mice (unpublished data from the Cicchetti lab), we evaluated the repeat instability activity induced by nicks in this mouse model for HD. Due to poor quality results, data from mice injected with AAV8-Cas9-D10A + AAV8-gCTG could not be compared to mice injected with only AAV8-Cas9-D10A (Figure III.III.9). Unfortunately, ratios of repeat distributions cannot be calculated yet. We can visually observe that repeat sizes are grouped in two different clusters. In one cluster repeats distribute around 175 repeat size, as the original repeat length with a certain variable range. However, a second group is characterized by repeats at 400 units. Due to poor quality results no conclusion can be drawn at the moment about Cas9 nickase efficiency in zQ175 mice and additional experiments need to be performed.

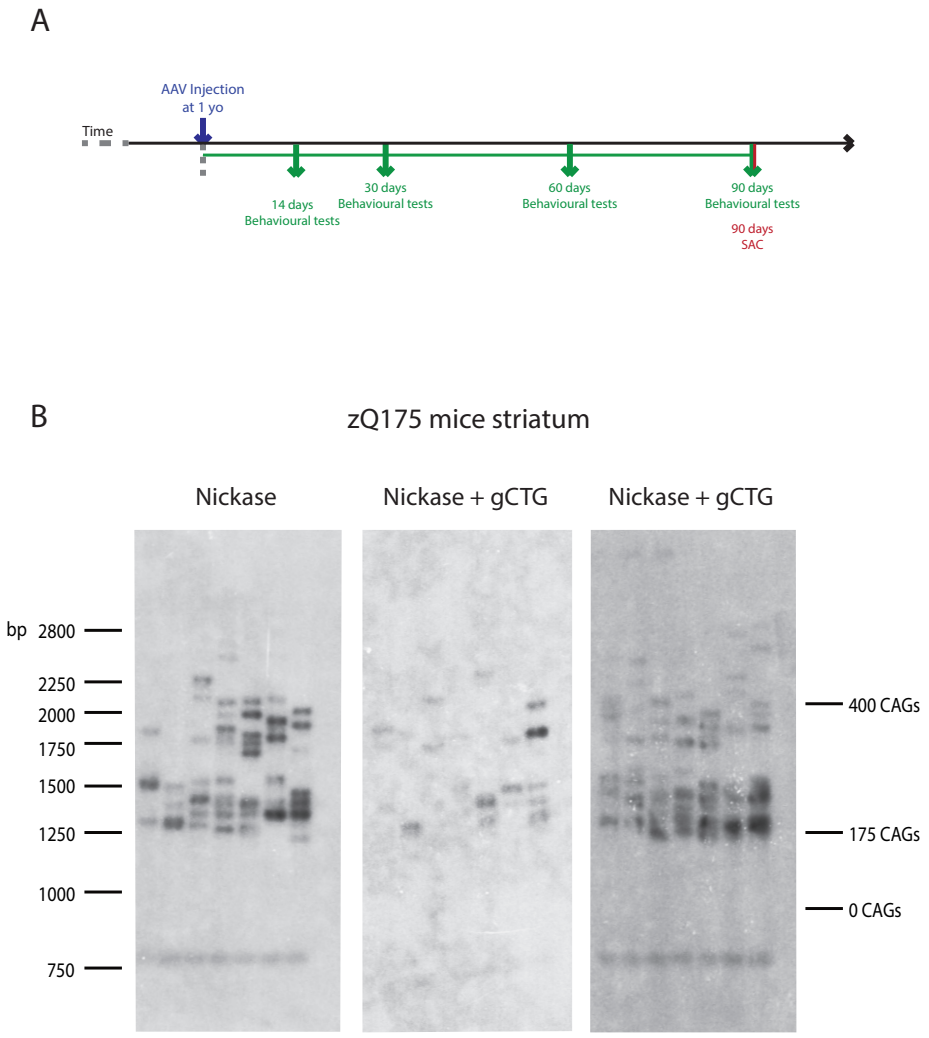

Figure III.III.9 zQ175 were injected with AAV8-Cas9-D10A + AAV8-gCTG
A) Experimental design of AAV8 Cas9 nickase and AAV8 gCTG injections in zQ175 mice. Mice have been injected with either one or both viruses at 1 year of age. Behavioral tests were performed at 14/30/60/90 days after injection. Mice were sacrificed at 90 days after injection. B) SP-PCR of striatum genomic DNA collected from zQ175 mice treated with AAV8 Cas9 nickase.

III.IV Conclusions

The main goal of this second part of the project was to evaluate Cas9 nickase activity, combined with gCTG, in patient-derived cells and *in vivo*. In this Chapter preliminary results have partially confirmed the promising conclusions presented in Chapter II.

The Cas9 nickase showed the ability to induce repeat shortening in both DM1 and HD patient-derived cells. The expanded allele slowly disappeared, giving rise to shorter bands that distributed in a wide size range. It will be interesting to determine the frequency of contracted alleles and the time of exposition of Cas9 nickase necessary to reach the healthy threshold, stabilizing the repeat tract. SP-PCRs will be repeated and longer time of treatment will be tested in HD-patient derived cells. WB and IF will also measure Cas9 protein presence and lentivirus transduction efficiency in treated LCLs. Additional experiments will determine better the efficiency and the mode of action of this tool.

Measurements of gene therapy experiment performed up to date did not reveal the expected results in mouse models. We observed appearance of contracted bands induced by Cas9 nickase activity in DM250 mice. However, it was not sufficiently to clarify and distinguish the result from spontaneous somatic instability. The Cas9 nickase protein presence was at undetectable levels by WB in liver, possibly explaining the low or absent ratio of contraction events. Repeat instability measurements by SP-PCR need to be repeated, in quadriceps, and additionally in liver samples. IF will also determine gCTG and Cas9 nickase presence with a different approach.

Repeat instability was measured by GeneScan in mouse tissues from Hdh^{Q111} injected mice. No variation in repeat size was observed in the tested tissues. This could be a result of the

absence of the Cas9 protein as suggested by the WBs of liver samples. Performing SP-PCR, more sensitive technique for variations in repeat instability, in tissues from Cas9 nickase + gCTG injected mice could uncover possible readouts not observed at the moment induced by the gene editing. Visual measurements of the Cas9 nickase and gCTG presence will be tested with IF.

In preliminary data, Cas9 nickase showed to improve motor deficits in zQ175 mice (unpublished data from the Cicchetti lab). Unfortunately, whether the Cas9 nickase activity in this mouse model induces repeat contractions remain inconclusive. More SP-PCR data are required to see the results.

The ultimate goal of this project is to develop a gene therapy-based system able to target expanded CAG/CTG and induce repeat shortening in patients. Combination of Cas9 D10A and AAV delivery could be the successful approach to cure 14 expanded TNR disorders.

Chapter IV

Conclusions and Discussion

IV.I The Cas9 nickase induces CAG/CTG repeat contractions in GFP(CAG)$_{101}$ cells and patient-derived cells.

The aim of this project was to discover and develop a therapeutic tool for expanded TNR disorders. The shortening of expanded repeats *in vivo* and the reversing the phenotype is the possibility raised by the data presented here. The Cas9 nickase fit the desired characteristics necessary to be an effective therapeutic tool and showed efficiency in mammalian cells and patient-derived cells.

We improved the GFP reporter previously published and used it to measure both CAG repeat contraction and expansion events induced by engineered nucleases (B. A. Santillan et al. 2014; Cinesi et al. 2016). Originally, the use of the GFP reporter allowed measurements of CAG repeat contraction events induced by an applied treatment. Due to not sufficiently long period of transcription through the GFP cassette, the GFP steady state levels was not reached masking possible expansion results. We prolonged expression of the GFP cassette over 72 hours, by addition of doxycycline, and reached the steady state level of GFP protein. This revealed hidden results, such as expansion events. Thus, the optimization of the experimental protocol allowed us to detect repeat instability, both contractions and expansions, at the same time. No system previously available could perform this result. The GFP(CAG)$_x$ assay is the first inducible chromosomal reporter able to detect repeat instability within 5 days in mammalian cells.

Our results suggested that induction of different types of DNA damage within trinucleotide repeats activate different DNA repair mechanisms (Cinesi et al. 2016). The induction of DSBs

within the repeat tract by ZFNs and Cas9 resulted in concomitant expansions and contractions. However, nick induction by the Cas9 nickase led predominantly to repeat contractions.

Investigation of the DNA repair mechanisms involved in repeat contraction induced by nick formation can highlight possible players useful for therapeutic approaches. Thus, we tested the involvement of well-known repair pathways. The inhibition of PARP and XRCC1, involved in SSBR, did not affected contraction frequency induced by the Cas9 nickase. This argued against the involvement of SSBR in the repair of the Cas9 nickase induced nicks. However, players from DDR showed contribution in the regulation of Cas9 nickase induced repeat contractions. In fact, ATR inhibition increased repeat instability possibly through DSB formation in a XPA- and MSH2-dependent manner. On the other hand, ATM kinase activity promoted repeat contractions. These results led us to the hypothesis that multiple nicks induced by the Cas9 nickase within the repeat tract form DNA gaps, as mutagenic intermediate, and result in contractions events.

The Cas9 nickase showed encouraging results from a potential therapeutic point of view. In fact, the induction of nicks within the CAG/CTG repeats in GFP$(CAG)_{101}$ cells led to 30% of contraction events in 12 days. We observed an increased number of contracted alleles over time with no off-target effects in the observed loci induced by Cas9 nickase activity. This engineered nickase showed a repeat length-dependent activity. These results revealed the Cas9 nickase as an efficient way of contracting expanded TNRs.

The transduction of patient-derived LCLs showed an increase in contracted alleles induced by the Cas9 nickase targeted on the repeat tract. In both DM1 and HD LCLs, the Cas9 nickase induced contractions were observed after only 3 days of activity. However, additional

experiments need to be performed to understand and explain different unclear results. Firstly, we cannot explain the presence/absence of the WT allele over the different membranes and period of treatment. Absence of large contractions to WT size could be caused by low sensitivity of the experimental technique for short repeats. In fact, the use of a 10 CAG long probe limits the detection to alleles with repeats longer than this size. It is also not clear at which exact point expanded allele is contracted to a WT size. At 29 days after transduction, we observed the disappearance of the expanded bands, converging to the WT size. At this point cells have already been through about 9 cell cycles and are under continuous selection for Cas9 expression and for expression of puromycin, which is expressed from the sgCTG lentivirus. With the knowledge of LCLs having a similar growth rate as HEK293 cells, contraction to the WT size of the whole population could happen after 29 days of the Cas9 nickase. This is a promising result, where in 1 month of Cas9 nickase activity the expanded repeat tract can possibly reach a healthy range size. However, at 56 days we observed the re-appearance of expended repeats. Different hypothesis can be exposed to explain this event. First and more probable, the WT size was not reached by the whole population at 29 days, and we observed a selection of contracted alleles caused by the dilution performed before PCR amplification. Alternatively, the expansion events occurred after 29 days of the Cas9 nickase activity due to possible advantageous growth of expanded alleles.

Since repeat instability is also caused by replication events, additional experiments are necessary to evaluate the involvement of somatic instability present in the observed results. Comparison of repeat instability between cells treated with Cas9 nickase for 56 days and cells that went through same passaging and replication events will be necessary. In case the observed results were induced by somatic instability, comparison between treated and untreated cells will show no difference in alleles distribution and frequencies. However, if the instability

observed is the result of Cas9 nickase activity, higher frequency of contracted alleles will be measured in treated cells.

The ratio of contracted repeats and the ability to bring repeat size below the pathogenic threshold are fundamental steps for reversing the pathogenic phenotypes and defining the Cas9 nickase as an effective approach for curing expanded TNR disorders.

These promising results, of Cas9 inducing repeat shortening in GFP$(CAG)_{101}$ cells and patient-derived cells, brought us to the attempt of developing a gene therapy approach for this tool, aimed to contract the expanded repeats as therapeutic avenue. Unfortunately, the injections of the Cas9 nickase into systemic models for DM1 and HD, such as mouse models, did not show a clear result as in cell cultures. Even if repeat sizes present in these mouse models were the same range as the ones in previously tested cells, GFP$(CAG)_x$ and patient-derived LCL, contractions events induced by Cas9 nickase activity were not as frequent as in tested cell cultures. In DM250 mice, the Cas9 activity over 6/10 weeks showed a small increased in number of contracted alleles under the 100 repeat units compared to the not-injected mice. However, presence of the Cas9 nickase protein was not detected by WB in liver. The Gene-Scan of repeat tract exposed to the Cas9 nickase activity for 1 month did not showed any repeat variations in different tissues from injected Hdh^{Q111} mice. Similar to the DM250 mice, the presence of the Cas9 protein was not observed in Hdh^{Q111} mouse livers.

The major difference that have been applied in mice for the Cas9 nickase treatment compared to cell culture experiments is the delivery system. In fact, for a safer and more efficiency delivery we decided to use AAVs instead of lentiviruses. Differently from the cell transduction experiments where lentiviruses were released into the media at high concentrations and we selected for transduced cells, the AAVs have been injected into the blood stream or directly into the mouse brain. Results showed an undetectable or complete absence of Cas9 protein in

injected mouse livers. Low presence of Cas9 nickase in tissues and consequent Cas9 inefficacy in inducing repeat instability could be caused by low expression levels and/or inefficient delivery of the Cas9 nickase to the cells. To determine if the Cas9 nickase gene is present in the transduced cells, qPCR for this gene coul be performed on genomic DNA from different tissues of the injected mice. Amplification of the Cas9 nickase gene would confirm presence and efficient transduction of the targeted cells. Differently, to understand whether the inefficient delivery is responsible for the absence of Cas9 nickase activity, detection of GFP fluorescence and Cas9 presence in transduced cells will be established by IF. This will determine whether AAV-Cas9-D10A and AAV-gRNA delivery happened efficiently.

Optimization of the AAV delivery system will be necessary if tissues of injected mice do not show GFP and Cas9 signals. Different variations can be done to increase Cas9 nickase expression and optimize AAV transduction in the affected tissues. Optimization of Cas9 nickase treatment will be discussed in the following section.

IV.II Further optimization for Cas9 nickase treatment in mouse models

Low or absence of Cas9 nickase expression could be caused by an inefficient promoter. Selection of a different promoter with expression specificity for the target tissues could increase Cas9 nickase expression and allow its activity. In fact, different promoters have shown to have specific expression pattern in function of the tissue localization (Watakabe et al. 2015; Salva et al. 2007). In our case, Cas9 nickase expression will be necessary in the most affected tissues in expanded TNR disorders: skeletal muscles, heart and brain. Since it has been used and demonstrated strong gene expression in muscles and brain, we selected and tested the minimal CMV promoter for Cas9 nickase expression (Monteys et al. 2017; Long et al. 2016; Tabebordbar et al. 2016; H. Lin et al. 2018). However, replacing the minimal CMV promoter with different alternative promoters specific for brain and muscle cells, such as CaMKII, MHCK7, Syn, could improve gene expression (Holehonnur et al. 2015; Watakabe et al. 2015; Salva et al. 2007).

Transduction efficiency of the target tissues could be increase by the packaging of the two components, Cas9 and gRNA with respective promoters, into a single AAV vector. This also removes the possibility of having cells ineffectively transduced expressing only one of the two components. Moreover, a single vector carrying Cas9 nickase and gRNA allows injections with reduced viral load since the single vector contains both Cas9 components. The packaging of Cas9 and gRNA in a single vector could lead to a greater improvement of the Cas9 treatment efficacy. Unfortunately, the *Streptococcus pyogenes* Cas9 (spCas9) sequence added to the gRNA and respective promoters exceed the upper limit that AAV vectors can carry. In fact, the recombinant AAV can carry a DNA sequence size up to 5 kb. Exceeding this sequence

length leads to the production of inefficient virions with truncated genome (Wu, Yang, and Colosi 2010; Grieger and Samulski 2005). To generate a functional AAV carrying Cas9 nickase and the gRNA, the use of alternative and shorter Cas9 nickases needs to be taken into consideration (Truong et al. 2015; Zetsche, Volz, and Zhang 2015). These shorter Cas9 alternatives have already been tested and showed their efficiency in different models. Distinct species Cas9 orthologues with shorter sizes have been previously selected and their efficacy have been tested (Friedland et al. 2015; Ran et al. 2015; Hou et al. 2013; E. Kim et al. 2017). The *Staphylococcus aureus* Cas9 (saCas9) orthologue showed comparable results to the spCas9, in both nuclease and nickase versions (Friedland et al. 2015). The saCas9 is the most common orthologue used with a 3'159 bps sequence. Ran et al. packaged saCas9 under a CMV promoter and the gRNA into a single AAV vector and injected it into mice. This saCas9 targeted to a cholesterol regulatory gene was able to induce more than 40% of insertions and deletions (indel) formations in liver cells in one week (Ran et al. 2015). The *Neisseria meningitidis* Cas9 (3'246 bps) and the *Campilobacter jejuni* Cas9 (2'952 bps) also showed their efficiency in target genomic DNAs in iPSCs and mice (Hou et al. 2013; E. Kim et al. 2017). We were able to generate the nmCas9 and the saCas9 nickase versions and their gRNAs in the laboratory and test them in GFP$(CAG)_{101}$ cell line (unpublished data). The expression of these orthologues combined with gRNAs targeted within the CAG/CTG repeat tract did not result in a strong activity such as shown by the spCas9 nickase, probably due to the inefficient PAM sequence. Although they showed more contractions than expansions. These results confirmed the nick generation as a successful step to induce repeat contractions and the feasibility of short Cas9 orthologues in reproducing the spCas9 nickase results.

The use of an alternative shorter Cas9 need consequent optimization of PAM sequences for CAG/CTG repeat in order to obtain efficient levels of activity. In fact, different Cas9s need specific gRNA scaffold sequences and PAMs. It has been shown how important the presence

of a proper nucleotide PAM sequence is to obtain a good cleavage efficiency (Anders et al. 2014; Kleinstiver et al. 2015). Non-specific PAM sequences drastically reduce the Cas9 cleavage efficiency. To select CAG/CTG repeat recognition and cleavage by the use of alternative Cas9, the PAM sequence needs to be optimized for CAG. PAM specificity can be improved by the induction and selection of specific modifications in the Cas9 sequence that allow non-canonical PAM, as shown by Kleinstiver et al. (Kleinstiver et al. 2015). In fact, PAM optimization is possible by the use of a bacterial selection system. Mutations in the PAM-interaction domains of Cas9 followed by the survival selection for a specific PAM gives rise to mutated Cas9 able to cleave DNA sequences in presence of the selected altered PAM. The specific selection for NAG or NTG could optimize alternative Cas9 nickases and improve contraction rates in expanded CAG/CTG repeats.

The undetected Cas9 protein levels observed in injected livers could be caused by inefficient delivery of the Cas9 gene due to unspecific tropism of the selected AAV. Detection and binding to receptors present on the target cells surface by the capsid determines the specific tropism and transduction efficiency of the AAV (Wu, Asokan, and Samulski 2006; Schmidt and Grimm 2015). However, to find virus with high tropism and good transduction efficiency for the target cells, different mutations and combinations of different serotypes need be generated and tested in mice (Kienle et al. 2012). We selected AAV8 and AAV9 since they have shown to efficiently infect muscles and brain tissues (Zincarelli et al. 2008; Z. Wang et al. 2005; Dufour et al. 2014; Foust et al. 2009; Bish et al. 2008). However, alternative serotypes, such as AAV1, could be taken into consideration to target these tissues (Zincarelli et al. 2008; Rabinowitz et al. 2002). Distinct serotypes for AAV could be tested for selecting a vector with specific tropism for brain and muscles tissues. Delivery to the correct tissues and expression of functional Cas9 nickase

will determine the ability of this engineered nickase in inducing repeat contraction in DM1 and HD mouse models.

Improvement in delivery efficiency, increased presence and prolonged activity of Cas9 nickase could increase off-targets and side effects. Patients affected by expanded TNR disorders do not need a constant presence of Cas9 nickase to reverse pathogenic symptoms, but only a certain time window of activity. In fact, once reached the healthy length induced by Cas9 nickase activity, the short repeat tract should remain stable and reverse the pathogenic symptoms. The temporary expression and functionality of Cas9 nickase can be achieved in different ways. The use of self-inactivating system can be efficiently applied and reduce time exposition of the Cas9 to the target locus. Providing a gRNA specific for the Cas9 sequence can induce self-cleavage and disruption of the Cas9 expression after a certain time (Merienne et al. 2017; A. Li et al. 2019). Alternatively, temporary presence of this tool can be achieved by the use of RNPs. During the last years, studies developed the Cas9/gRNA RNPs delivery as a valuable alternative to the DNA based approach (Ramakrishna et al. 2014; Mout et al. 2017; D'Astolfo et al. 2015). In fact, the delivery of a ready to use protein complex brings advantages compared to the use of the DNA-based Cas9. Efficient gene disruption, higher gene editing rate and reduced off-target effect are the major differences observed in RNP compared to Cas9 plasmid-based in cell cultures (Ramakrishna et al. 2014; S. Kim et al. 2014; Liang et al. 2015; Zuris et al. 2015; M. Wang et al. 2016). Zuris et al. observed an increased specificity and a lower off-target frequency induced by Cas9/gRNA RNP compared to DNA plasmid when transfected into 293 HEK cells (Zuris et al. 2015). They also observed efficient indel formation induced by the Cas9 protein:gRNA with cationic lipid when injected into mouse cochlea. Thus, Cas9/gRNA RNPs are promising alternative for DNA plasmid-based Cas9 form. In conclusion, reduced exposition of the Cas9 activity to the target gene can be achieved in different ways.

IV.III The Cas9 nickase treatment as the most promising gene therapy approach for expanded TNR disorders

The induction of nicks generation within the trinucleotide repeats is a promising strategy to cure the expanded TNR disorders. The silencing of an expanded allele has shown to reverse the symptoms (Yamamoto, Lucas, and Hen 2000; Mahadevan et al. 2006a; Zu et al. 2004). Thus, the use of gene editing to shrink repeat tract could ultimately reverse the symptoms. We decided to directly target the repeat tract and induce the DNA damage within the trinucleotide sequence. However, others have used a different approach to tackle expanded TNR disorders: a whole or partial excision of the repeats. Although this approach reversed pathogenic conditions in different models (van Agtmaal et al. 2017; Provenzano et al. 2017; Scrudato et al. 2017; Pribadi et al. 2016; Monteys et al. 2017; Shin et al. 2016; Merienne et al. 2017; Y. Li et al. 2015; Ouellet et al. 2017; Park et al. 2015), it showed several limitations, such as indels generation, high inversion frequency. The generation of a DSB in the proximity of the CGG repeats in *FMR1* gene resulted in repeat excision and reactivation of the gene expression (Park et al. 2015). However, this technique relies on the NHEJ repair and resection mechanisms and results in a random loss of the target sequence. With a therapeutic point of view, the uncontrollable and random nature of this excision is a dangerous condition that cannot be used. In fact, unpredictable genome changes on the site of cleavage, such as unwanted deletions, could result in worse phenotypic conditions. A more precise excision of the repeat tract can be achieved by the generation of two concomitant cuts upstream and downstream of the target locus (Y. Wang et al. 2018; Provenzano et al. 2017; Y. Li et al. 2015; van Agtmaal et al. 2017). However, in these studies the excision of the repeats by the use of two gRNAs or two ZFNs caused frequent inversion events of the expanded repeats, resulting in an unsuccessful amelioration of the pathogenesis. The excision of the CTG repeats at the *DMPK* locus by two

gRNAs with saCas9 resulted in 20% inversion events in DM1 neural stem cells (Y. Wang et al. 2018). The expanded CTGs were inverted to expanded CAG repeats leading to antisense-foci formation. Due to inversion events, the foci formation was not reversed to healthy phenotype in DM1 neural stem cells (Y. Wang et al. 2018).

The targeting of repeats flanking sequences does not discriminate the specific mutant allele from the WT. Thus, the DNA damage is also induced at the WT locus. In fact, presence of indels in the WT allele due to the unspecific-allele targeting has been observed in different studies induced by NHEJ mechanism (Pribadi et al. 2016; Dastidar et al. 2018). Depending on the type of mutations generated by the activity of the engineered nuclease, non-sense, frame-shit, truncated proteins can be produced resulting in even worse conditions (Mangiarini et al. 1996).

Allele specificity can be obtain by selection of specific SNPs present in the mutant allele (Dabrowska et al. 2018; Monteys et al. 2017; Shin et al. 2016; Merienne et al. 2017). However, this technique owns a major limitation: the specific treatment needs to be customized for every single disorder and individual.

By contrast, the use of the Cas9 nickase that directs the DNA damage within the CAG/CTG repeat solves all the limitations present in the previously mentioned approaches (Cinesi et al. 2016). The induction of nicks instead of DSBs within the repeat tract activates a DNA repair mechanism different than the NHEJ, reducing the possibility of dangerous on and off-target mutations (Cinesi et al. 2016). Even more, the Cas9 nickase showed repeat length-dependent specificity (Cinesi et al. 2016). In fact, variation in repeat sizes has been observed only in cells carrying expanded repeats, GFP$(CAG)_{101}$ and GFP$(CAG)_{270}$, transfected with Cas9 nickase and gCTG. This promising result demonstrated the specificity of Cas9 nickase for mutant alleles. Finally, the direct targeting of the repeat tract allows the use of the same tool for all 14 CAG/CTG disorders. For these reasons, direct action into the repeat tract and the induction of

contractions by the Cas9 nickase appears to be the most suitable and promising solution at the moment.

In conclusion, results from this project have increased the knowledge on TNR pathogenesis and established the basis for a possible treatment against expanded TNR disorders. The ultimate goal is to use a gene therapy approach to induce repeat contractions in the mutant allele for expanded CAG/CTG repeat disorders. Since in this study the Cas9 nickase showed to induce predominantly repeat contractions in HEK293-derived cells and patient-derived LCLs, we should be able observe repeat instability induced by the Cas9 nickase in mouse models. Results from this would be fundamental to determine whether the Cas9 nickase can be used to improve the pathology *in vivo* and be delivered via a gene therapy approach. Should our approach be successful in inducing repeat contractions using the Cas9 nickase in somatic tissues, this treatment could be applied to every 14 different neurological disorders caused by CTG/CAG expanded.

Chapter V

References

V. References

Acland, G. M., G. D. Aguirre, J. Ray, Q. Zhang, T. S. Aleman, A. V. Cideciyan, S. E. Pearce-Kelling, et al. 2001. "Gene Therapy Restores Vision in a Canine Model of Childhood Blindness." *Nature Genetics* 28 (1): 92–95. https://doi.org/10.1038/88327.

Aeschbach, Lorène, and Vincent Dion. 2017. "Minimizing Carry-over PCR Contamination in Expanded CAG/CTG Repeat Instability Applications." *Scientific Reports* 7 (1): 18026. https://doi.org/10.1038/s41598-017-18168-2.

Agtmaal, Ellen L. van, Laurène M. André, Marieke Willemse, Sarah A. Cumming, Ingeborg D. G. van Kessel, Walther J. A. A. van den Broek, Geneviève Gourdon, et al. 2017. "CRISPR/Cas9-Induced (CTG·CAG)n Repeat Instability in the Myotonic Dystrophy Type 1 Locus: Implications for Therapeutic Genome Editing." *Molecular Therapy* 25 (1): 24–43. https://doi.org/10.1016/j.ymthe.2016.10.014.

Aiuti, Alessandro, Federica Cattaneo, Stefania Galimberti, Ulrike Benninghoff, Barbara Cassani, Luciano Callegaro, Samantha Scaramuzza, et al. 2009. "Gene Therapy for Immunodeficiency Due to Adenosine Deaminase Deficiency." Research-article. Http://Dx.Doi.Org/10.1056/NEJMoa0805817. December 10, 2009. https://doi.org/10.1056/NEJMoa0805817.

Aiuti, Alessandro, Maria Grazia Roncarolo, and Luigi Naldini. 2017. "Gene Therapy for ADA-SCID, the First Marketing Approval of an Ex Vivo Gene Therapy in Europe: Paving the Road for the next Generation of Advanced Therapy Medicinal Products." *EMBO Molecular Medicine* 9 (6): 737–40. https://doi.org/10.15252/emmm.201707573.

Aiuti, Alessandro, Shimon Slavin, Memet Aker, Francesca Ficara, Sara Deola, Alessandra Mortellaro, Shoshana Morecki, et al. 2002. "Correction of ADA-SCID by Stem Cell Gene Therapy Combined with Nonmyeloablative Conditioning." *Science* 296 (5577): 2410–13. https://doi.org/10.1126/science.1070104.

Anders, Carolin, Ole Niewoehner, Alessia Duerst, and Martin Jinek. 2014. "Structural Basis of PAM-Dependent Target DNA Recognition by the Cas9 Endonuclease." *Nature* 513 (7519): 569–73. https://doi.org/10.1038/nature13579.

Andtbacka, Robert H.I., Howard L. Kaufman, Frances Collichio, Thomas Amatruda, Neil Senzer, Jason Chesney, Keith A. Delman, et al. 2015. "Talimogene Laherparepvec Improves Durable Response Rate in Patients With Advanced Melanoma." *Journal of Clinical Oncology* 33 (25): 2780–88. https://doi.org/10.1200/JCO.2014.58.3377.

Axford, Michelle M., Yuh-Hwa Wang, Masayuki Nakamori, Maria Zannis-Hadjopoulos, Charles A. Thornton, and Christopher E. Pearson. 2013. "Detection of Slipped-DNAs at the Trinucleotide Repeats of the Myotonic Dystrophy Type I Disease Locus in Patient Tissues." *PLOS Genetics* 9 (12): e1003866. https://doi.org/10.1371/journal.pgen.1003866.

Babačić, Haris, Aditi Mehta, Olivia Merkel, and Benedikt Schoser. 2019. "CRISPR-Cas Gene-Editing as Plausible Treatment of Neuromuscular and Nucleotide-Repeat-Expansion Diseases: A Systematic Review." *PLOS ONE* 14 (2): e0212198. https://doi.org/10.1371/journal.pone.0212198.

Bennett, Jean, Manzar Ashtari, Jennifer Wellman, Kathleen A. Marshall, Laura L. Cyckowski, Daniel C. Chung, Sarah McCague, et al. 2012. "AAV2 Gene Therapy Readministration in Three Adults with Congenital Blindness." *Science Translational Medicine* 4 (120): 120ra15. https://doi.org/10.1126/scitranslmed.3002865.

Bettencourt, Conceição, Davina Hensman-Moss, Michael Flower, Sarah Wiethoff, Alexis Brice, Cyril Goizet, Giovanni Stevanin, et al. 2016. "DNA Repair Pathways Underlie a Common Genetic Mechanism Modulating Onset in Polyglutamine Diseases." *Annals of Neurology* 79 (6): 983–90. https://doi.org/10.1002/ana.24656.

Beumer, Kelly J., Jonathan K. Trautman, Michelle Christian, Timothy J. Dahlem, Cathleen M. Lake, R. Scott Hawley, David J. Grunwald, Daniel F. Voytas, and Dana Carroll. 2013. "Comparing Zinc Finger Nucleases and Transcription Activator-Like Effector Nucleases for Gene Targeting in Drosophila." *G3: Genes|Genomes|Genetics* 3 (10): 1717–25. https://doi.org/10.1534/g3.113.007260.

Biagioni, Alessio, Anna Laurenzana, Francesca Margheri, Anastasia Chillà, Gabriella Fibbi, and Mario so. 2018. "Delivery Systems of CRISPR/Cas9-Based Cancer Gene Therapy." *Journal of Biological Engineering* 12 (December). https://doi.org/10.1186/s13036-018-0127-2.

Bish, Lawrence T., Kevin Morine, Meg M. Sleeper, Julio Sanmiguel, Di Wu, Guangping Gao, James M. Wilson, and H. Lee Sweeney. 2008. "Adeno-Associated Virus (AAV) Serotype 9 Provides Global Cardiac Gene Transfer Superior to AAV1, AAV6, AAV7, and AAV8 in the Mouse and Rat." *Human Gene Therapy* 19 (12): 1359–68. https://doi.org/10.1089/hum.2008.123.

Bisset, Darren R., Ewa A. Stepniak-Konieczna, Maja Zavaljevski, Jessica Wei, Gregory T. Carter, Michael D. Weiss, and Joel R. Chamberlain. 2015. "Therapeutic Impact of Systemic AAV-Mediated RNA Interference in a Mouse Model of Myotonic Dystrophy." *Human Molecular Genetics* 24 (17): 4971–83. https://doi.org/10.1093/hmg/ddv219.

Blaese, R. Michael, Kenneth W. Culver, A. Dusty Miller, Charles S. Carter, Thomas Fleisher, Mario Clerici, Gene Shearer, et al. 1995. "T Lymphocyte-Directed Gene Therapy for ADA− SCID: Initial Trial Results After 4 Years." *Science* 270 (5235): 475–80. https://doi.org/10.1126/science.270.5235.475.

Boch, Jens, Heidi Scholze, Sebastian Schornack, Angelika Landgraf, Simone Hahn, Sabine Kay, Thomas Lahaye, Anja Nickstadt, and Ulla Bonas. 2009. "Breaking the Code of DNA Binding Specificity of TAL-Type III Effectors." *Science* 326 (5959): 1509–12. https://doi.org/10.1126/science.1178811.

Broek, Walther J A A Van Den, Marcel R Nelen, Derick G Wansink, Marga M Coerwinkel, Hein Riele, Patricia J T A Groenen, and Bé Wieringa. 2002. "Somatic Expansion Behaviour of the (CTG)n Repeat in Myotonic Dystrophy Knock-in Mice Is Differentially Affected by Msh3 and Msh6 Mismatch – Repair Proteins." *Human Molecular Genetics* 11 (2): 191–98.

Brouns, Stan J. J., Matthijs M. Jore, Magnus Lundgren, Edze R. Westra, Rik J. H. Slijkhuis, Ambrosius P. L. Snijders, Mark J. Dickman, Kira S. Makarova, Eugene V. Koonin, and John van der Oost. 2008. "Small CRISPR RNAs Guide Antiviral Defense in Prokaryotes." *Science* 321 (5891): 960–64. https://doi.org/10.1126/science.1159689.

Campeau, Eric, Victoria E. Ruhl, Francis Rodier, Corey L. Smith, Brittany L. Rahmberg, Jill O. Fuss, Judith Campisi, Paul Yaswen, Priscilla K. Cooper, and Paul D. Kaufman. 2009. "A Versatile Viral System for Expression and Depletion of Proteins in Mammalian Cells." *PLoS ONE* 4 (8). https://doi.org/10.1371/journal.pone.0006529.

Carroll, D. 2008. "Progress and Prospects: Zinc-Finger Nucleases as Gene Therapy Agents." *Gene Therapy* 15 (22): 1463–68. https://doi.org/10.1038/gt.2008.145.

Carroll, Dana. 2008. "Zinc-Finger Nucleases as Gene Therapy Agents." *Gene Therapy* 15 (22): 1463–68. https://doi.org/10.1038/gt.2008.145.

Carroll, Jeffrey B, Simon C Warby, Amber L Southwell, Crystal N Doty, Sarah Greenlee, Niels Skotte, Gene Hung, C Frank Bennett, Susan M Freier, and Michael R Hayden.

2011. “Potent and Selective Antisense Oligonucleotides Targeting Single-Nucleotide Polymorphisms in the Huntington Disease Gene / Allele-Specific Silencing of Mutant Huntingtin.” *Molecular Therapy* 19 (12): 2178–85. https://doi.org/10.1038/mt.2011.201.

Cathomen, Toni, and J. Keith Joung. 2008a. “Zinc-Finger Nucleases: The next Generation Emerges.” *Molecular Therapy: The Journal of the American Society of Gene Therapy* 16 (7): 1200–1207. https://doi.org/10.1038/mt.2008.114.

Cattoglio, Claudia, Danilo Pellin, Ermanno Rizzi, Giulietta Maruggi, Giorgio Corti, Francesca Miselli, Daniela Sartori, et al. 2010. “High-Definition Mapping of Retroviral Integration Sites Identifies Active Regulatory Elements in Human Multipotent Hematopoietic Progenitors.” *Blood* 116 (25): 5507–17. https://doi.org/10.1182/blood-2010-05-283523.

Cavazzana-Calvo, Marina, Emmanuel Payen, Olivier Negre, Gary Wang, Kathleen Hehir, Floriane Fusil, Julian Down, et al. 2010. “Transfusion Independence and *HMGA2* Activation after Gene Therapy of Human β-Thalassaemia.” *Nature* 467 (7313): 318–22. https://doi.org/10.1038/nature09328.

Cermak, Tomas, Erin L. Doyle, Michelle Christian, Li Wang, Yong Zhang, Clarice Schmidt, Joshua A. Baller, Nikunj V. Somia, Adam J. Bogdanove, and Daniel F. Voytas. 2011. “Efficient Design and Assembly of Custom TALEN and Other TAL Effector-Based Constructs for DNA Targeting.” *Nucleic Acids Research* 39 (12): e82. https://doi.org/10.1093/nar/gkr218.

Chau, Anthony, and Auinash Kalsotra. 2015. “Developmental Insights into the Pathology of and Therapeutic Strategies for DM1: Back to the Basics.” *Developmental Dynamics: An Official Publication of the American Association of Anatomists* 244 (3): 377–90. https://doi.org/10.1002/dvdy.24240.

Chen, Jian-Min, David N. Cooper, Nadia Chuzhanova, Claude Férec, and George P. Patrinos. 2007. “Gene Conversion: Mechanisms, Evolution and Human Disease.” *Nature Reviews Genetics* 8 (10): 762–75. https://doi.org/10.1038/nrg2193.

Choudhury, Sourav R, Zachary Fitzpatrick, Anne F Harris, Stacy A Maitland, Jennifer S Ferreira, Yuanfan Zhang, Shan Ma, et al. 2016. “In Vivo Selection Yields AAV-B1 Capsid for Central Nervous System and Muscle Gene Therapy.” *Molecular Therapy* 24 (7): 1247–57. https://doi.org/10.1038/mt.2016.84.

Choudhury, Sourav R, Anne F Harris, Damien J Cabral, Allison M Keeler, Ellen Sapp, Jennifer S Ferreira, Heather L Gray-Edwards, et al. 2016. “Widespread Central Nervous System Gene Transfer and Silencing After Systemic Delivery of Novel AAV-AS Vector.” *Molecular Therapy* 24 (4): 726–35. https://doi.org/10.1038/mt.2015.231.

Chow, Ryan D., Christopher D. Guzman, Guangchuan Wang, Florian Schmidt, Mark W. Youngblood, Lupeng Ye, Youssef Errami, et al. 2017. “AAV-Mediated Direct *in Vivo* CRISPR Screen Identifies Functional Suppressors in Glioblastoma.” *Nature Neuroscience* 20 (10): 1329–41. https://doi.org/10.1038/nn.4620.

Christian, Michelle, Tomas Cermak, Erin L. Doyle, Clarice Schmidt, Feng Zhang, Aaron Hummel, Adam J. Bogdanove, and Daniel F. Voytas. 2010. “Targeting DNA Double-Strand Breaks with TAL Effector Nucleases.” *Genetics* 186 (2): 756–61. https://doi.org/10.1534/genetics.110.120717.

Cinesi, Cinzia, Lorène Aeschbach, Bin Yang, and Vincent Dion. 2016. “Contracting CAG/CTG Repeats Using the CRISPR-Cas9 Nickase.” *Nature Communications* 7 (November): 13272. https://doi.org/10.1038/ncomms13272.

Cong, Le, F. Ann Ran, David Cox, Shuailiang Lin, Robert Barretto, Naomi Habib, Patrick D. Hsu, et al. 2013. "Multiplex Genome Engineering Using CRISPR/Cas Systems." *Science* 339 (6121): 819–23. https://doi.org/10.1126/science.1231143.

Coonrod, Leslie a, Masayuki Nakamori, Wenli Wang, Samuel Carrell, Cameron L Hilton, Micah J Bodner, Ruth B Siboni, et al. 2013. "Reducing Levels of Toxic RNA with Small Molecules." *ACS Chemical Biology* 8 (11): 2528–37. https://doi.org/10.1021/cb400431f.

Dabrowska, Magdalena, Wojciech Juzwa, Wlodzimierz J. Krzyzosiak, and Marta Olejniczak. 2018. "Precise Excision of the CAG Tract from the Huntingtin Gene by Cas9 Nickases." *Frontiers in Neuroscience* 12 (February). https://doi.org/10.3389/fnins.2018.00075.

Dandelot, Elodie, and Geneviève Gourdon. 2018. "The Flash-Small-Pool PCR: How to Transform Blotting and Numerous Hybridization Steps into a Simple Denatured PCR." *BioTechniques* 64 (6): 262–65. https://doi.org/10.2144/btn-2018-0035.

Dastidar, Sumitava, Simon Ardui, Kshitiz Singh, Debanjana Majumdar, Nisha Nair, Yanfang Fu, Deepak Reyon, et al. 2018. "Efficient CRISPR/Cas9-Mediated Editing of Trinucleotide Repeat Expansion in Myotonic Dystrophy Patient-Derived IPS and Myogenic Cells." *Nucleic Acids Research* 46 (16): 8275–98. https://doi.org/10.1093/nar/gky548.

D'Astolfo, Diego S., Romina J. Pagliero, Anita Pras, Wouter R. Karthaus, Hans Clevers, Vikram Prasad, Robert Jan Lebbink, Holger Rehmann, and Niels Geijsen. 2015. "Efficient Intracellular Delivery of Native Proteins." *Cell* 161 (3): 674–90. https://doi.org/10.1016/j.cell.2015.03.028.

Deltcheva, Elitza, Krzysztof Chylinski, Cynthia M. Sharma, Karine Gonzales, Yanjie Chao, Zaid A. Pirzada, Maria R. Eckert, Jörg Vogel, and Emmanuelle Charpentier. 2011. "CRISPR RNA Maturation by Trans-Encoded Small RNA and Host Factor RNase III." *Nature* 471 (7340): 602–7. https://doi.org/10.1038/nature09886.

DePolo, Nicholas J., Joyce D. Reed, Philip L. Sheridan, Kay Townsend, Sybille L. Sauter, Douglas J. Jolly, and Thomas W. Dubensky. 2000. "VSV-G Pseudotyped Lentiviral Vector Particles Produced in Human Cells Are Inactivated by Human Serum." *Molecular Therapy* 2 (3): 218–22. https://doi.org/10.1006/mthe.2000.0116.

Deverman, Benjamin E., Piers L. Pravdo, Bryan P. Simpson, Sripriya Ravindra Kumar, Ken Y. Chan, Abhik Banerjee, Wei-Li Wu, et al. 2016. "Cre-Dependent Selection Yields AAV Variants for Widespread Gene Transfer to the Adult Brain." *Nature Biotechnology* 34 (2): 204–9. https://doi.org/10.1038/nbt.3440.

Díaz-Hernández, Miguel, Jesús Torres-Peraza, Alejandro Salvatori-Abarca, María A. Morán, Pilar Gómez-Ramos, Jordi Alberch, and José J. Lucas. 2005. "Full Motor Recovery Despite Striatal Neuron Loss and Formation of Irreversible Amyloid-Like Inclusions in a Conditional Mouse Model of Huntington's Disease." *Journal of Neuroscience* 25 (42): 9773–81. https://doi.org/10.1523/JNEUROSCI.3183-05.2005.

Dion, Vincent. 2014. "Tissue Specificity in DNA Repair: Lessons from Trinucleotide Repeat Instability." *Trends in Genetics* 30 (6): 220–29. https://doi.org/10.1016/j.tig.2014.04.005.

Dion, Vincent, Yunfu Lin, Leroy Hubert, Robert A. Waterland, and John H. Wilson. 2008. "Dnmt1 Deficiency Promotes CAG Repeat Expansion in the Mouse Germline." *Human Molecular Genetics* 17 (9): 1306–17. https://doi.org/10.1093/hmg/ddn019.

Drouet, Valérie, Valérie Perrin, Raymonde Hassig, Noëlle Dufour, Gwennaelle Auregan, Sandro Alves, Gilles Bonvento, et al. 2009. "Sustained Effects of Nonallele-Specific Huntingtin Silencing." *Annals of Neurology* 65 (3): 276–85. https://doi.org/10.1002/ana.21569.

Dufour, Brett D, Catherine A Smith, Randall L Clark, Timothy R Walker, and Jodi L McBride. 2014. “Intrajugular Vein Delivery of AAV9-RNAi Prevents Neuropathological Changes and Weight Loss in Huntington’s Disease Mice.” *Molecular Therapy* 22 (4): 797–810. https://doi.org/10.1038/mt.2013.289.

Dull, Tom, Romain Zufferey, Michael Kelly, R. J. Mandel, Minh Nguyen, Didier Trono, and Luigi Naldini. 1998. “A Third-Generation Lentivirus Vector with a Conditional Packaging System.” *Journal of Virology* 72 (11): 8463–71.

E M Doherty. 2017. “Screening Approaches to Identify Small-Molecule Modulators of Huntingtin Protein Levels.” *CHDI Foundation Annual Therapeutics Conference*.

European Medicines Agency. 2012. “European Medicines Agency Recommends First Gene Therapy for Approval.” European Medicines Agency. July 20, 2012. https://www.ema.europa.eu/en/news/european-medicines-agency-recommends-first-gene-therapy-approval.

———. 2015. “Imlygic.” European Medicines Agency. 2015. https://www.ema.europa.eu/en/medicines/human/EPAR/imlygic.

Finn, Jonathan D., Amy Rhoden Smith, Mihir C. Patel, Lucinda Shaw, Madeleine R. Youniss, Jane van Heteren, Tanner Dirstine, et al. 2018. “A Single Administration of CRISPR/Cas9 Lipid Nanoparticles Achieves Robust and Persistent In Vivo Genome Editing.” *Cell Reports* 22 (9): 2227–35. https://doi.org/10.1016/j.celrep.2018.02.014.

Foust, Kevin D., Emily Nurre, Chrystal L. Montgomery, Anna Hernandez, Curtis M. Chan, and Brian K. Kaspar. 2009. “Intravascular AAV9 Preferentially Targets Neonatal Neurons and Adult Astrocytes.” *Nature Biotechnology* 27 (1): 59–65. https://doi.org/10.1038/nbt.1515.

Friedland, Ari E., Reshica Baral, Pankhuri Singhal, Katherine Loveluck, Shen Shen, Minerva Sanchez, Eugenio Marco, et al. 2015. “Characterization of Staphylococcus Aureus Cas9: A Smaller Cas9 for All-in-One Adeno-Associated Virus Delivery and Paired Nickase Applications.” *Genome Biology* 16 (1): 257. https://doi.org/10.1186/s13059-015-0817-8.

Fu, Yanfang, Jennifer A. Foden, Cyd Khayter, Morgan L. Maeder, Deepak Reyon, J. Keith Joung, and Jeffry D. Sander. 2013. “High-Frequency off-Target Mutagenesis Induced by CRISPR-Cas Nucleases in Human Cells.” *Nature Biotechnology* 31 (9): 822–26. https://doi.org/10.1038/nbt.2623.

Furling, D., G. Doucet, M.-A. Langlois, L. Timchenko, E. Belanger, L. Cossette, and J. Puymirat. 2003. “Viral Vector Producing Antisense RNA Restores Myotonic Dystrophy Myoblast Functions.” *Gene Therapy* 10 (9): 795–802. https://doi.org/10.1038/sj.gt.3301955.

Gabriel, Richard, Angelo Lombardo, Anne Arens, Jeffrey C. Miller, Pietro Genovese, Christine Kaeppel, Ali Nowrouzi, et al. 2011. “An Unbiased Genome-Wide Analysis of Zinc-Finger Nuclease Specificity.” *Nature Biotechnology* 29 (9): 816–23. https://doi.org/10.1038/nbt.1948.

Gaj, Thomas, Charles A. Gersbach, and Carlos F. Barbas. 2013. “ZFN, TALEN, and CRISPR/Cas-Based Methods for Genome Engineering.” *Trends in Biotechnology* 31 (7): 397–405. https://doi.org/10.1016/j.tibtech.2013.04.004.

García-lópez, Amparo, Beatriz Llamusí, Mar Orzáez, and et al. 2011. “In Vivo Discovery of a Peptide That Prevents CUG – RNA Hairpin Formation and Reverses RNA Toxicity in Myotonic Dystrophy Models.” *PNAS* 108 (29): 11866–71. https://doi.org/10.1073/pnas.1018213108/-/DCSupplemental.www.pnas.org/cgi/doi/10.1073/pnas.1018213108.

Garriga-Canut, Mireia, Carmen Agustín-Pavón, Frank Herrmann, Aurora Sánchez, Mara Dierssen, Cristina Fillat, and Mark Isalan. 2012. “Synthetic Zinc Finger Repressors

Reduce Mutant Huntingtin Expression in the Brain of R6/2 Mice." *Proceedings of the National Academy of Sciences* 109 (45): E3136–45. https://doi.org/10.1073/pnas.1206506109.
Gaspar, H. Bobby, Samantha Cooray, Kimberly C. Gilmour, Kathryn L. Parsley, Stuart Adams, Steven J. Howe, Abdulaziz Al Ghonaium, et al. 2011. "Long-Term Persistence of a Polyclonal T Cell Repertoire After Gene Therapy for X-Linked Severe Combined Immunodeficiency." *Science Translational Medicine* 3 (97): 97ra79-97ra79. https://doi.org/10.1126/scitranslmed.3002715.
Gomes-Pereira, Mário, Thomas A. Cooper, and Geneviève Gourdon. 2011a. "Myotonic Dystrophy Mouse Models: Towards Rational Therapy Development." *Trends in Molecular Medicine* 17 (9). https://doi.org/10.1016/j.molmed.2011.05.004.
Gorbunova, Vera, Andrei Seluanov, Vincent Dion, Zoltan Sandor, James L. Meservy, and John H. Wilson. 2003. "Selectable System for Monitoring the Instability of CTG/CAG Triplet Repeats in Mammalian Cells." *Molecular and Cellular Biology* 23 (13): 4485–93. https://doi.org/10.1128/MCB.23.13.4485-4493.2003.
Gourdon, G, and G Meola. 2017. "Myotonic Dystrophies: State of the Art of New Therapeutic Developments for the CNS." *Frontiers in Cellular Neuroscience* in press (April): 1–14. https://doi.org/10.3389/FNCEL.2017.00101.
Gourdon, Geneviève, François Radvanyi, Anne-Sophie Lia, Chantal Duros, Martine Blanche, Marc Abitbol, Claudine Junien, and Hlène Hofmann-Radvanyi. 1997. "Moderate Intergenerational and Somatic Instability of a 55-CTG Repeat in Transgenic Mice." *Nature Genetics* 15 (2): 190. https://doi.org/10.1038/ng0297-190.
Grieger, Joshua C., and Richard J. Samulski. 2005. "Packaging Capacity of Adeno-Associated Virus Serotypes: Impact of Larger Genomes on Infectivity and Postentry Steps." *Journal of Virology* 79 (15): 9933–44. https://doi.org/10.1128/JVI.79.15.9933-9944.2005.
Group, Huntington's Disease Collaborative Research. 1993. "A Novel Gene Containing a Trinucleotide That Is Expanded and Unstable on Huntington ' s Disease Chromosomes." *Cell* 72: 971–83.
Hammans, S. R. 2002. "MYOTONIC DYSTROPHY, 3rd Edition." *Brain* 125 (8): 1225–26. https://doi.org/10.1093/brain/awf172.
Harper, Scott Q., Patrick D. Staber, Xiaohua He, Steven L. Eliason, Inês H. Martins, Qinwen Mao, Linda Yang, Robert M. Kotin, Henry L. Paulson, and Beverly L. Davidson. 2005. "RNA Interference Improves Motor and Neuropathological Abnormalities in a Huntington's Disease Mouse Model." *Proceedings of the National Academy of Sciences* 102 (16): 5820–25. https://doi.org/10.1073/pnas.0501507102.
Hashimoto, Masakazu, and Tatsuya Takemoto. 2015. "Electroporation Enables the Efficient MRNA Delivery into the Mouse Zygotes and Facilitates CRISPR/Cas9-Based Genome Editing." *Scientific Reports* 5 (June): 11315. https://doi.org/10.1038/srep11315.
Hernández-Hernández, Oscar, Céline Guiraud-Dogan, Géraldine Sicot, Aline Huguet, Sabrina Luilier, Esther Steidl, Stefanie Saenger, et al. 2013. "Myotonic Dystrophy CTG Expansion Affects Synaptic Vesicle Proteins, Neurotransmission and Mouse Behaviour." *Brain* 136 (3): 957–70. https://doi.org/10.1093/brain/aws367.
High, Federico Mingozzi and Katherine A. 2011. "Immune Responses to AAV in Clinical Trials." Current Gene Therapy. July 31, 2011. http://www.eurekaselect.com/74395/article.
Holehonnur, Roopashri, Srihari K. Lella, Anthony Ho, Jonathan A. Luong, and Jonathan E. Ploski. 2015. "The Production of Viral Vectors Designed to Express Large and

Difficult to Express Transgenes within Neurons." *Molecular Brain* 8 (1): 12. https://doi.org/10.1186/s13041-015-0100-7.
Holmans, Peter A., Thomas H. Massey, and Lesley Jones. 2017. "Genetic Modifiers of Mendelian Disease: Huntington's Disease and the Trinucleotide Repeat Disorders." *Human Molecular Genetics* 26 (R2): R83–90. https://doi.org/10.1093/hmg/ddx261.
Horii, Takuro, Yuji Arai, Miho Yamazaki, Sumiyo Morita, Mika Kimura, Masahiro Itoh, Yumiko Abe, and Izuho Hatada. 2014. "Validation of Microinjection Methods for Generating Knockout Mice by CRISPR/Cas-Mediated Genome Engineering." *Scientific Reports* 4 (March): 4513. https://doi.org/10.1038/srep04513.
Hou, Zhonggang, Yan Zhang, Nicholas E. Propson, Sara E. Howden, Li-Fang Chu, Erik J. Sontheimer, and James A. Thomson. 2013. "Efficient Genome Engineering in Human Pluripotent Stem Cells Using Cas9 from Neisseria Meningitidis." *Proceedings of the National Academy of Sciences* 110 (39): 15644–49. https://doi.org/10.1073/pnas.1313587110.
Huguet, Aline, Fadia Medja, Annie Nicole, Alban Vignaud, Céline Guiraud-Dogan, Arnaud Ferry, Valérie Decostre, et al. 2012. "Molecular, Physiological, and Motor Performance Defects in DMSXL Mice Carrying >1,000 CTG Repeats from the Human DM1 Locus." *PLoS Genetics* 8 (11). https://doi.org/10.1371/journal.pgen.1003043.
Huntington, George. 1872. "On Chorea." *Medical and Surgical Reporter. Philadelphia: SW Butler*.
Ishino, Y, H Shinagawa, K Makino, M Amemura, and A Nakata. 1987. "Nucleotide Sequence of the Iap Gene, Responsible for Alkaline Phosphatase Isozyme Conversion in Escherichia Coli, and Identification of the Gene Product." *Journal of Bacteriology* 169 (12): 5429–33.
Jansen, Ruud, Jan D. A. van Embden, Wim Gaastra, and Leo M. Schouls. 2002. "Identification of Genes That Are Associated with DNA Repeats in Prokaryotes." *Molecular Microbiology* 43 (6): 1565–75. https://doi.org/10.1046/j.1365-2958.2002.02839.x.
Jiang, Wenyan, David Bikard, David Cox, Feng Zhang, and Luciano a Marraffini. 2013. "RNA-Guided Editing of Bacterial Genomes Using CRISPR-Cas Systems." *Nature Biotechnology* 31 (3): 233–39. https://doi.org/10.1038/nbt.2508.
Jinek, Martin, Krzysztof Chylinski, Ines Fonfara, Michael Hauer, Jennifer A Doudna, and Emmanuelle Charpentier. 2012a. "A Programmable Dual-RNA – Guided" 337 (August): 816–22.
Jinek, Martin, Krzysztof Chylinski, Ines Fonfara, Michael Hauer, Jennifer A. Doudna, and Emmanuelle Charpentier. 2012b. "A Programmable Dual-RNA-Guided DNA Endonuclease in Adaptive Bacterial Immunity." *Science (New York, N.Y.)* 337 (6096): 816–21. https://doi.org/10.1126/science.1225829.
Johansen, Anne Katrine, Bas Molenaar, Danielle Versteeg, Ana Rita Leitoguinho, Charlotte Demkes, Bastiaan Spanjaard, Hesther de Ruiter, et al. 2017. "Postnatal Cardiac Gene Editing Using CRISPR/Cas9 With AAV9-Mediated Delivery of Short Guide RNAs Results in Mosaic Gene Disruption." *Circulation Research* 121 (10): 1168–81. https://doi.org/10.1161/CIRCRESAHA.116.310370.
Kaeppel, Christine, Stuart G. Beattie, Raffaele Fronza, Richard van Logtenstein, Florence Salmon, Sabine Schmidt, Stephan Wolf, et al. 2013. "A Largely Random AAV Integration Profile after LPLD Gene Therapy." *Nature Medicine* 19 (7): 889–91. https://doi.org/10.1038/nm.3230.
Kalman, Lisa, Jack Tarleton, Monica Hitch, Madhuri Hegde, Nick Hjelm, Elizabeth Berry-Kravis, Lili Zhou, et al. 2013. "Development of a Genomic DNA Reference Material

Panel for Myotonic Dystrophy Type 1 (DM1) Genetic Testing." *The Journal of Molecular Diagnostics* 15 (4): 518–25. https://doi.org/10.1016/j.jmoldx.2013.03.008.
Kang, Yoo Kyung, Kyu Kwon, Jea Sung Ryu, Ha Neul Lee, Chankyu Park, and Hyun Jung Chung. 2017. "Nonviral Genome Editing Based on a Polymer-Derivatized CRISPR Nanocomplex for Targeting Bacterial Pathogens and Antibiotic Resistance." *Bioconjugate Chemistry* 28 (4): 957–67. https://doi.org/10.1021/acs.bioconjchem.6b00676.
Kemaladewi, Dwi U., Eleonora Maino, Elzbieta Hyatt, Huayun Hou, Maylynn Ding, Kara M. Place, Xinyi Zhu, et al. 2017. "Correction of a Splicing Defect in a Mouse Model of Congenital Muscular Dystrophy Type 1A Using a Homology-Directed-Repair-Independent Mechanism." *Nature Medicine* 23 (8): 984–89. https://doi.org/10.1038/nm.4367.
Kennedy, L., and P. F. Shelbourne. 2000. "Dramatic Mutation Instability in HD Mouse Striatum: Does Polyglutamine Load Contribute to Cell-Specific Vulnerability in Huntington's Disease?" *Human Molecular Genetics* 9 (17): 2539–44.
Kielar, Catherine, and A. Jennifer Morton. 2018. "Early Neurodegeneration in R6/2 Mice Carrying the Huntington's Disease Mutation with a Super-Expanded CAG Repeat, Despite Normal Lifespan." *Journal of Huntington's Disease* 7 (1): 61–76. https://doi.org/10.3233/JHD-170265.
Kienle, Eike, Elena Senís, Kathleen Börner, Dominik Niopek, Ellen Wiedtke, Stefanie Grosse, and Dirk Grimm. 2012. "Engineering and Evolution of Synthetic Adeno-Associated Virus (AAV) Gene Therapy Vectors via DNA Family Shuffling." *JoVE (Journal of Visualized Experiments)*, no. 62 (April): e3819. https://doi.org/10.3791/3819.
Kim, Eunji, Taeyoung Koo, Sung Wook Park, Daesik Kim, Kyoungmi Kim, Hee-Yeon Cho, Dong Woo Song, et al. 2017. "*In Vivo* Genome Editing with a Small Cas9 Orthologue Derived from *Campylobacter Jejuni*." *Nature Communications* 8 (February): 14500. https://doi.org/10.1038/ncomms14500.
Kim, Hyongbum, and Jin-Soo Kim. 2014. "A Guide to Genome Engineering with Programmable Nucleases." *Nature Reviews Genetics* 15 (5): 321–34. https://doi.org/10.1038/nrg3686.
Kim, Sojung, Daesik Kim, Seung Woo Cho, Jungeun Kim, and Jin-Soo Kim. 2014. "Highly Efficient RNA-Guided Genome Editing in Human Cells via Delivery of Purified Cas9 Ribonucleoproteins." *Genome Research* 24 (6): 1012–19. https://doi.org/10.1101/gr.171322.113.
Kim, Yang-Gyun, Jooyeun Cha, and Srinivasan Chandrasegaran. 1996. "Hybrid Restriction Enzymes : Zinc Finger Fusions to Fok I Cleavage Domain." *Proceedings of the National Academy of Sciences* 93: 1156–60.
Kleinstiver, Benjamin P., Vikram Pattanayak, Michelle S. Prew, Shengdar Q. Tsai, Nhu T. Nguyen, Zongli Zheng, and J. Keith Joung. 2016. "High-Fidelity CRISPR–Cas9 Nucleases with No Detectable Genome-Wide off-Target Effects." *Nature* 529 (7587): 490–95. https://doi.org/10.1038/nature16526.
Kleinstiver, Benjamin P., Michelle S. Prew, Shengdar Q. Tsai, Ved V. Topkar, Nhu T. Nguyen, Zongli Zheng, Andrew P. W. Gonzales, et al. 2015. "Engineered CRISPR-Cas9 Nucleases with Altered PAM Specificities." *Nature* 523 (7561): 481–85. https://doi.org/10.1038/nature14592.
Kohwi, Y, H Wang, and T Kohwi-Shigematsu. 1993. "A Single Trinucleotide, 5'AGC3'/5'GCT3', of the Triplet-Repeat Disease Genes Confers Metal Ion-Induced Non-B DNA Structure." *Nucleic Acids Research* 21 (24): 5651–55.

Koike-Yusa, Hiroko, Yilong Li, E.-Pien Tan, Martin Del Castillo Velasco-Herrera, and Kosuke Yusa. 2014. "Genome-Wide Recessive Genetic Screening in Mammalian Cells with a Lentiviral CRISPR-Guide RNA Library." *Nature Biotechnology* 32 (3): 267–73. https://doi.org/10.1038/nbt.2800.

Kolli, Nivya, Ming Lu, Panchanan Maiti, Julien Rossignol, and Gary L. Dunbar. 2017. "CRISPR-Cas9 Mediated Gene-Silencing of the Mutant Huntingtin Gene in an In Vitro Model of Huntington's Disease." *International Journal of Molecular Sciences* 18 (4): 754. https://doi.org/10.3390/ijms18040754.

Kordasiewicz, Holly B., Lisa M. Stanek, Edward V. Wancewicz, Curt Mazur, Melissa M. McAlonis, Kimberly A. Pytel, Jonathan W. Artates, et al. 2012. "Sustained Therapeutic Reversal of Huntington's Disease by Transient Repression of Huntingtin Synthesis." *Neuron* 74 (6): 1031–44. https://doi.org/10.1016/j.neuron.2012.05.009.

Kouranova, Evguenia, Kevin Forbes, Guojun Zhao, Joe Warren, Angela Bartels, Yumei Wu, and Xiaoxia Cui. 2016. "CRISPRs for Optimal Targeting: Delivery of CRISPR Components as DNA, RNA, and Protein into Cultured Cells and Single-Cell Embryos." *Human Gene Therapy* 27 (6): 464–75. https://doi.org/10.1089/hum.2016.009.

Kovalenko, Marina, Ella Dragileva, Jason St. Claire, Tammy Gillis, Jolene R. Guide, Jaclyn New, Hualing Dong, et al. 2012. "Msh2 Acts in Medium-Spiny Striatal Neurons as an Enhancer of CAG Instability and Mutant Huntingtin Phenotypes in Huntington's Disease Knock-In Mice." *PLoS ONE* 7 (9). https://doi.org/10.1371/journal.pone.0044273.

Kovtun, I V, and C T Mcmurray. 2001. "Trinucleotide Expansion in Haploid Germ Cells by Gap Repair." *Nature Genetics* 27: 407–11.

Kovtun, I V, a R Thornhill, and C T McMurray. 2004. "Somatic Deletion Events Occur during Early Embryonic Development and Modify the Extent of CAG Expansion in Subsequent Generations." *Human Molecular Genetics* 13 (24): 3057–68. https://doi.org/10.1093/hmg/ddh325.

Kumar, Ashish, Jennifer Zhang, Sara Tallaksen-Greene, Michael R. Crowley, David K. Crossman, A. Jennifer Morton, Thomas Van Groen, et al. 2016. "Allelic Series of Huntington's Disease Knock-in Mice Reveals Expression Discorrelates." *Human Molecular Genetics* 25 (8): 1619–36. https://doi.org/10.1093/hmg/ddw040.

Lee, Johanna E., C. Frank Bennett, and Thomas A. Cooper. 2012. "RNase H-Mediated Degradation of Toxic RNA in Myotonic Dystrophy Type 1." *Proceedings of the National Academy of Sciences of the United States of America* 109 (11): 4221–26. https://doi.org/10.1073/pnas.1117019109.

Lee, Jong-Min, Vanessa C. Wheeler, Michael J. Chao, Jean Paul G. Vonsattel, Ricardo Mouro Pinto, Diane Lucente, Kawther Abu-Elneel, et al. 2015. "Identification of Genetic Factors That Modify Clinical Onset of Huntington's Disease." *Cell* 162 (3): 516–26. https://doi.org/10.1016/j.cell.2015.07.003.

Lee, Jong-Min, Jie Zhang, Andrew I. Su, John R. Walker, Tim Wiltshire, Kihwa Kang, Ella Dragileva, et al. 2010. "A Novel Approach to Investigate Tissue-Specific Trinucleotide Repeat Instability." *BMC Systems Biology* 4 (1): 29. https://doi.org/10.1186/1752-0509-4-29.

Lewinski, Mary K., Masahiro Yamashita, Michael Emerman, Angela Ciuffi, Heather Marshall, Gregory Crawford, Francis Collins, et al. 2006. "Retroviral DNA Integration: Viral and Cellular Determinants of Target-Site Selection." *PLOS Pathogens* 2 (6): e60. https://doi.org/10.1371/journal.ppat.0020060.

Li, Ang, Ciaran M. Lee, Ayrea E. Hurley, Kelsey E. Jarrett, Marco De Giorgi, Weiqi Lu, Karol S. Balderrama, et al. 2019. "A Self-Deleting AAV-CRISPR System for In Vivo

Genome Editing." *Molecular Therapy - Methods & Clinical Development* 12 (March): 111–22. https://doi.org/10.1016/j.omtm.2018.11.009.
Li, Yanjie, Urszula Polak, Angela D. Bhalla, Natalia Rozwadowska, Jill Sergesketter Butler, David R. Lynch, Sharon Y. R. Dent, and Marek Napierala. 2015. "Excision of Expanded GAA Repeats Alleviates the Molecular Phenotype of Friedreich's Ataxia." *Molecular Therapy: The Journal of the American Society of Gene Therapy* 23 (6): 1055–65. https://doi.org/10.1038/mt.2015.41.
Liang, Xiquan, Jason Potter, Shantanu Kumar, Yanfei Zou, Rene Quintanilla, Mahalakshmi Sridharan, Jason Carte, et al. 2015. "Rapid and Highly Efficient Mammalian Cell Engineering via Cas9 Protein Transfection." *Journal of Biotechnology* 208 (August): 44–53. https://doi.org/10.1016/j.jbiotec.2015.04.024.
Lin, HuiQian, HaoJie Hu, WeiSong Duan, YaLing Liu, GuoJun Tan, ZhongYao Li, YaKun Liu, et al. 2018. "Intramuscular Delivery of ScAAV9-HIGF1 Prolongs Survival in the HSOD1G93A ALS Mouse Model via Upregulation of D-Amino Acid Oxidase." *Molecular Neurobiology* 55 (1): 682–95. https://doi.org/10.1007/s12035-016-0335-z.
Lin, Yunfu, Sharon Y. R. Dent, John H. Wilson, Robert D. Wells, and Marek Napierala. 2010. "R Loops Stimulate Genetic Instability of CTG·CAG Repeats." *Proceedings of the National Academy of Sciences* 107 (2): 692–97. https://doi.org/10.1073/pnas.0909740107.
Lin, Yunfu, Vincent Dion, and John H. Wilson. 2005. "A Novel Selectable System for Detecting Expansion of CAG·CTG Repeats in Mammalian Cells." *Mutation Research/Fundamental and Molecular Mechanisms of Mutagenesis* 572 (1): 123–31. https://doi.org/10.1016/j.mrfmmm.2005.01.013.
Liu, X. Shawn, Hao Wu, Marine Krzisch, Xuebing Wu, John Graef, Julien Muffat, Denes Hnisz, et al. 2018. "Rescue of Fragile X Syndrome Neurons by DNA Methylation Editing of the FMR1 Gene." *Cell* 172 (5): 979-992.e6. https://doi.org/10.1016/j.cell.2018.01.012.
Logigian, E L, W B Martens, R T Moxley Iv, M P McDermott, N Dilek, A W Wiegner, A T Pearson, et al. 2010. "Mexiletine Is an Effective Antimyotonia Treatment in Myotonic Dystrophy Type," 9.
Long, Chengzu, Leonela Amoasii, Alex A. Mireault, John R. McAnally, Hui Li, Efrain Sanchez-Ortiz, Samadrita Bhattacharyya, John M. Shelton, Rhonda Bassel-Duby, and Eric N. Olson. 2016. "Postnatal Genome Editing Partially Restores Dystrophin Expression in a Mouse Model of Muscular Dystrophy." *Science* 351 (6271): 400–403. https://doi.org/10.1126/science.aad5725.
López Castel, Arturo, John D. Cleary, and Christopher E. Pearson. 2010. "Repeat Instability as the Basis for Human Diseases and as a Potential Target for Therapy." *Nature Reviews Molecular Cell Biology* 11 (3): 165–70. https://doi.org/10.1038/nrm2854.
MacLaren, Robert E, Markus Groppe, Alun R Barnard, Charles L Cottriall, Tanya Tolmachova, Len Seymour, K Reed Clark, et al. 2014. "Retinal Gene Therapy in Patients with Choroideremia: Initial Findings from a Phase 1/2 Clinical Trial." *The Lancet* 383 (9923): 1129–37. https://doi.org/10.1016/S0140-6736(13)62117-0.
Maguire, Albert M., Francesca Simonelli, Eric A. Pierce, Edward N. Pugh, Federico Mingozzi, Jeannette Bennicelli, Sandro Banfi, et al. 2008. "Safety and Efficacy of Gene Transfer for Leber's Congenital Amaurosis." *The New England Journal of Medicine* 358 (21): 2240–48. https://doi.org/10.1056/NEJMoa0802315.
Mahadevan, Mani S, Ramesh S Yadava, Qing Yu, Sadguna Balijepalli, Carla D Frenzel-McCardell, T David Bourne, and Lawrence H Phillips. 2006a. "Reversible Model of RNA Toxicity and Cardiac Conduction Defects in Myotonic Dystrophy." *Nature Genetics* 38 (9): 1066–70. https://doi.org/10.1038/ng1857.

Mali, Prashant, Luhan Yang, Kevin M. Esvelt, John Aach, Marc Guell, James E. DiCarlo, Julie E. Norville, and George M. Church. 2013. "RNA-Guided Human Genome Engineering via Cas9." *Science (New York, N.Y.)* 339 (6121): 823–26. https://doi.org/10.1126/science.1232033.

Mangiarini, Laura, Kirupa Sathasivam, Amarbirpal Mahal, Richard Mott, Mary Seller, and Gillian P. Bates. 1997. "Instability of Highly Expanded CAG Repeats in Mice Transgenic for the Huntington's Disease Mutation." *Nature Genetics* 15 (2): 197–200. https://doi.org/10.1038/ng0297-197.

Mangiarini, Laura, Kirupa Sathasivam, Mary Seller, Barbara Cozens, Alex Harper, Colin Hetherington, Martin Lawton, et al. 1996. "Exon 1 of the HD Gene with an Expanded CAG Repeat Is Sufficient to Cause a Progressive Neurological Phenotype in Transgenic Mice." *Cell* 87 (3): 493–506. https://doi.org/10.1016/S0092-8674(00)81369-0.

Mankodi, A. 2000. "Myotonic Dystrophy in Transgenic Mice Expressing an Expanded CUG Repeat." *Science* 289: 1769–73.

Mankodi, Ami, Eric Logigian, Linda Callahan, Carolyn McClain, Robert White, Don Henderson, Matt Krym, and Charles A. Thornton. 2000. "Myotonic Dystrophy in Transgenic Mice Expressing an Expanded CUG Repeat." *Science* 289 (5485): 1769–72. https://doi.org/10.1126/science.289.5485.1769.

Manley, K, T L Shirley, L Flaherty, and A Messer. 1999. "Msh2 Deficiency Prevents in Vivo Somatic Instability of the CAG Repeat in Huntington Disease Transgenic Mice." *Nature Genetics* 23: 471–73.

Marquis Gacy, A., Geoffrey Goellner, Nenad Juranić, Slobodan Macura, and Cynthia T. McMurray. 1995. "Trinucleotide Repeats That Expand in Human Disease Form Hairpin Structures in Vitro." *Cell* 81 (4): 533–40. https://doi.org/10.1016/0092-8674(95)90074-8.

McMurray, Cynthia T. 2010. "Mechanisms of Trinucleotide Repeat Instability during Human Development." *Nature Reviews Genetics* 11 (11): 786–99. https://doi.org/10.1038/nrg2828.

Memi, Fani, Aglaia Ntokou, and Irinna Papangeli. 2018. "CRISPR/Cas9 Gene-Editing: Research Technologies, Clinical Applications and Ethical Considerations." *Seminars in Perinatology*, Gene Editing (CRISPR), 42 (8): 487–500. https://doi.org/10.1053/j.semperi.2018.09.003.

Menalled, Liliana B., Andrea E. Kudwa, Sam Miller, Jon Fitzpatrick, Judy Watson-Johnson, Nicole Keating, Melinda Ruiz, et al. 2012. "Comprehensive Behavioral and Molecular Characterization of a New Knock-In Mouse Model of Huntington's Disease: ZQ175." *PLOS ONE* 7 (12): e49838. https://doi.org/10.1371/journal.pone.0049838.

Menalled, Liliana B., Jessica D. Sison, Ioannis Dragatsis, Scott Zeitlin, and Marie-Françoise Chesselet. 2003. "Time Course of Early Motor and Neuropathological Anomalies in a Knock-in Mouse Model of Huntington's Disease with 140 CAG Repeats." *Journal of Comparative Neurology* 465 (1): 11–26. https://doi.org/10.1002/cne.10776.

Mendell, Jerry R, Zarife Sahenk, Vinod Malik, Ana M Gomez, Kevin M Flanigan, Linda P Lowes, Lindsay N Alfano, et al. 2015. "A Phase 1/2a Follistatin Gene Therapy Trial for Becker Muscular Dystrophy." *Molecular Therapy* 23 (1): 192–201. https://doi.org/10.1038/mt.2014.200.

Merienne, Nicolas, Gabriel Vachey, Lucie de Longprez, Cécile Meunier, Virginie Zimmer, Guillaume Perriard, Mathieu Canales, et al. 2017. "The Self-Inactivating KamiCas9 System for the Editing of CNS Disease Genes." *Cell Reports* 20 (12): 2980–91. https://doi.org/10.1016/j.celrep.2017.08.075.

Mirkin, Sergei M. 2007. “Expandable DNA Repeats and Human Disease.” *Nature* 447 (June): 932–40. https://doi.org/10.1038/nature05977.
Mitchell, Rick S., Brett F. Beitzel, Astrid R. W. Schroder, Paul Shinn, Huaming Chen, Charles C. Berry, Joseph R. Ecker, and Frederic D. Bushman. 2004. “Retroviral DNA Integration: ASLV, HIV, and MLV Show Distinct Target Site Preferences.” *PLOS Biology* 2 (8): e234. https://doi.org/10.1371/journal.pbio.0020234.
Mittelman, David, Christopher Moye, Jason Morton, Kristen Sykoudis, Yunfu Lin, Dana Carroll, and John H Wilson. 2009a. “Zinc-Finger Directed Double-Strand Breaks within CAG Repeat Tracts Promote Repeat Instability in Human Cells.” *Proceedings of the National Academy of Sciences of the United States of America* 106 (24): 9607–12. https://doi.org/10.1073/pnas.0902420106.
Modlich, Ute, Jens Bohne, Manfred Schmidt, Christof von Kalle, Sabine Knöss, Axel Schambach, and Christopher Baum. 2006. “Cell-Culture Assays Reveal the Importance of Retroviral Vector Design for Insertional Genotoxicity.” *Blood* 108 (8): 2545–53. https://doi.org/10.1182/blood-2005-08-024976.
Moehle, Erica A., Jeremy M. Rock, Ya-Li Lee, Yann Jouvenot, Russell C. DeKelver, Philip D. Gregory, Fyodor D. Urnov, and Michael C. Holmes. 2007. “Targeted Gene Addition into a Specified Location in the Human Genome Using Designed Zinc Finger Nucleases.” *Proceedings of the National Academy of Sciences* 104 (9): 3055–60. https://doi.org/10.1073/pnas.0611478104.
Mojica, Francisco J.M., Chc)sar Díez-Villaseñor, Jesús García-Martínez, and Elena Soria. 2005. “Intervening Sequences of Regularly Spaced Prokaryotic Repeats Derive from Foreign Genetic Elements.” *Journal of Molecular Evolution* 60 (2): 174–82. https://doi.org/10.1007/s00239-004-0046-3.
Monckton, D. G., L. J. Wong, T. Ashizawa, and C. T. Caskey. 1995. “Somatic Mosaicism, Germline Expansions, Germline Reversions and Intergenerational Reductions in Myotonic Dystrophy Males: Small Pool PCR Analyses.” *Human Molecular Genetics* 4 (1): 1–8.
Monteys, Alex Mas, Shauna A. Ebanks, Megan S. Keiser, and Beverly L. Davidson. 2017. “CRISPR/Cas9 Editing of the Mutant Huntingtin Allele In Vitro and In Vivo.” *Molecular Therapy* 25 (1): 12–23. https://doi.org/10.1016/j.ymthe.2016.11.010.
Montini, Eugenio, Daniela Cesana, Manfred Schmidt, Francesca Sanvito, Maurilio Ponzoni, Cynthia Bartholomae, Lucia Sergi Sergi, et al. 2006. “Hematopoietic Stem Cell Gene Transfer in a Tumor-Prone Mouse Model Uncovers Low Genotoxicity of Lentiviral Vector Integration.” *Nature Biotechnology* 24 (6): 687–96. https://doi.org/10.1038/nbt1216.
Mosbach, Valentine, Lucie Poggi, David Viterbo, Marine Charpentier, and Guy-Franck Richard. 2018. “TALEN-Induced Double-Strand Break Repair of CTG Trinucleotide Repeats.” *Cell Reports* 22 (8): 2146–59. https://doi.org/10.1016/j.celrep.2018.01.083.
Moscou, Matthew J., and Adam J. Bogdanove. 2009. “A Simple Cipher Governs DNA Recognition by TAL Effectors.” *Science* 326 (5959): 1501–1501. https://doi.org/10.1126/science.1178817.
Moss, Davina J Hensman, Antonio F Pardiñas, Douglas Langbehn, Kitty Lo, Blair R Leavitt, Raymund Roos, Alexandra Durr, et al. 2017. “Identification of Genetic Variants Associated with Huntington’s Disease Progression: A Genome-Wide Association Study.” *The Lancet Neurology* 16 (9): 701–11. https://doi.org/10.1016/S1474-4422(17)30161-8.
Mout, Rubul, Moumita Ray, Gulen Yesilbag Tonga, Yi-Wei Lee, Tristan Tay, Kanae Sasaki, and Vincent M. Rotello. 2017. “Direct Cytosolic Delivery of CRISPR/Cas9-

Ribonucleoprotein for Efficient Gene Editing." *ACS Nano* 11 (3): 2452–58. https://doi.org/10.1021/acsnano.6b07600.
Mulders, Susan A. M., Walther J. A. A. van den Broek, Thurman M. Wheeler, Huib J. E. Croes, Petra van Kuik-Romeijn, Sjef J. de Kimpe, Denis Furling, et al. 2009. "Triplet-Repeat Oligonucleotide-Mediated Reversal of RNA Toxicity in Myotonic Dystrophy." *Proceedings of the National Academy of Sciences* 106 (33): 13915–20. https://doi.org/10.1073/pnas.0905780106.
Murlidharan, Giridhar, Kensuke Sakamoto, Lavanya Rao, Travis Corriher, Dan Wang, Guangping Gao, Patrick Sullivan, and Aravind Asokan. 2016. "CNS-Restricted Transduction and CRISPR/Cas9-Mediated Gene Deletion with an Engineered AAV Vector." *Molecular Therapy. Nucleic Acids* 5 (7): e338. https://doi.org/10.1038/mtna.2016.49.
Mussolino, Claudio, and Toni Cathomen. 2011. "On Target? Tracing Zinc-Finger-Nuclease Specificity." *Nature Methods* 8 (9): 725–26. https://doi.org/10.1038/nmeth.1680.
Naldini, Luigi, Ulrike Blömer, Philippe Gallay, Daniel Ory, Richard Mulligan, Fred H. Gage, Inder M. Verma, and Didier Trono. 1996. "In Vivo Gene Delivery and Stable Transduction of Nondividing Cells by a Lentiviral Vector." *Science* 272 (5259): 263–67. https://doi.org/10.1126/science.272.5259.263.
Nance, M. A., V. Mathias-Hagen, G. Breningstall, Myra J. Wick, and R. C. McGlennen. 1999. "Analysis of a Very Large Trinucleotide Repeat in a Patient with Juvenile Huntington's Disease." *Neurology* 52 (2): 392–94.
Nathwani, A.C., U.M. Reiss, E.G.D. Tuddenham, C. Rosales, P. Chowdary, J. McIntosh, M. Della Peruta, et al. 2014. "Long-Term Safety and Efficacy of Factor IX Gene Therapy in Hemophilia B." *The New England Journal of Medicine* 371 (21): 1994–2004. https://doi.org/10.1056/NEJMoa1407309.
Nelson, Christopher E., Chady H. Hakim, David G. Ousterout, Pratiksha I. Thakore, Eirik A. Moreb, Ruth M. Castellanos Rivera, Sarina Madhavan, et al. 2016. "In Vivo Genome Editing Improves Muscle Function in a Mouse Model of Duchenne Muscular Dystrophy." *Science* 351 (6271): 403–7. https://doi.org/10.1126/science.aad5143.
Nienhuis, Arthur W., Cynthia E. Dunbar, and Brian P. Sorrentino. 2006. "Genotoxicity of Retroviral Integration In Hematopoietic Cells." *Molecular Therapy* 13 (6): 1031–49. https://doi.org/10.1016/j.ymthe.2006.03.001.
Orr, Harry T., and Huda Y. Zoghbi. 2007a. "Trinucleotide Repeat Disorders." *Annual Review of Neuroscience* 30 (1): 575–621. https://doi.org/10.1146/annurev.neuro.29.051605.113042.
Ouellet, D. L., K. Cherif, J. Rousseau, and J. P. Tremblay. 2017. "Deletion of the GAA Repeats from the Human Frataxin Gene Using the CRISPR-Cas9 System in YG8R-Derived Cells and Mouse Models of Friedreich Ataxia." *Gene Therapy* 24 (5): 265–74. https://doi.org/10.1038/gt.2016.89.
Ousterout, David G., Ami M. Kabadi, Pratiksha I. Thakore, William H. Majoros, Timothy E. Reddy, and Charles A. Gersbach. 2015. "Multiplex CRISPR/Cas9-Based Genome Editing for Correction of Dystrophin Mutations That Cause Duchenne Muscular Dystrophy." *Nature Communications* 6 (February): 6244. https://doi.org/10.1038/ncomms7244.
Panaite, Petrica-Adrian, Emilien Gantelet, Rudolf Kraftsik, Geneviève Gourdon, Thierry Kuntzer, and Ibtissam Barakat-Walter. 2008. "Myotonic Dystrophy Transgenic Mice Exhibit Pathologic Abnormalities in Diaphragm Neuromuscular Junctions and Phrenic Nerves." *Journal of Neuropathology & Experimental Neurology* 67 (8): 763–72. https://doi.org/10.1097/NEN.0b013e318180ec64.

Park, Chul-Yong, Tomer Halevy, Dongjin R. Lee, Jin Jea Sung, Jae Souk Lee, Ofra Yanuka, Nissim Benvenisty, and Dong-Wook Kim. 2015. "Reversion of FMR1 Methylation and Silencing by Editing the Triplet Repeats in Fragile X IPSC-Derived Neurons." *Cell Reports* 13 (2): 234–41. https://doi.org/10.1016/j.celrep.2015.08.084.

Pattanayak, Vikram, Cherie L. Ramirez, J. Keith Joung, and David R. Liu. 2011. "Revealing Off-Target Cleavage Specificities of Zinc Finger Nucleases by In Vitro Selection." *Nature Methods* 8 (9): 765–70. https://doi.org/10.1038/nmeth.1670.

Pearson, Christopher E, Kerrie Nichol Edamura, and John D Cleary. 2005. "Repeat Instability: Mechanisms of Dynamic Mutations." *Nature Reviews. Genetics* 6 (10): 729–42. https://doi.org/10.1038/nrg1689.

Perez, Elena E, Jianbin Wang, Jeffrey C Miller, Yann Jouvenot, Kenneth a Kim, Olga Liu, Nathaniel Wang, et al. 2008a. "Establishment of HIV-1 Resistance in CD4+ T Cells by Genome Editing Using Zinc-Finger Nucleases." *Nature Biotechnology* 26 (7): 808–16. https://doi.org/10.1038/nbt1410.

Pešović, Jovan, S. Perić, M. Brkušanin, G. Brajušković, V. Rakočević-Stojanović, and Dušanka Savić-Pavićević. 2017. "Molecular Genetic and Clinical Characterization of Myotonic Dystrophy Type 1 Patients Carrying Variant Repeats within DMPK Expansions." *Neurogenetics* 18 (4): 207–18. https://doi.org/10.1007/s10048-017-0523-7.

Pinto, Belinda S., Tanvi Saxena, Ruan Oliveira, Héctor R. Méndez-Gómez, John D. Cleary, Lance T. Denes, Ona McConnell, et al. 2017. "Impeding Transcription of Expanded Microsatellite Repeats by Deactivated Cas9." *Molecular Cell* 68 (3): 479-490.e5. https://doi.org/10.1016/j.molcel.2017.09.033.

Pribadi, Mochtar, Zhongan Yang, Tanya S. Kim, Elliot W. Swartz, Alden Y. Huang, Jason A. Chen, Deepika Dokuru, et al. 2016. "CRISPR-Cas9 Targeted Deletion of the C9orf72 Repeat Expansion Mutation Corrects Cellular Phenotypes in Patient-Derived IPS Cells." *BioRxiv*, May, 051193. https://doi.org/10.1101/051193.

Provenzano, Claudia, Marisa Cappella, Rea Valaperta, Rosanna Cardani, Giovanni Meola, Fabio Martelli, Beatrice Cardinali, and Germana Falcone. 2017. "CRISPR/Cas9-Mediated Deletion of CTG Expansions Recovers Normal Phenotype in Myogenic Cells Derived from Myotonic Dystrophy 1 Patients." *Molecular Therapy - Nucleic Acids* 9 (December): 337–48. https://doi.org/10.1016/j.omtn.2017.10.006.

Puumalainen, Anu-Maaria, Matti Vapalahti, Reitu S. Agrawal, Maija Kossila, Johanna Laukkanen, Pauliina Lehtolainen, Helena Viita, Leo Paljärvi, Ritva Vanninen, and Seppo Ylä-Herttuala. 1998. "β-Galactosidase Gene Transfer to Human Malignant Glioma In Vivo Using Replication-Deficient Retroviruses and Adenoviruses." *Human Gene Therapy* 9 (12): 1769–74. https://doi.org/10.1089/hum.1998.9.12-1769.

Rabinowitz, Joseph E., Fabienne Rolling, Chengwen Li, Hervè Conrath, Weidong Xiao, Xiao Xiao, and R. Jude Samulski. 2002. "Cross-Packaging of a Single Adeno-Associated Virus (AAV) Type 2 Vector Genome into Multiple AAV Serotypes Enables Transduction with Broad Specificity." *Journal of Virology* 76 (2): 791–801. https://doi.org/10.1128/JVI.76.2.791-801.2002.

Ramakrishna, Suresh, Abu-Bonsrah Kwaku Dad, Jagadish Beloor, Ramu Gopalappa, Sang-Kyung Lee, and Hyongbum Kim. 2014. "Gene Disruption by Cell-Penetrating Peptide-Mediated Delivery of Cas9 Protein and Guide RNA." *Genome Research* 24 (6): 1020–27. https://doi.org/10.1101/gr.171264.113.

Ran, F. Ann, Le Cong, Winston X. Yan, David A. Scott, Jonathan S. Gootenberg, Andrea J. Kriz, Bernd Zetsche, et al. 2015. "In Vivo Genome Editing Using Staphylococcus Aureus Cas9." *Nature* 520 (7546): 186–91. https://doi.org/10.1038/nature14299.

Ran, F. Ann, Patrick D. Hsu, Chie-Yu Lin, Jonathan S. Gootenberg, Silvana Konermann, Alexandro E. Trevino, David A. Scott, et al. 2013. "Double Nicking by RNA-Guided CRISPR Cas9 for Enhanced Genome Editing Specificity." *Cell* 154 (6): 1380–89. https://doi.org/10.1016/j.cell.2013.08.021.

Rauch, Benjamin J., Melanie R. Silvis, Judd F. Hultquist, Christopher S. Waters, Michael J. McGregor, Nevan J. Krogan, and Joseph Bondy-Denomy. 2017. "Inhibition of CRISPR-Cas9 with Bacteriophage Proteins." *Cell* 168 (1): 150-158.e10. https://doi.org/10.1016/j.cell.2016.12.009.

Rawlins, Michael D., Nancy S. Wexler, Alice R. Wexler, Sarah J. Tabrizi, Ian Douglas, Stephen J. W. Evans, and Liam Smeeth. 2016. "The Prevalence of Huntington's Disease." *Neuroepidemiology* 46 (2): 144–53. https://doi.org/10.1159/000443738.

Richard, G. F., B. Dujon, and J. E. Haber. 1999. "Double-Strand Break Repair Can Lead to High Frequencies of Deletions within Short CAG/CTG Trinucleotide Repeats." *Molecular and General Genetics* 261 (4–5): 871–82.

Richard, Guy-Franck, David Viterbo, Varun Khanna, Valentine Mosbach, Lauriane Castelain, and Bernard Dujon. 2014a. "Highly Specific Contractions of a Single CAG/CTG Trinucleotide Repeat by TALEN in Yeast." *PloS One* 9 (4): e95611. https://doi.org/10.1371/journal.pone.0095611.

Ross, Colin J.D., Jaap Twisk, Janneke M. Meulenberg, Guoqing Liu, Karin Van Den Oever, Ewoud Moraal, Wim T. Hermens, et al. 2004. "Long-Term Correction of Murine Lipoprotein Lipase Deficiency with AAV1-Mediated Gene Transfer of the Naturally Occurring LPLS447X Beneficial Mutation." *Human Gene Therapy* 15 (9): 906–19. https://doi.org/10.1089/hum.2004.15.906.

Salmon, Patrick, and Didier Trono. 2007. "Production and Titration of Lentiviral Vectors." *Current Protocols in Human Genetics* 54 (1): 12.10.1-12.10.24. https://doi.org/10.1002/0471142905.hg1210s54.

Salva, Maja Z, Charis L Himeda, Phillip WL Tai, Eiko Nishiuchi, Paul Gregorevic, James M Allen, Eric E Finn, et al. 2007. "Design of Tissue-Specific Regulatory Cassettes for High-Level RAAV-Mediated Expression in Skeletal and Cardiac Muscle." *Molecular Therapy* 15 (2): 320–29. https://doi.org/10.1038/sj.mt.6300027.

Sanjana, Neville E., Ophir Shalem, and Feng Zhang. 2014. "Improved Vectors and Genome-Wide Libraries for CRISPR Screening." *Nature Methods* 11 (8): 783–84. https://doi.org/10.1038/nmeth.3047.

Santillan, Beatriz A., Christopher Moye, David Mittelman, and John H. Wilson. 2014. "GFP-Based Fluorescence Assay for CAG Repeat Instability in Cultured Human Cells." *PLOS ONE* 9 (11): e113952. https://doi.org/10.1371/journal.pone.0113952.

Saudou, Frédéric, Steven Finkbeiner, Didier Devys, and Michael E Greenberg. 1998. "Huntingtin Acts in the Nucleus to Induce Apoptosis but Death Does Not Correlate with the Formation of Intranuclear Inclusions." *Cell* 95 (1): 55–66. https://doi.org/10.1016/S0092-8674(00)81782-1.

Savouret, Â, E Brisson, J Essers, R Kanaar, A Pastink, and H Riele. 2003. "CTG Repeat Instability and Size Variation Timing in DNA Repair-de ® Cient Mice." *The EMBO Journal* 22 (9): 2264–73.

Savouret, C., C Garcia-cordier, H Riele, C Junien, and I U Ge. 2004. "MSH2-Dependent Germinal CTG Repeat Expansions Are Produced Continuously in Spermatogonia from DM1 Transgenic Mice." *Molecular and Cellular Biology* 24 (2): 629–37. https://doi.org/10.1128/MCB.24.2.629.

Schmidt, Florian, and Dirk Grimm. 2015. "CRISPR Genome Engineering and Viral Gene Delivery: A Case of Mutual Attraction." *Biotechnology Journal* 10 (2): 258–72. https://doi.org/10.1002/biot.201400529.

Schröder, Astrid R. W., Paul Shinn, Huaming Chen, Charles Berry, Joseph R. Ecker, and Frederic Bushman. 2002. "HIV-1 Integration in the Human Genome Favors Active Genes and Local Hotspots." *Cell* 110 (4): 521–29. https://doi.org/10.1016/S0092-8674(02)00864-4.

Scrudato, M. Lo, K. Poulard, A. Klein, S. Tomé, S. Martin, G. Gourdon, D. Furling, and A. Buj-Bello. 2017. "CRISPR/Cas9-Mediated Genome Editing Corrects Splicing Alterations in Myotonic Dystrophy Type 1." *Neuromuscular Disorders* 27 (October): S181. https://doi.org/10.1016/j.nmd.2017.06.318.

Segal, David J., Birgit Dreier, Roger R. Beerli, and Carlos F. Barbas. 1999. "Toward Controlling Gene Expression at Will: Selection and Design of Zinc Finger Domains Recognizing Each of the 5′-GNN-3′ DNA Target Sequences." *Proceedings of the National Academy of Sciences* 96 (6): 2758–63. https://doi.org/10.1073/pnas.96.6.2758.

Sengillo, Jesse D., Sally Justus, Thiago Cabral, and Stephen H. Tsang. 2017. "Correction of Monogenic and Common Retinal Disorders with Gene Therapy." *Genes* 8 (2): 53. https://doi.org/10.3390/genes8020053.

Seznec, Hervé, Anne-Sophie Lia-Baldini, Chantal Duros, Coralie Fouquet, Céline Lacroix, Hélène Hofmann-Radvanyi, Claudine Junien, and Geneviève Gourdon. 2000a. "Transgenic Mice Carrying Large Human Genomic Sequences with Expanded CTG Repeat Mimic Closely the DM CTG Repeat Intergenerational and Somatic Instability." *Human Molecular Genetics* 9 (8): 1185–94. https://doi.org/10.1093/hmg/9.8.1185.

Shin, Jun Wan, Kyung-Hee Kim, Michael J. Chao, Ranjit S. Atwal, Tammy Gillis, Marcy E. MacDonald, James F. Gusella, and Jong-Min Lee. 2016. "Permanent Inactivation of Huntington's Disease Mutation by Personalized Allele-Specific CRISPR/Cas9." *Human Molecular Genetics* 25 (20): 4566–76. https://doi.org/10.1093/hmg/ddw286.

Sobczak, Krzysztof, Thurman M Wheeler, Wenli Wang, and Charles a Thornton. 2013. "RNA Interference Targeting CUG Repeats in a Mouse Model of Myotonic Dystrophy." *Molecular Therapy : The Journal of the American Society of Gene Therapy* 21 (2): 380–87. https://doi.org/10.1038/mt.2012.222.

Staahl, Brett T., Madhurima Benekareddy, Claire Coulon-Bainier, Ashwin A. Banfal, Stephen N. Floor, Jennifer K. Sabo, Cole Urnes, Gabriela Acevedo Munares, Anirvan Ghosh, and Jennifer A. Doudna. 2017. "Efficient Genome Editing in the Mouse Brain by Local Delivery of Engineered Cas9 Ribonucleoprotein Complexes." *Nature Biotechnology* 35 (5): 431–34. https://doi.org/10.1038/nbt.3806.

Stolberg, Sheryl Gay. 1999. "The Biotech Death of Jesse Gelsinger." *The New York Times*, November 28, 1999, sec. Magazine. https://www.nytimes.com/1999/11/28/magazine/the-biotech-death-of-jesse-gelsinger.html.

Stroes, E. S., M. C. Nierman, J. J. Meulenberg, R. Franssen, J. Twisk, C. P. Henny, M. M. Maas, et al. 2008. "Intramuscular Administration of AAV1-Lipoprotein Lipase S447X Lowers Triglycerides in Lipoprotein Lipase-Deficient Patients." *Arteriosclerosis, Thrombosis, and Vascular Biology* 28 (12): 2303–4. https://doi.org/10.1161/ATVBAHA.108.175620.

Suresh, Bharathi, Suresh Ramakrishna, and Hyongbum Kim. 2017. "Cell-Penetrating Peptide-Mediated Delivery of Cas9 Protein and Guide RNA for Genome Editing." In *Eukaryotic Transcriptional and Post-Transcriptional Gene Expression Regulation*, edited by Narendra Wajapeyee and Romi Gupta, 81–94. Methods in Molecular Biology. New York, NY: Springer New York. https://doi.org/10.1007/978-1-4939-6518-2_7.

Swiech, Lukasz, Matthias Heidenreich, Abhishek Banerjee, Naomi Habib, Yinqing Li, John Trombetta, Mriganka Sur, and Feng Zhang. 2015. "*In Vivo* Interrogation of Gene Function in the Mammalian Brain Using CRISPR-Cas9." *Nature Biotechnology* 33 (1): 102–6. https://doi.org/10.1038/nbt.3055.

Tabebordbar, Mohammadsharif, Kexian Zhu, Jason K. W. Cheng, Wei Leong Chew, Jeffrey J. Widrick, Winston X. Yan, Claire Maesner, et al. 2016. "In Vivo Gene Editing in Dystrophic Mouse Muscle and Muscle Stem Cells." *Science* 351 (6271): 407–11. https://doi.org/10.1126/science.aad5177.

Tardieu, Marc, Michel Zérah, Béatrice Husson, Stéphanie de Bournonville, Kumaran Deiva, Catherine Adamsbaum, Fanny Vincent, et al. 2014. "Intracerebral Administration of Adeno-Associated Viral Vector Serotype Rh.10 Carrying Human SGSH and SUMF1 CDNAs in Children with Mucopolysaccharidosis Type IIIA Disease: Results of a Phase I/II Trial." *Human Gene Therapy* 25 (6): 506–16. https://doi.org/10.1089/hum.2013.238.

Tervo, D. Gowanlock R., Bum-Yeol Hwang, Sarada Viswanathan, Thomas Gaj, Maria Lavzin, Kimberly D. Ritola, Sarah Lindo, et al. 2016. "A Designer AAV Variant Permits Efficient Retrograde Access to Projection Neurons." *Neuron* 92 (2): 372–82. https://doi.org/10.1016/j.neuron.2016.09.021.

Tomé, S, I Holt, W Edelmann, G E Morris, A Munnich, C E Pearson, and G Gourdon. 2009. "MSH2 ATPase Domain Mutation Affects CTG*CAG Repeat Instability in Transgenic Mice." *PLoS Genetics* 5 (5): e1000482. https://doi.org/10.1371/journal.pgen.1000482.

Truong, Dong-Jiunn Jeffery, Karin Kühner, Ralf Kühn, Stanislas Werfel, Stefan Engelhardt, Wolfgang Wurst, and Oskar Ortiz. 2015. "Development of an Intein-Mediated Split–Cas9 System for Gene Therapy." *Nucleic Acids Research* 43 (13): 6450–58. https://doi.org/10.1093/nar/gkv601.

Udd, Bjarne, and Ralf Krahe. 2012a. "The Myotonic Dystrophies: Molecular, Clinical, and Therapeutic Challenges." *The Lancet. Neurology* 11 (10): 891–905. https://doi.org/10.1016/S1474-4422(12)70204-1.

Wang, Gary P, Bruce L Levine, Gwendolyn K Binder, Charles C Berry, Nirav Malani, Gary McGarrity, Pablo Tebas, Carl H June, and Frederic D Bushman. 2009. "Analysis of Lentiviral Vector Integration in HIV+ Study Subjects Receiving Autologous Infusions of Gene Modified CD4+ T Cells." *Molecular Therapy* 17 (5): 844–50. https://doi.org/10.1038/mt.2009.16.

Wang, Guey-Shin, Debra L Kearney, Mariella De Biasi, George Taffet, and Thomas a Cooper. 2007. "Elevation of RNA-Binding Protein CUGBP1 Is an Early Event in an Inducible Heart-Specific Mouse Model of Myotonic Dystrophy." *The Journal of Clinical Investigation* 117 (10): 2802–11. https://doi.org/10.1172/JCI32308.

Wang, Ming, John A. Zuris, Fantao Meng, Holly Rees, Shuo Sun, Pu Deng, Yong Han, et al. 2016. "Efficient Delivery of Genome-Editing Proteins Using Bioreducible Lipid Nanoparticles." *Proceedings of the National Academy of Sciences* 113 (11): 2868–73. https://doi.org/10.1073/pnas.1520244113.

Wang, Yanlin, Lei Hao, Hongcai Wang, Katherine Santostefano, Arjun Thapa, John Cleary, Hui Li, et al. 2018. "Therapeutic Genome Editing for Myotonic Dystrophy Type 1 Using CRISPR/Cas9." *Molecular Therapy* 26 (11): 2617–30. https://doi.org/10.1016/j.ymthe.2018.09.003.

Wang, Zhong, Tong Zhu, Chunping Qiao, Liqiao Zhou, Bing Wang, Jian Zhang, Chunlian Chen, Juan Li, and Xiao Xiao. 2005. "Adeno-Associated Virus Serotype 8 Efficiently Delivers Genes to Muscle and Heart." *Nature Biotechnology* 23 (3): 321–28. https://doi.org/10.1038/nbt1073.

Warf, M B, M Nakamori, C Matthys, C Thornton, and J A Berglund. 2009. “Pentamidine Reverses the Splicing Defects Associated with Myotonic Dystrophy.” *Proceedings of the National Academy of Sciences of the United States of America* 106 (44): 18551–56.

Watakabe, Akiya, Masanari Ohtsuka, Masaharu Kinoshita, Masafumi Takaji, Kaoru Isa, Hiroaki Mizukami, Keiya Ozawa, Tadashi Isa, and Tetsuo Yamamori. 2015. “Comparative Analyses of Adeno-Associated Viral Vector Serotypes 1, 2, 5, 8 and 9 in Marmoset, Mouse and Macaque Cerebral Cortex.” *Neuroscience Research*, Marmoset Neuroscience, 93 (April): 144–57. https://doi.org/10.1016/j.neures.2014.09.002.

Wheeler, V. C., W. Auerbach, J. K. White, J. Srinidhi, A. Auerbach, A. Ryan, M. P. Duyao, et al. 1999. “Length-Dependent Gametic CAG Repeat Instability in the Huntington’s Disease Knock-in Mouse.” *Human Molecular Genetics* 8 (1): 115–22.

Wheeler, V. C., Lori-Anne Lebel, Vladimir Vrbanac, Allison Teed, Hein te Reile, and Marcy E MacDonal. 2003. “Mismatch Repair Gene Msh2 Modifies the Timing of Early Disease in HdhQ111 Striatum.” *Human Molecular Genetics* 12 (3): 273–81. https://doi.org/10.1093/hmg/ddg056.

Wheeler, Vanessa C., Jacqueline K. White, Claire-Anne Gutekunst, Vladimir Vrbanac, Meredith Weaver, Xiao-Jiang Li, Shi-Hua Li, et al. 2000. “Long Glutamine Tracts Cause Nuclear Localization of a Novel Form of Huntingtin in Medium Spiny Striatal Neurons in HdhQ92 and HdhQ111 Knock-in Mice.” *Human Molecular Genetics* 9 (4): 503–13. https://doi.org/10.1093/hmg/9.4.503.

White, Jacqueline K., Wojtek Auerbach, Mabel P. Duyao, Jean-Paul Vonsattel, James F. Gusella, Alexandra L. Joyner, and Marcy E. MacDonald. 1997a. “Huntingtin Is Required for Neurogenesis and Is Not Impaired by the Huntington’s Disease CAG Expansion.” *Nature Genetics* 17 (4): 404. https://doi.org/10.1038/ng1297-404.

Wu, Zhijian, Aravind Asokan, and R. Jude Samulski. 2006. “Adeno-Associated Virus Serotypes: Vector Toolkit for Human Gene Therapy.” *Molecular Therapy* 14 (3): 316–27. https://doi.org/10.1016/j.ymthe.2006.05.009.

Wu, Zhijian, Hongyan Yang, and Peter Colosi. 2010. “Effect of Genome Size on AAV Vector Packaging.” *Molecular Therapy* 18 (1): 80–86. https://doi.org/10.1038/mt.2009.255.

Xiao, X., J. Li, and R. J. Samulski. 1996. “Efficient Long-Term Gene Transfer into Muscle Tissue of Immunocompetent Mice by Adeno-Associated Virus Vector.” *Journal of Virology* 70 (11): 8098–8108.

Yamamoto, Ai, José J Lucas, and René Hen. 2000. “Reversal of Neuropathology and Motor Dysfunction in a Conditional Model of Huntington’s Disease.” *Cell* 101 (1): 57–66. https://doi.org/10.1016/S0092-8674(00)80623-6.

Yang, Hui, Haoyi Wang, Chikdu S. Shivalila, Albert W. Cheng, Linyu Shi, and Rudolf Jaenisch. 2013. “One-Step Generation of Mice Carrying Reporter and Conditional Alleles by CRISPR/Cas-Mediated Genome Engineering.” *Cell* 154 (6): 1370–79. https://doi.org/10.1016/j.cell.2013.08.022.

Yang, Su, Renbao Chang, Huiming Yang, Ting Zhao, Yan Hong, Ha Eun Kong, Xiaobo Sun, et al. 2017. “CRISPR/Cas9-Mediated Gene Editing Ameliorates Neurotoxicity in Mouse Model of Huntington’s Disease.” *The Journal of Clinical Investigation* 127 (7): 2719–24. https://doi.org/10.1172/JCI92087.

Yang, Yang, Lili Wang, Peter Bell, Deirdre McMenamin, Zhenning He, John White, Hongwei Yu, et al. 2016. “A Dual AAV System Enables the Cas9-Mediated Correction of a Metabolic Liver Disease in Newborn Mice.” *Nature Biotechnology* 34 (3): 334–38. https://doi.org/10.1038/nbt.3469.

Yee, Jiing-Kuan. 2016. “Off-Target Effects of Engineered Nucleases.” *The FEBS Journal* 283 (17): 3239–48. https://doi.org/10.1111/febs.13760.

Yero, Tatiana, and Jose A. Rey. 2008. “Tetrabenazine (Xenazine), An FDA-Approved Treatment Option For Huntington’s Disease–Related Chorea.” *Pharmacy and Therapeutics* 33 (12): 690–94.

Ylä-Herttuala, Seppo. 2012. “Endgame: Glybera Finally Recommended for Approval as the First Gene Therapy Drug in the European Union.” *Molecular Therapy* 20 (10): 1831–32. https://doi.org/10.1038/mt.2012.194.

Zetsche, Bernd, Sara E. Volz, and Feng Zhang. 2015. “A Split-Cas9 Architecture for Inducible Genome Editing and Transcription Modulation.” *Nature Biotechnology* 33 (February): 139–42. https://doi.org/10.1038/nbt.3149.

Zhang, Yilan, Xianglian Ge, Fayu Yang, Liping Zhang, Jiayong Zheng, Xuefang Tan, Zi-Bing Jin, Jia Qu, and Feng Gu. 2014. “Comparison of Non-Canonical PAMs for CRISPR/Cas9-Mediated DNA Cleavage in Human Cells.” *Scientific Reports* 4 (June): 5405. https://doi.org/10.1038/srep05405.

Zhao, Xiao-Nan, and Karen Usdin. 2015. “The Repeat Expansion Diseases: The Dark Side of DNA Repair.” *DNA Repair*, Cutting-edge Perspectives in Genomic Maintenance, 32 (August): 96–105. https://doi.org/10.1016/j.dnarep.2015.04.019.

Zincarelli, Carmela, Stephen Soltys, Giuseppe Rengo, and Joseph E Rabinowitz. 2008. “Analysis of AAV Serotypes 1–9 Mediated Gene Expression and Tropism in Mice After Systemic Injection.” *Molecular Therapy* 16 (6): 1073–80. https://doi.org/10.1038/mt.2008.76.

Zu, Tao, Lisa A. Duvick, Michael D. Kaytor, Michael S. Berlinger, Huda Y. Zoghbi, H. Brent Clark, and Harry T. Orr. 2004. “Recovery from Polyglutamine-Induced Neurodegeneration in Conditional SCA1 Transgenic Mice.” *The Journal of Neuroscience: The Official Journal of the Society for Neuroscience* 24 (40): 8853–61. https://doi.org/10.1523/JNEUROSCI.2978-04.2004.

Zuris, John A., David B. Thompson, Yilai Shu, John P. Guilinger, Jeffrey L. Bessen, Johnny H. Hu, Morgan L. Maeder, J. Keith Joung, Zheng-Yi Chen, and David R. Liu. 2015. “Cationic Lipid-Mediated Delivery of Proteins Enables Efficient Protein-Based Genome Editing *in Vitro* and *in Vivo*.” *Nature Biotechnology* 33 (1): 73–80. https://doi.org/10.1038/nbt.3081.

Appendix: Protocols

Production of lentivirus with the third generation vector

Protocol from (Salmon and Trono 2007).

- Plate 2.5 x 10^6 HEK 293 T in 4 x 15 cm/dish in 20 mL of DMEM/glutamax supplemented with 10% fetal bovine serum (FBS), 100 U/mL penicillin, 100 µg/mL streptomycin.
- Incubate at 37°C for 56 hours.
- Replace medium with 22.5mL of fresh medium 2 hours before the transfection.
- CalPhos Mammalian Transfection:

  All the plasmids need to be at a concentration of 1 µg/µL.

  Mix in one 15 mL tube as followed:

  - 2.64 mL of TE 0.1X
  - 1.09 mL of H_2O
  - 90 µg of vector containing gene of interest = 90 µL
  - 31.6 µg of pMD2G (bVIN-374) = 31.6 µL
  - 58.4 µg of pMDL g/pRRE (bVIN-376) = 58.4 µL
  - 24 µg of pRSV-Rev (bVIN-375) = 24 µL
  - 0.562 mL of CaCl2 2M (0.25M final)

  Mix well by vortexing

  - Add the mix drop by drop vortexing into a second tube with 4.5 mL of HeBs 2X
  - Incubate at RT for 5 min.
  - Distribute transfection solution 2.25 mL per dish.
  - Incubate for 24 hours.

- Replace medium with 14 mL of fresh medium in the early morning.
- 8 hours after, collect the medium and store it 4°C. Add 14 mL of fresh medium to the plates.
- Leave overnight in the incubator.

- In the early morning, collect the medium and store at 4°C. Add 14 mL of fresh medium.
- 8 hours after, collect the last aliquot of the medium and store it at 4°C.

Centrifugation

- Mix all collected of medium containing virus and filter with a 0.22 µm Stericup 250 mL
- Distribute the medium in Ultracentrifuge tube 38.5ml (Beckman).
- Ultracentrifuge 2 hours at 19500 rpm 16°C
- Discard the supernatant by aspiration and dry tubes placing them upside down on a paper.
- Resuspension total in 200µL 1X PBS: add 100 µL of PBS in first tube and 20 µL in five other tubes; incubate at RT for 15 min.
- Resuspend the virus in PBS by pipetting with this technique:

  - Start by resuspending the pellet in the first tube (100 µL). Choose one side of the tube and do 10 ups and downs to detach the pellet, then rotate the tube of ¼.
  - 10 ups and downs to detach the pellet, then rotate the tube of ¼.
  - 10 ups and downs to detach the pellet, then rotate the tube of ¼.
  - Finish with 10-20 ups and downs in the middle of the tube.
  - Transfer the 100ul to the second tube and process in the same way.
  - Repeat until collecting the entire PBS volume into the last tube.
  - Avoid as much as possible to make bubbles.
  - At the end, collect all 200 µL and aliquot the volume, 10 µL per tube.
  - Store at -80°C.

Protocol from (Salmon and Trono 2007).

Cells transduction with the lentivirus

Day 0: Plate 100'000 HEK 293 T cells in 7 wells of coated 12 wells plate.

Day 1: Collect cells from 1 well and count.

Change the medium with 500ul of fresh medium in the other wells.

Cells infection with designed lentivirus:

-1 well: no infection

-1 well: 3 ul of virus

-1 well: 2 ul of virus

-1 well: 10 ul of dilution 1 (27 ul of PBS + 3ul of virus)

-1 well: 10 ul of dilution 2 (27 ul of PBS + 3ul of dilution 1)

-1 well: 10 ul of dilution 2 (27 ul of PBS + 3ul of dilution 2)

Day 3: Collect and DNA extract with NucleoSpin Tissue Kit (MACHEREY-NAGEL, Düren, Germany)

qPCR

qPCR was performed with the FastStart Universal SYBR Green Master (Roche) using a 7900HT Fast Real-Time PCR System in a 384-Well Block Module (Applied Biosystems™).

1. Setup qPCR reaction. Prepare and run each sample per primers couple in triplicate (standard and viral).

2. For one sample make a serial dilution of $1x10^{11}$ copies/mL stock to generate $1x10^{10}$, $1x10^{9}$, $1x10^{8}$, $1x10^{7}$, $1x10^{6}$, $1x10^{5}$ copy/mL solutions.

qPCR conditions

SybrGreen Master	3.2 uL
Forward primer (100 uM)	0.3 uL
Reverse Primer (100 uM)	0.3 uL
Water	1.3 uL

The primers used are:
oVIN-1663 For Gag
oVIN-1664 Rev Gag
oVIN-1665 For WPRE
oVIN-1666 Rev WPRE
oVIN-2018 Rev Albumin
oVIN-2019 Rev Albumin

qPCR program:

I.	95°C	10 min	
II.	95°C	15 sec	
III.	60°C	1 min	50 cycles

3. Use the standard curve to predict the titer of the vector. Make sure to account for the dilution factor and the single-stranded nature of the lentiviral vector genome.

Ct values were analyzed using the SDS Software v2.4. The reported enrichments were obtained using the ΔCt method:

ΔCt= Ct2-Ct1
Ct1: viral gene
Ct2: Actin

$2^{-\Delta C}$= copy number

N° of cells at infection x 2 x copy number x dilution factor x 1000 = TU /mL

Consider the final titer as the average of the triplicates of the same dilutions.

Adapted from (Dion et al. 2008).

gDNA dilutions

For each 10 µL PCR reaction: 1 µL of gDNA dilution is required.

Dilute the genomic DNA to a concentration of 1 $^{ng}/_{\mu L}$ (*HTT*) or 1 $^{ng}/_{\mu L}$ (*DMPK*).

Small-pool PCR reaction

Prepare a PCR reaction mastermix according to the following:

HTT CAG repeats	10 µL reaction	*DMPK* CTG repeats	10 µL reaction
5X Mango Taq buffer	2 µL (1X)	5X MyFi buffer	2 µL
$MgCl_2$	0.2 µL (1mM)	10 µM oVIN-1251	0.4 µL (0.4 µM)
dNTPs	0.2 µL (200µM)	10 µM oVIN-1252	0.4 µL (0.4 µM)
10 µM oVIN-1333/ oVIN-2548	0.5 µL (0.5µM)	MyFi Pol	0.4 µL
		H_2O	5.8 µL
10 µM oVIN-1334/ oVIN-2530	0.5 µL (0.5µM)		
DMSO	0.3 µL (3%)		
TAQ	0.2 µL (1U)		
H_2O	6.1 µL		

Human *HTT*: F/R primers (oVIN-1333 + oVIN-1334)

Murine *HTT*: F/R primers (oVIN-2548 + oVIN-2530)

Human *DMPK*: F/R primers (oVIN-1252 + oVIN-1251)

Multiply by the number of the PCR:

7.5 PCR mastermix per dilution

+ 1 negative control per dilution

- Add 7.5 µL of gDNA dilution [1.5 $^{ng}/_{\mu L}$] + 67.5 µL of PCR reaction mastermix.
- Mix well and distribute 10 µL into each individual PCR tubes.
- For negative controls: 9 µL of master mix + 1 µL of H_2O.

PCR Program for murine and human *HTT*

1. 95°C	5 min	
2. 95°C	20 sec	
3. 52°C	20 sec	
4. 72°C	2 min	4 cycles, steps: from 2 to 4
5. 95°C	30 sec	
6. 55°C	30 sec	
7. 72°C	90 sec	25 cycles: steps: from 5 to 7
8. 72°C	10 min	
9. 15°C	Pause	

PCR Program for *DMPK*

1. 95°C	1 min	
2. 95°C	15 sec	
3. 60°C	15 sec	
4. 72°C	2 min	32 cycles, steps: from 2 to 4
8. 72°C	10 min	
9. 15°C	Pause	

Gel electrophoresis

- Make a large 2% agarose gel, around 300 mL volume
- Load 10 µL of PCR reactions and 5 µL of molecular markers.
- Run at 180 V for 4 hours in TAE 1X.

Transfer

- Cut the excess of the gel. Take a picture of the gel
- Incubate the gel 2 times for 20min in Alkaline Transfer Buffer.
- Fill both ends of a transfer apparatus with Alkaline Transfer Buffer.
- Cut a piece of Whatman paper wide enough to cover the surface where your gel will sit and long enough so that it dips into the Alkaline Transfer Buffer at both ends. Pour some more Alkaline Transfer Buffer on top so that the filter paper is wet.

- Place your gel onto the filter paper upside down. Make sure there are no bubbles between the filter paper and the gel (bubbles will prevent transfer at that spot).
- Cut a piece of nitrocellulose membrane exactly the size of your gel.
- Place the membrane on top of the gel. Make sure there are no bubbles between the gel and the membrane (bubbles will prevent transfer at that spot).
- Cut 2 pieces of filter paper the size of your membrane and place them on top of the membrane.
- Every bit of filter paper not touching the gel MUST be covered with parafilm.
- Add paper towels on top of the filter papers.
- Add some weight on top in order to allow capillary movement and transfer of the DNA from the gel to membrane.
- Transfer overnight. You can transfer over the weekend. The longer the better, as long as you don't run out of alkaline transfer buffer or paper towel.

Probe preparation + Hybridization

- Wash membrane in Neutralization buffer for 5 minutes.
- Preheat oven, hybridization cylinders and hybridization buffer at 48°C for murine *HTT* and 52 ºC for *DMPK* or human *HTT*.
- Prepare a CAG repeat probe as follows:

T4 PNK Buffer	2.5 µL
oVIN-100 (100X dilution)	5 µL
H2O	11.5 µL
(Continue in C lab)	
α-P32-dATP	5 µL
T4 PNK	1 µL
1 hour 37 ºC	
10 minutes 65 ºC	

Meanwhile prehibridize the membrane as follow:

- Boil 500 µL salmon sperm for 5 min. Then put it on ice for ~1 min.
- Add 15 mL of Ultrahyb buffer and 500 µL salmon sperm into the pre-heated hybridization tube.
- Place membrane inside the hybridization tube with the DNA facing the inside.

- Get rid of any bubbles between the membrane and the tube.
- Block the membrane by incubating for 1 hour at 48°C for murine *HTT* or 52 ºC for *DMPK* or human *HTT*.
- Once the probe is ready, add it directly to the membrane. One probe can be shared in maximum 3 cylinders.
- Hybridize for 2 hours at 48°C for murine *HTT* or 52 ºC for *DMPK* or human *HTT*.

Washing

- Pre-heat washing buffer at 48 ºC for murine *HTT* or 52°C for *DMPK* or human *HTT*.
- Remove hybridization buffer.
- Wash twice with ~15 mL warm Wash buffer for 30 min.

Reveal

- Place the membrane inside plastic sheet protectors.
- Put the membrane inside the cassette and expose to a "clean" phosphoscreen at RT overnight.

Materials and solutions

- MyFi DNA polymerase (bioline # BIO-21117)
- MangoTaq polymerase (bioline # BIO-21083)
- Alkaline transfer buffer (0.4M NaOH, 1M NaCl)
- Nylon membrane (Fisher Scientific #NP0HYA0010)
- Neutralization buffer (1.5M NaCl, 0.5M Tris base pH7.4)
- Salmon sperm DNA 10 mg/ml (Roche #11467140001)
- T4 PNK kit (New England Biolabs #M0201S)
- γ-^{32}P-dATP (Perkin Elmer #BLU502Z250UC)
- oVIN-100: AGCAGCAGCAGCAGCAGCAGCAGCAGC
- dCTP, dATP, and dGTP at 100mM each (LabGene #KK1007)
- Ultrahyb buffer (Thermo Fisher Scientific #AM8670)
- 20X SSC (3M NaCl, 0.3M NaCitrate pH7.0)
- Wash buffer (0.5X SSC, 0.1% SDS)